ASD TECHNICAL REPORT 61-192

A THEORETICAL AND EXPERIMENTAL STUDY OF GAS FLOW THROUGH CLOTH OVER A RANGE OF PRESSURES AND TEMPERATURES

FREDERICK O. SMETANA

UNIVERSITY OF SOUTHERN CALIFORNIA

SEPTEMBER 1961

AERONAUTICAL SYSTEMS DIVISION

NOTICES

When Government drawings, specifications, or other data are used for any purpose other than in connection with a definitely related Government procurement operation, the United States Government thereby incurs no responsibility nor any obligation whatsoever; and the fact that the Government may have formulated, furnished, or in any way supplied the said drawings, specifications, or other data, is not to be regarded by implication or otherwise as in any manner licensing the holder or any other person or corporation, or conveying any rights or permission to manufacture, use, or sell any patented invention that may in any way be related thereto.

Qualified requesters may obtain copies of this report from the Armed Services Technical Information Agency, (ASTIA), Arlington Hall Station, Arlington 12, Virginia.

This report has been released to the Office of Technical Services, U. S. Department of Commerce, Washington 25, D. C., for sale to the general public.

Copies of ASD Technical Reports and Technical Notes should not be returned to the Aeronautical Systems Division unless return is required by security considerations, contractual obligations, or notice on a specific document.

ASD TECHNICAL REPORT 61-192

A THEORETICAL AND EXPERIMENTAL STUDY OF GAS FLOW THROUGH CLOTH OVER A RANGE OF PRESSURES AND TEMPERATURES

FREDERICK O. SMETANA

ENGINEERING CENTER
UNIVERSITY OF SOUTHERN CALIFORNIA
LOS ANGELES 7, CALIFORNIA

SEPTEMBER 1961

DIRECTORATE OF MATERIALS AND PROCESSES
CONTRACT No. AF 33(616)-7102
PROJECT No. 7320

AERONAUTICAL SYSTEMS DIVISION
AIR FORCE SYSTEMS COMMAND
UNITED STATES AIR FORCE
WRIGHT-PATTERSON AIR FORCE BASE, OHIO

900 - January 1962 - 16-674 & 675

FOREWORD

This report was prepared by University of Southern California under Contract No. AF 33(616)-7102. This contract was initiated under Project No. 7320, "Fibrous Materials for Decelerators and Structures," Task No. 73203, "Fibrous Structural Materials." The work was administered under the direction of Directorate for Materials and Processes, Deputy for Technology, Aeronautical Systems Division, with Captain Clarence O. Little, Jr. acting as project engineer.

This report covers work conducted from February 1960 to May 1961.

The author wishes to thank Dr. H. T. Yang for his careful and critical review of the manuscript and for his assistance in clarifying the theoretical aspects of the flow phenomena.

Mr. Kenneth Yost contributed materially to the experimental portion of the program by conducting many of the tests and keeping the apparatus functional.

The author also wishes to thank the project monitor, Capt. C. O. Little, Jr. for his assistance in securing reference material, arranging conferences with users of permeability information, and becoming thoroughly acquainted with the problems of and results of the work. His efforts have been responsible for widening the scope of the investigation and, it is hoped, have resulted in a more useful work.

ABSTRACT

Measurements were made of the permeability of five fabrics at downstream pressures from sea level to 150,000', pressure drops across the samples of 1 mm Hg to 900 mm Hg, and stagnation temperatures from 300°K to 930°K. In addition to this basic information, the investigation sought to provide a means of predicting high altitude results from those at sea level. It was found that: (a) the geometry of the test apparatus can have a marked influence on the results, (b) the major elastic effects on permeability arise from the change in fabric pore inclination with load rather than through simple extension of the yarn itself, (c) viscous effects are present for all except the very highest pressures, (d) rarefaction effects appear at altitudes above about 60,000', (e) the most satisfactory model for explaining the results appears to be one likening the flow to that between two noninteracting cylinders, and (f) as long as the fabric retains its elasticity and does not take a permanent set, temperature changes affect the permeability only insofar as the air density is changed. Some of these findings have not as yet been described quantitatively; for this reason, a satisfactory prediction procedure is not yet available.

PUBLICATION REVIEW

This report has been reviewed and is approved.

FOR THE COMMANDER:

C. A. WILLIS, Chief
Fibrous Materials Branch
Nonmetallic Materials Laboratory
Directorate of Materials and Processes

TABLE OF CONTENTS

		Page
I.	INTRODUCTION	1
II.	REVIEW OF PREVIOUS WORK	3
III.	GENERALIZED ANALYSIS OF FLOW THROUGH CLOTH	16
IV.	EXPERIMENTAL APPARATUS	27
V.	EFFECT OF APPARATUS GEOMETRY ON PERMEABILITY MEASUREMENTS	35
VI.	EXPERIMENTAL PROCEDURE AND HANDLING OF DATA	39
VII.	DISCUSSION OF RESULTS	42
VIII.	CONCLUSIONS	49
IX.	REFERENCES	52
	APPENDIX I - AN EXTENDED THEORY OF GAS FLOW RATE THROUGH A NOZZLE	54

LIST OF FIGURES

Figure		Page
A1	Discharge Characteristics Of Venturi Meter. . . .	76
A2	Agreement Of Empirical Formulae $C_d \frac{1}{1+\frac{B}{\sqrt{R_e}}}$, $C_d \geq 0.65$; $C_d = \frac{\sqrt{R_e}}{2.86\,B}$; $C_d \leq 0.65$ With Values Given In The Literature.	77
A3	Viscous Flow Characteristics Through Three Geometries-Incompressible Flow.	78
1(a)	Nozzle Discharge Characteristics, Nitrogen At 300°K, d = 1.147 cm.	79
1(b)	Nozzle Discharge Characteristics, Nitrogen At 300°K, d = 0.0115 cm.	80
2(a)	Orifice Discharge Characteristics, Nitrogen At 300°K, d = 1.147 cm.	81
2(b)	Orifice Discharge Characteristics, Nitrogen At 300°K, d = 0.0115 cm.	82
3	Screen Discharge Characteristics, Nitrogen At 300°K.	83
4	Maximum Solidity Possible For Supersonic Approach Velocity.	84
5	Low Pressure High Temperature Permeability Apparatus.	85
6	Apparatus Details	86
7	Apparatus Details	86
8	Sample Holder (Shown With Stainless Steel Fabric) Diameter 3.5".	87

List of Figures (contd.)

Figure		Page
9	Estimated Characteristics Of Test Sections. . . .	88
9a	Estimated Characteristics Of Test Sections. . . .	89
10	Permeability Of Experimental Stainless Steel Fabrics, Sample Area = 15.5 cm^2.	90
11	Permeability Of Experimental Stainless Steel Fabrics, Sample Area = 15.5 cm^2.	91
12	Permeability Of Experimental Stainless Steel Fabrics, Sample Area $\approx$ 0.203 cm^2.	92
13	Permeability Of Mil-C-7350B Type I Fabric, Sample Area = 15.5 cm^2.	93
14	Permeability Of High Temperature Organic Fiber Woven According To Mil-C-7350B Type I, Sample Area = 15.5 cm^2.	94
15	Permeability Of HT-1 Woven According To Mil-C-7350B Type I, Sample Area = 15.5 cm^2. . .	95
16	Permeability Of Mil-C-8021B Type II Fabric, Sample Area = 15.5 cm^2.	96
17	Permeability Of Mil-C-8021B Type II Fabric, Sample Area = 31.7 cm^2.	97
18	Permeability Of Mil-C-8021B Type II Fabric, Sample Area $\approx$ 0.203 cm^2.	98
19	Permeability Of Mil-F-9084A Type VIII Fabric, Sample Area = 15.5 cm^2.	99
20	Permeability Of Mil-F-9084A Type VIII Fabric, Sample Area = 31.7 cm^2.	100
21	Permeability Of Experimental Stainless Steel Fabric, Sample Area = 15.5 cm^2.	101
22	Permeability Of Mil-C-7350B Type I Fabric, Sample Area = 15.5 cm^2.	102

Figure		Page
23	Permeability Of High Temperature Organic Fiber Woven According To Mil-C-7350 Type I, Sample Area = 15.5 cm^2.	103
24	Permeability Of Mil-C-8021B Type II Fabric, Sample Area = 15.5 cm^2.	104
25	Permeability Of Mil-C-8021B Type II Fabric, Sample Area = 31.7 cm^2.	105
26	Permeability Of Mil-F-9084A Type VIII Fabric, Sample Area = 15.5 cm^2.	106
27	Permeability Of Mil-F-9084A Type VIII Fabric, Sample Area = 31.7 cm^2.	107
28	Comparison Of Results Of Several Investigations Of Permeability Of Mil-C-7350B Type I Fabric. . .	108
29	Comparison Of Results For Test At Several Altitudes Mil-C-7350B Type I.	109
30	Comparison Of Results Of Several Investigations Of Permeability Of Mil-C-8021B Type II Fabric. . .	110
31	Comparison Of Results Of Several Investigations Of Permeability Of Mil-C-8021B Type II Fabric. . .	111
32	Mil-C-8021B Type II Fabric After Tests During Which Airflow Temperature Exceeded Melting Temperature Of Material, Diameter Of Melted Section Is About 1".	112
33	HT-1 Fabric After Tests During Which Airflow Temperature Exceeded Melting Temperature Of Material.	113
34	Effect Of Temperature On Permeability Of Mil-C-8021B Type II, $\dot{m}$ = 0.113 gm/sec.	114
35	Effect Of Temperature On Permeability Of Mil-C-8021B Type II, $\dot{m}$ = 1 gm/sec.	115
36	Effect Of Temperature On Permeability Of Mil-C-8021B Type II, $\dot{m}$ = 2.35 gm/sec.	116

Figure		Page
37	Effect Of Temperature On Permeability Of Mil-C-8021B Type II, $\dot{m}$ = 7.5 gm/sec.	117
38	Effect Of Temperature On Permeability Of HT-1 Fabric, $\dot{m}$ = .95 gm/sec.	118
39	Effect Of Temperature On Permeability Of HT-1 Fabric, $\dot{m}$ = 2.5 gm/sec.	119
40	Effect Of Temperature On Permeability Of Mil-F-9084 Type VIII, P_2 = 46 mm Hg.	120
41	Effect Of Temperature On Permeability Of Glass 9084 Type VIII, $\dot{m}$ = 1.0 gm/sec.	121
42	Effect Of Temperature On Permeability Of Stainless Steel Fabric, $\dot{m}$ = 1 gm/sec.	122
43	Effect Of Temperature On Permeability Of Stainless Steel Fabric, $\dot{m}$ = 2.5 gm/sec.	123
44	Effect Of Temperature On Permeability Of Stainless Steel Fabric, $\dot{m}$ = 11.8 gm/sec.	124

LIST OF SYMBOLS

A	sample area
A_2	throat area
A_f	open area
A_f'/A_f	open area increase due to load
A_θ/A_f	defined by Eq. (15)
B	empirical nozzle constant
C_D	drag coefficient
C_d	discharge coefficient
D	sample diameter
d	nozzle or orifice throat diameter
d_{eff}	effective pore diameter of cloth
d'	screen wire diameter
G	gain function
$g(P_2/P_1)$	$\frac{P_1}{\sqrt{T_s}} \sqrt{(P_2/P_1)^{2/\gamma} \left(1 - \left[P_2/P_1\right]^{\frac{\gamma - 1}{\gamma}}\right)}$
h	deflection of cloth sample due to air load
K_1, K_2	numerical constants Eq. (25)
ℓ	cylinder length
M	Mach number
$\dot{m}$	mass flow
$\dot{m}_i$	inviscid mass flow
P_1	upstream pressure
P_2	downstream

List of Symbols (contd.)

ΔP	pressure drop across sample
q	dynamic pressure, $1/2\,\rho U^2$
R	nozzle inlet radius
$\mathcal{R}$	gas constant
r	thread radius
R_e	Reynolds number
R_{e_d}	Reynolds number based on diameter
s	solidity or ratio of blocked area to total area
T_s	stagnation temperature
T_1	upstream temperature
u	velocity
w	projected spacing between threads
x	exponent in Eq. (22); also linear dimension in nozzle
y	expansion factor
δ^*	boundary layer displacement thickness
ρ	density
γ	ratio of specific heats
μ	dynamic viscosity
θ	inclination of pore
ν	kinematic viscosity
λ	molecular mean free path length

I. INTRODUCTION

The permeability to gas flow is one of the physical properties of cloth of most interest to parachute designers because of the relation which it has to the inflation ability, stability, drag, and opening shock of the parachute. Permeability measurements on parachute fabrics have been made for many years but the realization that the permeability will change with pressure ratio as well as with ΔP is of fairly recent origin. Since the flow mechanisms through cloth are still relatively poorly understood, despite intensive efforts to obtain analytical representations for them, they must still be investigated experimentally. This involves the use of vacuum facilities of considerable capacity and is therefore both expensive and time consuming. Hence, it was the intent of the present work to

(a) extend the range of pressures over which accurate measurements of permeability on selected fabrics have been made, and

(b) study the results of these and other tests in an effort to describe at least the laws by which measurements at a single downstream pressure (atmospheric) can be converted to those at any other downstream pressure.

Results of previous studies had indicated that the region of chief interest was that for which $\Delta P < 190$ mm Hg.

Manuscript released May 1961 for publication as an ASD Technical Report.

Since changes in temperature affect the density and viscosity of the air flow and may affect the elastic properties of the cloth, an additional object of the present program was to measure for the first time the effects of high gas temperature on permeability at various simulated altitudes. It was desired also that any effects of temperature found in this investigation be included in the expressions for converting results at one altitude to those at another.

The materials investigated were:

(a) Nylon Fabric, Mil-C-7350, Type I

(b) Nylon Fabric, Mil-C-8021, Type II

(c) Glass Fabric, Mil-F-9084, Type VIII

(d) An experimental organic fiber (HT - 1) woven to meet the requirements of Mil-C-7350, Type I

(e) A high porosity stainless steel fabric. The fabric is constructed from wire 0.0014" in diameter and is a broadcloth with approximately 220 wires per inch in both warp and fill. The solidity is approximately 52%.

The term permeability as used herein refers generally to the mass flow which will pass through a unit area of the material. This differs somewhat from the more common usage in which permeability refers to the number of standard cubic feet per minute which will pass through a square foot of the material. The conversion from one to the other, however, involves only multiplication or division by the actual gas density.

II. REVIEW OF PREVIOUS WORK

Although screens and cloth are similar in many respects from an aerodynamic viewpoint, they appear to have been treated quite differently in the literature on gas flow through porous media. For example, the screen data is frequently presented as the variation of $\Delta P/q$ with approach Reynolds number or Mach number, while the cloth data is most often reported in terms of the variation of the volume rate of flow through a unit area with pressure drop (ΔP). Possibly this difference in presentation was a result of the end use of the data, that on screens having been used primarily by wind tunnel designers and others to calculate the power losses resulting from the use of screens to improve velocity profiles. That on cloth was used primarily by parachute designers to correlate the performance of parachutes. Nevertheless, the aerodynamic similarities present should permit the use of screen data in the study of the mechanisms of flow through cloth. Screen data have the advantage that the geometrical configuration involved is better defined and less subject to change with air load than is that of cloth. Consequently, screens can be analyzed more readily than cloth. In spite of this, however, Cornell (Ref. 1) concluded that losses through screens were best determined empirically.

A. FLOW THROUGH PERFORATED PLATES

In an effort to reduce number of factors influencing the results and thus to render the problem more tractable theoretically, Cornell considered the flow through closely spaced holes in a thin plate. With this configuration, the losses in formation of the jets which issue from the holes and those in the plate are negligible if the flow velocities and/or densities are high enough so that the Reynolds number based on local conditions in the holes exceeds 10^3. The entire loss can therefore be assumed to take place downstream of the plate as a result of mixing of the jets and wakes. This is a problem which has been studied to some extent and fairly reliable theoretical solutions are known. Following earlier treatments, Cornell expressed the pressure drop across the plate in incompressible flow as

$$\frac{\Delta P}{q} = \left[\frac{1-\phi(1-S)}{\phi(1-S)}\right]^2 \qquad (1)$$

where ϕ is the contraction ratio of the jet leaving the orifice and s is the ratio of the blocked area to the total area of the plate. They used the value of $\phi(s)$ calculated by von Mises in 1917 which was confirmed by later experiment on large, single orifices. For plates with large holes and/or low solidity this equation appears to give satisfactory results. It may be converted to a form more familiar to parachute designers as follows:

$$\frac{\dot{m}}{A} = \left[\frac{\phi(1-S)}{1-\phi(1-S)}\right]\sqrt{\frac{2\Delta P(P_2+\Delta P)}{\mathcal{R}T_1}} \qquad (2)$$

Some study of the problem will reveal that no matter what the loss mechanism downstream of the plate – whether P_1 is fully recovered, whether all the dynamic head is lost, or whether some condition in between actually occurs — the form of Eq. (2) remains the same. Only the term in brackets will change. As long as the flow is incompressible it depends only on the plate geometry. To illustrate this point, it is rather easy to show that if one assumes that all the dynamic head is lost, i.e., that the pressure far downstream of the plate is the same as the minimum pressure in the jets, then Eq. (2) would be written

$$\frac{\dot{m}}{A} = \frac{\phi(1-S)}{\sqrt{1-\phi^2(1-S)^2}}\sqrt{\frac{2\Delta P(P_2+\Delta P)}{\mathcal{R}T_1}} \qquad (2a)$$

So that the conditions under which Eq. (1) was derived are not violated, one must restrict its application to cases where P_2 is large and ΔP small. For these conditions, Eq. (2) could be written

$$\frac{\dot{m}}{A} = \left[\frac{\phi(1-S)}{1-\phi(1-S)}\right]\sqrt{\frac{2P_2\Delta P}{\mathcal{R}T_1}} \qquad (3)$$

Cornell attempted to extend the range of applicability of Eq. (1) by including compressibility effects on the left hand side of the equation and using empirically determined values for $\phi(s)$. These were for $P_2/P_1 > 0.528$, however. The agreement which Morgan (Ref. 2)

obtained between this revised equation and his experimental results was increasingly poor for $P_2/P_1 < 0.8$. Cornell's relation seemed to consistently underestimate the pressure drop, indicating possibly that more of the dynamic head was being lost (probably through shock waves) than for $P_2/P_1 \longrightarrow 1.0$ or that $\phi(s)$ at the pressure ratios involved was different than assumed. Despite this lack of agreement it seems clear from fundamental considerations that one can always represent the mass flow through porous plates at high Reynolds numbers by the functional form

$$\frac{\dot{m}}{A} = f(s, P_2/P_1)\, g(P_2/P_1) \tag{4}$$

where $g(P_2/P_1)$ is the familiar isentropic nozzle flow function. Whether one can arrive at a satisfactory prediction for $f(s, P_2/P_1)$, however, is another matter. In order to do this conveniently, one must be able to develop an expression for the mixing losses which is simultaneously valid for all of the following cases:

(1) Wherein the individual jets are perturbed primarily by wakes such as occurs when the solidity is less than about 0.4 (Ref. 3).

(2) Wherein the individual jets — because of relatively large distance between them, as for example, in a plate with high solidity — react rather violently upon contact.

(3) A situation between cases (1) and (2).

(4) Wherein the pressure ratio across the plate is high enough to produce expansion and acceleration of the jets (see Appendix I for an elaboration of this point).

(5) Wherein the jet flow may be assumed to be incompressible This is obviously a difficult task, one which has as yet not been completed successfully. One could, perhaps, attempt to split the task into parts, i.e., develop expressions valid only for given regions of P_2/P_1 and s, but this then leads to problems in determining the applicability of the results and fairing between regions of applicability. At the present, therefore, one must conclude that while exact values are available for certain special cases of $f(s, P_2/P_1)$ and the qualitative behavior is understood in general, no general quantitative description is within sight. Thus, one could not be expected to predict accurately the mass flow through an arbitrary perforated plate for any arbitrary ΔP and P_2 even if the results are known to be insensitive to changes in Reynolds number. Similarly, it is virtually impossible to predict the geometric solidity of a plate from experimental data except for isolated cases.

B. FLOW THROUGH ROUND WIRE SCREENS

In reviewing earlier work on incompressible flow through screens, Cornell found that the semi-empirical equation proposed by Wieghardt

$$\frac{\Delta P}{q} = \frac{6S}{Re^{1/3}(1-S)^2} \quad \text{for } 60 < R_e < 1000 \tag{5}$$

and that proposed by MacDougall

$$\frac{\Delta P}{q} = \frac{33.93}{Re} \frac{S(1-S)^{-1.27}}{1+(1-S)^{.5}} \quad \text{for } .006 < R_e < 20, \tag{6}$$

where

$$Re = \frac{U, d'}{\nu (1-S)} \tag{7}$$

and d' is the wire diameter, agreed well with his own results and that of others. For $1000 < R_e < 17,000$, Cornell found that the results were for practical purposes independent of Reynolds number.

Apparently the initial form of these results were obtained by considering the screen to be made up of a number of independent circular cylinders and converting empirical $C_D \sim R_e$ data to a suitable form. Since

$$D \approx \Delta P A, \tag{8}$$

$$C_D \approx \frac{\Delta P}{q} \tag{9}$$

On this basis, one would assume that

$$\frac{\Delta P}{q} \sim \frac{1}{R_{ed}{}^{0.75}} \quad \text{for } R_e < 2 \tag{10}$$

$$\frac{\Delta P}{q} \sim \frac{1}{R_{ed}{}^{0.25}} \quad \text{for } 10 < R_{ed} < 1000 \tag{11}$$

$$\frac{\Delta P}{q} = \text{constant} \qquad \text{for } 10^3 < R_{e_d} < 2 \times 10^5 \qquad (12)$$

Little or no data is available to indicate the behavior of C_D when $M > 0.4$ and $R_{e_d} < 10^5$. One would speculate, however, that a Reynolds number effect, superimposed on the usual Mach number effects is to be expected. A more quantitative analysis of screen flow based on this approach is given in Appendix I.

Study of Eqs. (5) and (6) reveals that they can be written in the form

$$\frac{\dot{m}}{A} = h(s, P_2/P_1, R_e)\, g(P_2/P_1) \qquad (13)$$

The losses which occur upstream of and in the screen can be included in the dependence on Reynolds number. (This question is discussed at some length in Appendix I.) Thus, the form is basically the same as for Eq. (4) except for the inclusion of the Reynolds number dependence.

C. FLOW THROUGH CLOTH

With this background, one can proceed somewhat more knowledgably to review the efforts made to predict the flow through cloth. During the discussion which follows it should be remembered that compared with screens or perforated plates, most cloth samples are

quite elastic and have a relatively high solidity. The high solidity usually leads to complete loss of the dynamic head while the elasticity leads to changes in effective solidity with ΔP.

Lavier (Ref. 4) after studying earlier work on the flow of air through cloth and results of his own experiments concluded that:

(a) For very low pressure differentials (i.e., < 50 in.H_2O) across the cloth, the flow "is like that of viscous flow through a porous medium". [Study of works on this subject, for example Ref. 5, shows that for such cases $\dot{m}/A \sim \Delta P$. A similar result is observed in Eq. (6)].

(b) For higher pressure differentials, "the air flow through the cloth may be like the air flow through a screen or grid". Presumably, the dependence of the mass flow through the cloth on Reynolds number is different than in (a).

(c) For still higher pressure differences, "compressibility effects will be experienced", as well as elastic effects.

(d) Specification of the proper characteristic length presents the chief problem in obtaining a better description of the viscous effects.

Lavier also reviewed efforts to apply the theory of Green and Duez (Ref. 6) to the flow through cloth. In this theory, it is assumed that the flow is incompressible and isothermal and that the pressure drop across the cloth can be represented as a linear sum of a viscous term (for which the pressure drop is linearly proportional to flow

velocity) and an inviscid term (for which the pressure drop is proportional to the square of the velocity); the coefficients are left undetermined to be evaluated from experimental data and are presumably functions of the geometry only. He found that, generally, for $\Delta P > 50$ in.H_2O, the theory predicted increasingly less mass flow (compared with the measured values) with increasing pressure drops for both parachute cloth and 100 mesh screen; he was, therefore, unable to determine constant values for the coefficients. He attributed this to disappearance of the viscous effects more rapidly than predicted by the theory.

In a later report, Lavier and Boteler (Ref. 7) concluded that the flow through cloth for large pressure ratios across the cloth should be treated by a compressible theory; however, in calculating an effective discharge coefficient, i.e., the ratio of the actual mass flow to that predicted by theory, they employed incompressible theory and based their Reynolds number on the conditions in front of the fabric.

The MIT group which examined these results, concluded (Ref. 8) that such assumptions are tantamount to assuming that the flow through the cloth is similar to the flow through an orifice (presumably in incompressible flow). This, they suggest, is incorrect; rather, the flow can be represented more satisfactorily and more correctly by assuming it analogous to flow in an isentropic nozzle. They attribute the pressure drop experienced across the cloth entirely to mixing losses downstream of the fabric. Implicit in their approach, although not expressed, is the

assumption that all the velocity head is lost in the mixing process. They apparently felt that although the specification of effective open area was still a procedure of uncertain results, a method whereby measured permeabilities could be extrapolated to other values of P_2 would be very useful in reducing the number of tests required to describe the permeability completely. By this device, the elastic effects need not be known explicitly, and the problem is reduced to describing the aerodynamic behavior of the cloth for a constant geometry.

The scaling relations which they developed are based on the variation in mass flow through an isentropic nozzle. If the elastic properties are functions of ΔP alone, then according to this analogy, the permeability at one P_2 and ΔP may be transformed to that at another P_2 by multiplying by the appropriate ratio of $g_2(P_2/P_1)/g_1(P_2/P_1)$ for the same ΔP. They suggest that isentropic theory is valid for $\Delta P > 100$ in. H_2O.

The agreement with experiment achieved by these scaling relations is only fair. In particular, the slopes of the individual curves appear to be different from those given by theory although the magnitudes of the higher altitude data have about the predicted relation to the sea level results in most cases. It would seem, therefore, that while this approach may offer a coarse means of extrapolating sea level data to higher altitudes, it is not sufficiently inclusive or it does not employ a sufficiently correct model to permit accurate calculation.

D. SPECIFICATION OF THE EFFECTIVE OPEN AREA

The most complete study to date of means for specifying the effective open area seems to have been given in Ref. 9. In this work they define the discharge coefficient by

$$C_d = \frac{\dot{m}}{A_f\left(\frac{A_\theta}{A_f}\right)\left(\frac{A_f'}{A_f}\right)\sqrt{\frac{2P_1\,\Delta P}{RT_1}}} \tag{14}$$

where

A_f = the open area when $\Delta P = 0$ as determined from light penetrability measurements

$\frac{A_\theta}{A_f}$ = the ratio of the actual open area which is inclined to the plane of the cloth to the projected open area, i.e., the open area as seen from light penetrability tests

$$= \left(1 + \frac{2r}{w}\right)\left[\frac{1}{2\cos\theta} + \frac{1}{4\tan\theta}\,\ln\left(\frac{1+\sin\theta}{1-\sin\theta}\right)\right] - \frac{2r}{w} \tag{15}$$

r = the thread radius

w = the projected spacing between threads

θ = the inclination relative to the plane of the cloth of the line between thread centers, i.e., pore inclination

$\frac{A_f'}{A_f}$ = the open area increase due to air load

The pore Reynolds number is defined by

$$R_e = \frac{V}{\nu}\left[\frac{w(1+\sec\theta) + 2r(\sec\theta - 1)}{2}\right] \tag{16}$$

θ is determined from the empirical relation

$$\theta = \tan^{-1} \frac{0.136 \sqrt{\text{percent crimp in filling yarn}}}{\text{warp threads per inch} \times \text{spacing of fill threads (in./thread)}} \quad (17)$$

r is determined by measurement or from experimental relations between yarn diameter and twist. w is then determined from the relation between yarn diameter and threads per inch. The change in open area due to air load was found from measurement of linear extension and light penetrability. These data indicate that

$$\frac{A_f'}{A_f} \approx 1 + 0.2 \quad \Delta P^{0.2} \quad (18)$$

for the fabrics tested.

Assuming these relationships to be correct, it was found that

$$C_{d_\theta} = C_{d_{\theta=0}} - 0.0041\,\theta \quad (19)$$

(θ in degrees)

$$C_{d_{\theta=0}} = 0.565\, R_e^{0.1} \quad (20)$$

for $100 \leq R_e \leq 300$

Good agreement with experiment was obtained for a number of different fabrics for $\Delta P \leq 30"H_2O$ and $P_2 = 406"H_2O$. Similar correlation for data with $\Delta P > 30"H_2O$ was not attempted.

Several interesting conclusions can be drawn from this work:

1. From the measurements of linear extension of the cloth fibers under load it seems apparent that the change in total surface area (and thus, the change in pore size related to the

change in area) is small, being between 7 and 11 percent for the fabrics of interest in the current study at $\Delta P = 680$ mm.

2. The change in light penetrability with load, on the other hand, is much larger [see Eq. (18), for example] indicating that changes in θ resulting from air load are the principal reasons for changes in the effective open area. This would appear to be an area for fruitful analytical work since the momentum transport and thus the load (ΔP) on the cloth for a given mass flow depend on the changes in direction which the flow must make in traversing the cloth. It is interesting also, that the light penetrability measurements reported by Klein, et al, appear to correlate well with the measurements of θ as a function of ΔP reported in Ref. 8.

3. The Reynolds number effect shown by Eq. (20) seems to be confined to too small a range to permit attaching much credence to it. Generally, one would expect that the Reynolds number dependance would be at least as strong as that for turbulent pipe flow, i.e., $R_e^{0.25}$ to R_e^o as R_e increases.

In the next section, an attempt is made to combine the significant features of the various analyses and experimental results cited above to obtain a more general semi-empirical description of gas flow through cloth.

III. GENERALIZED ANALYSIS OF FLOW THROUGH CLOTH

It is evident from the foregoing that a prediction of the flow through a given sample must be based on rather complete measurements of the construction of the cloth and its variation with load. It is not the purpose of this section to deal explicitly with this portion of the problem, however, and thus, no general prediction procedure can result. What is sought is a method whereby experimental results on a group of fabrics can be correlated to determine the influence of air density. If this is successful, then the technique can be used with fair assurance of success to predict the change in permeability with altitude for a variety of fabrics from their sea level permeability measurements. To do this, it is necessary to know the effect of elasticity on the permeability or to determine the viscous effects independently. Subsection A is a study of the latter. Since success in this endeavor would obviate the need for detailed study of the elastic effects, the analysis of these effects — described in Subsections B and C — sought qualitative results only. It should be pointed out in this connection that even a completely successful description of the effects of elasticity on permeability by itself would not permit attainment of the objectives of the program, except in a wholly empirical fashion. A satisfactory physical description of the flow phenomena is still required to obtain an analytical expression valid over the entire range of interest.

A. EFFECTS OF VISCOSITY

Following the approach used by the MIT group, initial efforts of the present study centered on obtaining a satisfactory description of the mass transfer characteristics of a nozzle when viscous effects are important. It was soon found that nothing short of a numerical solution of the general equations of motion would yield analytical results in which much confidence could be placed. Since the proper boundary conditions for the flow through cloth are at best poorly known, the correspondence of a solution of the nozzle flow equations to the flow through cloth may not be good. The very large effort required to obtain numerical solutions was therefore not justified. As a result, the effort was made to describe nozzle flow in a relatively simple, semi-empirical fashion. The details of this analysis are given in Appendix A and the results shown in Figs. A1, A2 and A3. Basically, this procedure uses one-dimensional flow theory modified by a discharge coefficient. It was found that as long as the Knudsen number of the throat is less than 0.01, and the entrance radius is greater than 0.25 times the throat diameter, the discharge coefficient can be expressed as a function of Reynolds number which contains only one empirical constant; further, fairly crude theoretical estimates of this constant for a particular geometry indicate good agreement with experiment, particularly for $R_{e_d} > 500$. By writing the Reynolds number in the form

$$R_{e_d} = \frac{\dot{m}}{\pi/4\, d\mu} \tag{21}$$

where d is the nozzle throat diameter one may then find an explicit expression for the mass flow in terms of P_1, P_2, T_s, A_2, A_1/A_2, μ, and the empirical constant B. This equation is graphed in Figs. 1(a) and 1(b) for two values of d and B = 4.0. The effects of viscosity are evident from a comparison of the curves for the two diameters.

To obtain some feeling for the change in appearance of the $\dot{m}$ vs. ΔP curves resulting from a change in the flow model, similar curves were computed for a sharp-edged orifice and for an idealized screen. These are shown in Figs. 2(a), 2(b) and 3. The curves for an orifice were computed assuming that the viscous and inviscid effects could be treated separately as indicated by the data discussed in Appendix I. The curves for the screen were computed from published values of C_D vs. M and C_D vs. R_e for a cylinder according to Eq. (A26). It is evident upon examination that there is considerable difference in the magnitudes and slopes of the curves for the three models, particularly at the lower densities and flow velocities. Thus, unless some single model can be shown to represent flow through cloth it is not possible to determine the viscous effects independently of the elastic effects. Unfortunately, data available in the literature at this time is either too limited in range, contains effects of the test setup geometry (see Section V), or does not provide corresponding results on A_f'/A_f vs. ΔP to allow one to assign a definite model.

It will be noted, however, that for small ranges of ΔP and T_s all the curves can be represented by the relation

$$\dot{m} = G \left(\frac{300}{T_s}\right)^{\frac{1}{2}} \Delta P^x \qquad (22)$$

where G is a constant which depends on geometry and P_2, and x is a constant whose value lies between 0.5 and 1.5.* For inviscid flow x is 0.5 when ΔP is small. When $P_2/P_1 < 0.528$, x increases toward 1.0. For fully developed viscous flow, 0.5 is added to the inviscid result. As the Reynolds number increases, something less than 0.5 is added to the inviscid result.

Eq. (22) being consistent with Eq. (13), has therefore, quite general validity if G is also allowed to vary with changes in loss mechanism. It will be seen that Eq. (22) can be used to represent flow through cloth as well if x is also made to include elastic effects. The change which temperature variations produce in the viscous and elastic characteristics can also be accommodated by changes in x. Thus, it would appear that the permeability characteristics of a particular cloth sample can be represented quite adequately by evaluating G as a function of pressure ratio and x as a function of $\dot{m}/A$, P_2/P_1, and T_s. While these functions

* The observation that Eq. (22) can be fit, using constant values of x, to all low ΔP permeability data seems to have been made first in Ref. 10. Apparently, subsequent investigators make no mention of it.

must, for the present, be empirical they provide a common basis for comparison of various fabrics which is more indicative of the significant aerodynamic parameters than representations used heretofore.

Despite the handicaps imposed by such a semi-empirical analysis, it is, nevertheless, possible to arrive at some conclusions regarding the significance of experimental data:

(1) x can be less than 0.5 only if the discharge coefficient decreases with increasing Reynolds number. This can occur over small ranges of R_e for which there is flow separation from the surface such as through orifice plates. This would not be expected for a round wire screen of fairly close mesh and for cloth; therefore, any experimental data evidencing such a trend should be regarded with extreme suspicion.

(2) If x is greater than 1.5, significant elastic effects are present.

(3) If both viscous and elastic effects are present, it is extremely difficult to deduce their individual contributions to x.

Some elaboration of this last point is in order. Presumably, the elastic properties at a given ΔP and T_s are independent of P_2; thus, it should be possible to find the variation in x with $\dot{m}/A$ at constant ΔP if some assumptions regarding G can be made. It is necessary to assume that the effective open area remains constant, and that the variation in G with P_2 is directly related to that for an isentropic nozzle,

i.e., there is no change in loss mechanism with P_2. This procedure permits one to determine the change in the viscous contribution to x_b with P_2, but does not allow one to find the absolute value of this contribution to x at any P_2. At some larger ΔP, the effective fabric pore size increases. In order to determine the change in x due to elastic effects, it is necessary to hold the Reynolds number constant. To do this, however, it is necessary to hold the ratio of $\dot{m}/A$ to the effective pore diameter constant. This is obviously not possible so that the best one can do is to maintain $\dot{m}/A$ constant as ΔP is increased and hope that the change in d_{eff} is not sufficient to produce marked changes in the viscous effects or loss mechanism. If this is true, then the elastic contribution to x should be the same at all $\dot{m}/A$. By iterating back and forth until a consistent set of values is obtained one can probably arrive at a reasonably good picture of the combined effects of fabric elasticity and flow losses, provided the assumptions in regard to loss mechanisms are justified. It is evident, however, that this entire process is time consuming and because of data scatter and lack of knowledge of constancy of the loss mechanisms, may be of limited accuracy. The results should, nevertheless, be valuable in making qualitative comparisons between various fabrics and establishing trends with altitude, load and temperature.

In an effort to remove some of the uncertainty from the aforementioned procedure, an attempt was made to find an analytical, if somewhat idealized, description for the change in pore dimension with load and its effect on mass flow. While a complete description of the change in pore size with load, rate of load, load history, etc., would be extremely complex and difficult to use even if it could be found, an analysis assuming the material to be perfectly elastic probably accounts for most of the change. Such an analysis can be divided into two parts for simplicity.

B. CHANGE IN SAMPLE OPEN AREA DUE TO SAMPLE DEFLECTION WITH LOAD

If one assumes that the test sample deflects under load to form a portion of a sphere, then the total surface area is

$$A = \pi\left(h^2 + \frac{D^2}{4}\right) \qquad (23)$$

where h is the deflection. If the area closed to air flow remains essentially constant for reasonable values of h and the deflection due to load is analogous to that of a thin membrane, then

$$h \sim \Delta P^{1/3} \qquad (24)$$

$$A_{open} = K_1 + K_2\ \Delta P^{2/3} \qquad (25)$$

and

$$Z = 1 + C\ \Delta P^{2/3} \tag{26}$$

Z is the ratio of strained to unstrained fiber length. Examination of the data in Ref. 8 shows that this prediction for Z is quite accurate and thus, one would expect Eq. (25) to represent closely the change in open area resulting from linear extension of the threads. Since C has a value on the order of 10^{-3}, according to the MIT measurements, $K_2/K_1 \sim 10^3$ which means that ΔP must be quite large ($\sim$ 1000) to produce changes in area of 10%. For most practical purposes, then, one may neglect this effect.

C. CHANGE IN EFFECTIVE OPEN AREA DUE TO ROTATION OF THREADS WITH LOAD

In the unstrained condition with the actual pore making some angle θ with the normal to the cloth, the flow must turn θ^o on the average before entering the pore. Such a turn will cause a pressure drop in the flow so that the force driving the air through the cloth is not ΔP but rather some smaller force. Assuming that this drop in driving force does not depend upon Reynolds number and that the approach velocity is always relatively small, it appears from the hydraulic literature that the drop in effective P_1 may be written

$$\Delta P_1 = \Delta P\ f(s)\ \sin\theta \tag{27}$$

Inspection of data in Ref. 8 indicates that for moderate values of ΔP

$$\sin \theta \sim \frac{1}{\Delta P^{y}} \tag{28}$$

where y is 0.2 to 0.5 or so. Thus, on the average,

$$\Delta P_1 \approx f_1(s)\, \Delta P^{.7} \tag{29}$$

The effective change in open areas may therefore be written

$$\frac{A_f'}{A_f} = \left[\frac{1}{1 + f_1(s)\, \Delta P^{-.3}}\right]^{x} \approx f_2(s)\, \Delta P^{0.3x} \tag{30}$$

When $x = 0.5$, $A_f'/A_f \sim \Delta P^{0.15}$ which agrees fairly well with the trends shown by Eq. (18). It would be expected that the losses represented by Eq. (30) will be the only additional effect of pore inclination since it appears that whatever dynamic head exists in the flow issuing from the pores is lost in mixing regardless of the pore inclination.

The analysis given above is, of course, of a very qualitative nature and not suitable for quantitative determinations. It serves to point out, however, that the major elastic effect in parachute cloth so far as permeability is concerned is the rotation of the pores under load. From measurements available of this rotation, it seems reasonable to conclude that the elastic contribution to x at low ΔP is 0.15 to 0.2 for P_1/P_2 near 1.0 and 0.2 to 0.5 for $P_1/P_2 > 4$. At larger ΔP the

elastic contribution approaches that given by Eq. (25). A more complete analysis of the effects of pore rotation was not possible because of limitations in the time available but it is an area where very fruitful efforts can be applied in the future. Once the effects of pore rotation are established quantitatively, it will be relatively simple matter to determine the viscous aspects of flow through parachute cloth.

D. EFFECTS OF LOW SOLIDITY ON FLOW CHARACTERISTICS

When the solidity of the fabric is less than 95%, the approach velocity will begin to be significant. This has the effect of shifting the critical pressure toward 1.0 as indicated in Fig. 3 and $\dot{m}/A$ will be higher for the same ΔP. The reduction in solidity also permits the character of the approach flow to change from incompressible to compressible. For supersonic approach velocities, the effect of adjacent filaments on the flow over any given filament or thread can be reduced. This happens when the flow between the threads is supersonic. The maximum solidity for which this is possible is shown in Fig. 4. Under these conditions the drag coefficient of the screen may be considerably less than with subsonic approach velocities, and the permeabilities considerably higher for the same P_1. Because the shock detachment distance is small, however, the pressure drop across the screen measured in the conventional fashion will be negative. For such

conditions the use of Eq. (22) is obviously not warranted. Thus, if the use of low solidity fabrics is contemplated in parachutes operating at high Mach numbers, an analysis not based on an analogy to nozzle flow must be developed to treat experimental data.

IV. EXPERIMENTAL APPARATUS

The test apparatus is shown in Figs. 5, 6, 7, and 8. The figures are for the most part self-explanatory. Some comments on the design philosophy and experience with the use of the equipment are perhaps in order to serve as food for thought for future investigators.

A. MASS FLOW METERING

Reference to the results will show that for these tests, mass flow varies over a range of 10^4. The tolerable error was on the order of 2% of actual indication over the entire range. Originally, it had been planned to use two venturi meters with throat diameters of approximately 0.45" and 0.9" for this purpose. Venturi meters were favored because

1. A very large range of mass flows can be covered accurately with a single instrument, provided the throat velocity remains high, i.e., the pressure drop is large enough to be read accurately.

2. Very little pressure drop must be accepted compared to an orifice meter. This is important when the maximum pressure of the system is limited.

3. The reduction of data is simpler than with an orifice meter because the flow characteristics are better understood.

As it developed, the larger venturi meter was abandoned because it could not be calibrated easily with the pumping capacity available and because the smaller meter would measure the maximum flow which the nitrogen supply would deliver without excessive manometer lengths. Considerable time and effort had to be expended in shaping the remaining venturi throat to produce pressure ratios in agreement with theory. This was necessary, however, to take advantage of the simplicity afforded by the theory. To avoid disturbing the flow, very small (.028") pressure source holes were needed. To keep the lag within reasonable bounds, a number (4) of these holes were drilled around the periphery. Because of very small drifts the axial locations of the holes during drilling the measured pressure at each hole was slightly different ($\pm$ 2%). By using only those taps which averaged nearest 0.528 P_1 for choked flow, it was possible to measure the choked flow value within the reading accuracy of the manometers.

A well-made venturi meter should require calibration only at low Reynolds numbers. This simplifies the calibration task considerably since the capacity of the calibrating meter or device need not be large. This assumption seems to be born out in the calibration results shown in Fig. A1. The scatter in the calibration at very low Reynolds number is undesirable, but since the device was not used at these conditions, it is not important to the data reduction.

During operation with fabrics under test, it was found that the mass flows and pressure levels were such that the venturi meter could not be used accurately for mass flows less than 0.5 gm/sec, except with the very porous stainless steel fabric. Accordingly, rotometers were used to measure $\dot{m}$ down to 0.01 gm/sec.

The rotometers were found to be within guaranteed accuracy only for supply pressures above atmospheric. With a supply pressure limit of 30 psig, each rotometer could therefore cover about a decade in mass flow. Thus, two rotometers were required to cover the range. The first covered the range from 0.011 gm/sec to 0.25 gm/sec. The second covered the range from 0.1 gm/sec to 2.4 gm/sec.

The rotometers were not calibrated further. The prediction charts supplied by the manufacturers were used to compute curves of indication vs. mass rate for a range of supply pressures and temperatures. During testing, efforts were made to operate on these curves. Individual rotometers are guaranteed by the manufacturer to be within 2% of these curves. This was considered acceptable.

Temperatures used in computing the mass flow were measured with a sensitive ASTM mercury bulb thermometer inserted into the stream.

B. PRESSURE MEASUREMENT

Because of the need for accuracy over a wide range, at least two instruments were required for each pressure except that upstream of the rotometer. This was measured with a single gauge having 0.1 psi divisions. The venturi meter employed a mercury U-tube with one side open to atmosphere (measured by a mercury barometer), a Wallace and Tiernan 6" dial gauge (0-100 mm, 1/2 mm divisions) accurate to $\pm$ 0.3 mm and a Todd Scientific McLeod gauge (0-.5 mm, 0 - 5 mm, 0 - 25 mm scales) to measure the upstream pressure. The differential pressure was measured by a mercury and a silicone oil (Dow Corning DC-200, sp.gr. = .97) manometer. The silicone oil has a very low vapor pressure but is hygroscopic; frequent cleaning of manometer oil from the pressure lines was necessary because of violent outgassing which occurred whenever the system was exposed to atmosphere for any length of time. As a result, the system was later kept under vacuum at all times except during model changes and repairs.

The test sample pressures were measured in a similar fashion. Provisions were made on both panels for sealing off the McLeod gauges and the dial gauges for tests when their ranges were exceeded. This proved necessary inspite of other possible arrangements when the dial gauges were damaged during leak checking, and mercury from the McLeod gauge was blown into the small vacuum pump. A trap was later provided for this pump.

The manometer valving arrangement was developed when other simpler techniques could not be operated with sufficient rapidity or reliability to prevent the oil manometers from blowing over. The valves are ordinary bronze steam cocks. They proved to require constant attention to keep them reasonably leak free, however. Lower pressure tests will obviously require a completely different type.

Originally, neoprene rubber tubing was used for the pressure lines, but this proved too susceptible to small leaks and degassing and it was replaced by copper where practical.

Even with these precautions, it developed that small pressure differentials (< 2 mm), particularly at low P_2, were difficult to measure because of the relatively large volume of the measuring system and the small mass flow going through the sample. If tests are ever to be confined to the low ΔP, low P_2 regime, design changes are indicated.

It should be noted in passing that in designing the apparatus and associated instrumentation for this experiment, the effort was made to keep it as simple and, hopefully therefore, as reliable and inexpensive as possible. In research work, some changes are always necessary no matter how careful the initial design. It was felt, therefore, that the procedure adopted, while undoubtedly requiring more changes than a more elaborate system, was in the long run just as accurate and reliable and considerably less expensive.

C. TEST SECTION

As elaborated more fully in Section V, the test section was designed to test as large a sample as possible, to provide a more uniform velocity profile than a straight tube, and to keep the flow approximately normal to the cloth, i.e., prevent spreading downstream of the sample. Originally, a 2.5" test sample was used but because the mass flow did not fall off as rapidly with P_2 as had been expected, this area proved to be too large for the pumping capacity available at low P_2. Accordingly, a 1.75" diameter test section was constructed. This was used for most of the tests. For the very porous materials, however, even this proved too large to get large pressure drops and a 0.20" test section was constructed. To avoid excessive length in the recovery section downstream, a sudden expansion to 1.75" was accepted. This entailed the possibility of jet spreading and results different from those with the other sections. A thin rubber sheet was used to confine the open area to 0.20" diameter should the sample be blown away from the face of the upstream section.

These test sections were constructed from solid aluminum. For the hot tests, the test section was constructed of copper sheets in a manner which provided space for circulation of a coolant (water). Some cooling was necessary to protect the vacuum seals from the heat and to

protect the operator and other portions of the equipment. As discussed later, however, the heat transfer to wall was too large and a significant temperature gradient existed at high temperatures.

For tests below 750° F, an ASTM mercury bulb thermometer placed in the center of the flow upstream of the contraction was used for temperature measurement. For tests above this temperature, a copper-constantan thermocouple was used.

D. HEATER

The heater consisted of 48 coils of nichrome wire inside quartz tubes. These tubes, dimpled at the upstream end to prevent motion downstream, were held loosely in part baffles. This arrangement required almost all the flow to pass through the tubes. The walls of the flow channel were made of thin stainless steel insulated from the steel case by MgO. Changes in heat output were effected by changing the voltage on the coils.

The heater operation was generally satisfactory except for the long lag time at low mass flow. At mass flows less than 1 gm/sec, cool down time from 250° F was on the order of 2 hours. Since the heater was designed to meet the high power requirements associated with high temperatures and large mass flows, this lag is unavoidable. Broken tubes and wires resulted on occasion when the mass flow was changed suddenly during operation at very high temperatures.

E. COOLER

The cooler was a conventional, straight gas-tube type and functioned satisfactorily under all heat inputs with minimum pressure drop.

F. PUMP

The laboratory's 130 CFM vacuum pump was used for most of the tests. Near the end of the program, a larger 350 CFM pump was placed in service. The apparatus was modified to make use of this added capacity and a few of the later runs utilized both pumps.

V. EFFECT OF APPARATUS GEOMETRY ON PERMEABILITY MEASUREMENTS

When the apparatus for the present investigation was designed at the beginning of the program, the influence of the apparatus geometry on the test results was not fully appreciated. The object had been merely to provide a reasonably uniform approach velocity without excessive pressure drops and to maintain the flow normal to the cloth. After the calibration of the venturi meter, however, it became clear that the velocity distribution of the flow as it approaches the test sample determines the mass flow passed by the cloth for a given ΔP and P_2. This can be seen very readily from the following considerations. If one assumes that the test channel walls are parallel, then the pressure normal to the wall is constant across the channel. The velocity profile, however, may range from nearly uniform to fully parabolic. When a parabolic profile exists, most of the mass flow is concentrated near the center. Because the pressure drop across the cloth increases with increasing mass flow, the flow near the center will have a higher than average pressure drop. Since the drop must be the same across the entire cloth, the net effect is that for a parabolic profile the pressure drop will be higher than for a uniform profile with the same mass flow.

The deficit in mass flow for a given ΔP and P_2 would seem to be related to the discharge coefficient of the test channel. Assuming that the test channel in the present experiments - because of its geometric similarity to the venturi meter - can be analyzed by the method described in the Appendix and that B is approximately the same as for the venturi meter, one may then write the mass flow which would be passed for a given ΔP and P_2 if the profile is uniform in terms of the actual mass flow as follows:

$$\dot{m}_{uniform} = \dot{m}_{actual} + 3.55 \sqrt{\mu_1 D \dot{m}_{actual}}$$

This relation is shown graphically for the test sections used in these experiments in **Figs.** 9. Because of the large mass flows necessary to obtain reasonable pressure drops along the channel, it was not possible to verify this relation directly.

The test setup used by the MIT group would, on the basis of its design, also be expected to reduce the mass flow through the sample compared with that which would be passed if the approach velocity were uniform. Although the present writer has less theoretical or experimental basis for an accurate estimate of the characteristics of the MIT apparatus than his own, he is inclined to believe that the curves in Figs. 9 provide a reasonable first approximation. Many other permeability apparatus probably are also amenable to such relatively simple analysis.

The apparatus used in the tests at Georgia Institute of Technology seems to be in a different category with respect to estimating its contribution to the test results. In this apparatus, the metering section is followed by an expanding channel which is terminated by the test sample. Although the test sample itself is relatively large (4" diameter in one version and 4" square in another), there may be significant nonuniformity in the flow resulting from separations from the wall in the expanding section. These nonuniformities are virtually impossible to estimate without detailed information on the geometry, turbulence level, and mass flow. Thus, one can conclude only that while there may be effects due to flow nonuniformities in this apparatus, they are undetermined at present.

The discussion thus far has dealt only with the geometry of the channel upstream of the test specimen. It can be shown, however, that the geometry downstream of the test specimen and the location or characteristics of the gas pump also contribute to the results. If, for example, the channel immediately downstream of the sample enlarges discontinuously, or even very rapidly, the downstream pressure may be considerably lower for the same mass flow than if the diameter remains constant. Whether this happens will depend on the dispersive power of the sample and the admittance of the downstream mass sink (atmosphere or pump). If the sample produces little dispersion in the stream, or if the downstream pressure is held constant, no matter what the mass flow through the sample, then the $m \sim \Delta P$ relation will be independent of

downstream geometry. On the other hand, if the sample produces a large dispersion, the downstream pressure will be lower for the same mass flow in order to satisfy mass conservation. This drop may not materialize, however, if it will result in changes in the inlet conditions of a constant volume pump. Rather, the upstream pressure will tend to rise.

It must now be evident to the reader that permeabilities of given cloth samples in the present apparatus will be quite different from those measured in the MIT apparatus. Generally because the approach velocity is probably more nonuniform and the channel enlarges discontinuously downstream of the test sample, the MIT data would be expected to show a larger pressure drop for the same mass flow. The MIT data can also be expected to show a larger percentage drop in mass flow with decrease in P_2 than the present data.

While one may argue that flow through a parachute canopy is certainly dispersed, it would seem that cloth permeability measurements per se should be carried out in a constant area stream tube with a uniform approach velocity which is normal to the sample surface. Study of pressure distributions on complete parachute canopies reported in Ref. 11 suggest that this is the most reasonable basis for generalizing test data on small cloth samples to full scale canopies.

VI. EXPERIMENTAL PROCEDURE AND HANDLING OF DATA

A. COLD FLOW TEST PROCEDURE

Runs were usually begun at a downstream pressure of approximately 760 mm Hg. The downstream fine metering valve was opened slightly and dry nitrogen was admitted through one of the rotometers. The pressure upstream of the rotometer was adjusted commensurate with the upstream temperature so that the density through the rotometer was 1, 2, or 3 atmospheres. The pressure drop across the cloth was recorded. Oil manometers were used for $\Delta P < 60$ mm Hg. By opening the downstream metering valve and increasing the gas in-flow rate, the downstream pressure was held at 760 mm and the ΔP increased. At mass flows higher than 1 to 2.5 gm/sec, the flow was diverted from the rotometers and passed directly through the venturi. Upstream venturi pressure was read with a mercury manometer for $P_1 > 100$ mm Hga and with a Wallace and Tiernan dial gauge for $P_1 < 100$ mm Hga. ΔP was read with the silicone oil manometer for $\Delta P < 60$ mm and with the mercury manometer for $\Delta P > 60$ mm.

Points were taken more or less at random, the effort being to take sufficient points to permit fairing through the usual random variations and to keep the log ΔP interval fairly constant. The upper limit

was determined by which came first: (a) gas supply limitations of 65 gm/sec max, (b) pump capacity limitation of approximately 0.1 P_2 mm Hg gm/sec, (c) manometer deflection limitations of 990 mm Hg, or (d) fabric failure.

Following the completion of a run at P_2 = 760 mm, the downstream pressure was decreased and the procedure repeated, usually for descending ΔP. The third P_2 run utilized an ascending ΔP, etc. The selection of P_2 was made to facilitate definition of the trends with P_2. At the low P_2's, the McLeod gauge was used to check the pressures.

Usually a second or a third sample was spot checked to determine the degree of scatter from the results of the first sample. Four different test apparatus were available; a particular material, however, was tested in only three. For the most part, different samples were used in the tests in the different test sections.

Perhaps it might be well to comment at this point on the use of dry nitrogen as the test gas in place of air. First of all, nitrogen was available in the laboratory and a dry air supply suitable for mass flows less than 30 gm/sec but more than 1 gm/sec was not. Secondly, nitrogen is very similar to air in density and viscosity so that the results should be comparable. Thirdly, the life of open wound and other simple heating elements is much longer in nitrogen than in air which made the design and construction of the heater easier and less costly. The only area where the use of nitrogen may make a difference is in the high

temperature degradation of organic fibers. There is evidence in the literature to indicate that oxygen causes more rapid degradation than nitrogen. This point was left for future investigation, however.

B. HOT FLOW PROCEDURE

Because of the difficulty in regulating the output of the heater, the data at a given temperature level were taken at constant mass flow. The variation in pressure drop with changes in P_2 was recorded. The temperature was then increased and when a stable value was reached, the procedure repeated. The temperature was increased in increments until failure was observed or to a planned 1500°F, whichever occurred first. The temperature increments were chosen in an effort to define the effects of temperature with the minimum number of points.

C. DATA REDUCTION PROCEDURE

Except for the viscous corrections applied to the measured mass flow and the correction for approach velocity nonuniformity, the basic data reduction procedure is self-indicating. The viscous corrections applied to the venturi mass flow were obtained from the venturi calibration (see Appendix and Fig. A1). The rotometer data was used directly. All the results so obtained are shown in Figs. 10 through 20. Later, the estimated effects of approach velocity nonuniformity were applied to the faired curves and these were then redrawn as Figs. 21 through 27.

VII. DISCUSSION OF RESULTS

A. COLD FLOW TESTS

1. Variations from Sample to Sample

Generally, the thinner and more rigid the sample, the less the variation in permeability from sample to sample. The permeability of the stainless steel fabric was virtually the same for all samples. Deviations were usually confined to the scatter band for any particular run. The Mil-C-7350B Type I fabric also gave reasonably good agreement from sample to sample. The Mil-C-8021B Type II fabric showed variations on the order of 20% while the Mil-F-9084 Type VIII fabric showed variations of around 50% from sample to sample. The HT-1 fabric showed the same variations of the Mil-C-7350B Type I fabric.

It is important to note, however, that the ratio of permeability at one downstream pressure to that of another for the same ΔP was nearly the same for all samples of the same material, indicating that while there may be minor differences in construction of the various samples, these do not affect the qualitative air flow characteristics. The results of other tests on the same fabric can thus be converted to higher altitude results by multiplying the present data by the ratio

$$\frac{G_{760} \text{ new test}}{G_{760} \text{ present data}}$$

2. Effect of Sample Area

The two heavier materials were tested in both the 2.5" and 1.75" test sections. After correcting the results for flow nonuniformity, it was found that the mass flow per unit area was the same within 20% for the 8021B fabric and 50% for the 9084 fabric. This would indicate that (a) the smaller sample size is sufficient for good average results, and (b) that the corrections for flow nonuniformity were proper.

3. Comparison with Results of Other Investigations

Figs. 28, 29, 30, and 31 give comparisons between the uncorrected (i.e., for approach velocity nonuniformity and downstream spreading) results of several investigations of the same material. At sea level, the USC and MIT tests of the 7350B Type I fabric show approximately the same trend, but a different "gain", the difference being somewhat more than that found between samples of 7350B Type I. It seems reasonable to expect that this is a result of downstream spreading in the MIT apparatus. It will be noted that the Georgia Institute of Technology apparatus gave results which agreed more closely with the USC results in magnitude, but with a slope indicative of either different elastic properties or a change in the velocity distribution approaching the cloth.

At the higher altitudes the results obtained with the MIT apparatus show a much greater drop in G and a higher value of x than with the USC apparatus. This is to be expected since the approach velocity may

be somewhat more nonuniform in the MIT apparatus and the downstream spreading can be expected to increase with decreasing Reynolds number.

The sea level results obtained with the 8021B fabric are somewhat anomalous. The gain of USC results is only about 70% of the MIT results, although the slopes are the same. From tests of other samples of the 8021B fabric it would be expected that the curve marked USC represents the lower limit. Even if one adds 20% or 30% the results will still fall 25% below the MIT data. The material, being quite dense, would tend to promote downstream spreading and thus, the results are even less understandable. The GIT results because of their peculiar slope must be regarded as affected by increasing separation from the walls of the stream approaching the test sample.

At the higher altitudes, the effect of apparatus geometry on the MIT results as opposed to the USC results is evident.

4. Predictability of Results

Fig. 3 shows the predicted permeability of the stainless steel fabric based on the two cylinder flow analogy. Comparison with the measured results (Figs. 11 and 21) yields excellent agreement for $P_2 > 46$ mm (about 63,000). For $P_2 \leq 46$ the measured data is increasingly higher than the predicted, indicating that the predicted viscous effects did not materialize. At $P_2 = 46$ mm, the Knudsen

number of the fabric is about 0.03 and thus, one would expect that the characteristics will begin to deviate from those of continuum theory. However, measurements of the characteristics of cylinders in the transition region, between continuum flow and free molecule flow, are not yet well enough established to permit inclusion of these effects in the prediction. The present predictability limit is thus about 50,000'. For altitudes below this, it has been demonstrated that the two cylinder model gives excellent results for solidities, at least as high as .52. Morgan's results (Ref. 20) show the same feature at higher Reynolds numbers.

Fig. 3 was also compared with the measured permeabilities of the other materials. The qualitative agreement with the 7350B Type I fabric was good for $P_2 > 46$ mm, but some elastic effects or altered viscous effects did produce some differences. It is difficult, as noted earlier, to assign the cause to one or the other. The trends, however, seem in closer agreement with the two-cylinder model than with either the smooth nozzle or the orifice.

The permeabilities of the two heavier fabrics showed somewhat poorer agreement with the qualitative predictions for the screen at $P_2 > 46$ mm, indicating that the viscous effects may be somewhat different than assumed.

For $P_2 < 46$ mm, the permeabilities of all fabrics evidenced rarefaction effects. It appears, therefore, that satisfactory prediction of the permeabilities of fabrics at high altitudes must await a satisfactory description of their transition flow characteristics.

5. Empirical Description of Change in Permeability with Altitude

An attempt was made to obtain from the experimental results the functional dependence of G and x on P_2/P_1, ΔP, and $\dot{m}$, but no satisfactory correlation has been obtained so far. For the present, one must accept the corrected experimental results in lieu of a valid scaling procedure or a complete analytical description of the permeability.

B. HOT FLOW TESTS

At temperatures below the melting point of the material, one would expect that either the material will stretch slightly under load or that it will begin to yield, in which case it is impossible to obtain steady state permeability indications. Since it has been shown that simple extension of the fibers results in an almost negligible increase in permeability, one would expect the mass flow at a given ΔP and P_2 to depend almost entirely on density. For experimental convenience, however, the tests were designed to measure the variation in ΔP with T at constant $\dot{m}$ and P_2. For this case one would expect that since

$$\frac{\dot{m}}{A} = \frac{G'}{\sqrt{T_s}} \Delta P^x \qquad \text{at constant } P_2,$$

one would find that

$$\Delta P = G_o T_s^{\frac{0.5}{x}}$$

The results showed the exponent of T_s to be somewhat more than predicted in every case. The reason for this is that the heat transfer to the test section wall tends to make the mass flow distribution over the face of the sample more uniform, thus making the value of x slightly smaller. That this is the case seems evident from an examination of a typical sample which has been exposed to a temperature much higher than its melting point (Fig. 32). It will be seen that only the center 1" is melted, the outer 3/8 of an inch on all sides is unmelted.

While such high heat transfer is undesirable from the point of view of data interpretation, the analysis above and the experimental results seem to demonstrate conclusively that the long term effects on permeability of changes in stagnation temperature can be accounted for entirely by multiplying by $\sqrt{T_{s_o}/T_{s_1}}$.

The 8021B fabric was tested to a temperature of 400° F without failure. Tests at intermediate values of 275° F and 325° F were also made. Temperature overshoot of the heater, however, made it impossible to approach the melting temperature more closely without sample failure.

The new organic fiber HT-1 was tested to 650° F without failure. Tests at intermediate temperatures of 400° F, 500° F and 600° F were also run. The sample failed when an attempt was made to test it at 700° F. The sample is shown in Fig. 33.

The glass fabric was tested at 275° F, 500° F, and 750° F without evidence of any damage. It had been hoped to test it at higher temperatures but failure of the heater in the last days of the testing program prevented this.

The stainless steel fabric was tested at 750° F and an indicated 1200° F. There is reason to believe, however, that the thermocouple indication may have been too low (due to heat losses along the wires and reradiation to the wall). This temperature was the maximum on the galvanometer scale. It had been planned to use another indicator for higher temperatures, but failure of the heater at this point forced abandonment of this plan since repair of the heater would have required about a week and the time was not available.

The results of the various hot tests are shown in Figs. 34 through 44.

VIII. CONCLUSIONS

The present program has shown for the first time that:

1. The internal geometry of the permeometer can have an important effect on the measured permeability. Results most similar to those for a portion of a parachute canopy should be obtained with a permeometer employing a bell-mouth inlet, with the sample placed across the end of the inlet followed by a tube having the same internal diameter as the end of the inlet.

2. Viscous effects are present under all, except the very highest, mass flows for all materials tested.

3. Rarefaction effects appear to be present at altitudes above 60,000'.

4. The general equation for mass flow through the cloth is

$$\frac{\dot{m}}{A} = f\left(\frac{P_2}{P_1}, s, \Delta P, R_e\right) \frac{P_1}{\sqrt{T_s}} \left(\frac{P_2}{P_1}\right)^{\frac{1}{\gamma}} \sqrt{1 - \left(\frac{P_2}{P_1}\right)^{\frac{\gamma-1}{\gamma}}}$$

The expression $f(P_2/P_1, s, \Delta P, R_e)$ is in general different for each type of material and cannot as yet be determined analytically. For constructions where the dependence on P_2/P_1 and ΔP is small, satisfactory predictions can be obtained for $f(s, R_e)$ if $s < 0.5$ or so and the Knudsen number is less than .01.

5. The principal change in permeability resulting from material elasticity is connected with the rotation of the fabric pores under load. Changes associated with linear extension of the yarn arises only at very high ΔP's.

For the materials tested, the effects of elevated temperatures on permeability are derived entirely from changes in air density.

A. RECOMMENDATIONS

1. From the point of view of basic research, the flow characteristics through typical cloth samples should be determined under very low density conditions to delineate the rarefaction effects. Tests should be conducted with P_2 as low as 30μ Hg and with $\Delta P/P_2$ up to about 4.

2. This will require that the test sample be at least 4" in diameter to avoid excessive approach velocity nonuniformity.

3. A qualitative analysis - both theoretical and experimental - of the effect of pore inclination on its mass transfer characteristics should be initiated. This should be coupled with an investigation to determine the discharge characteristics of smooth nozzles, orifices and two-cylinder nozzles at low densities.

4. Analysis of the data already on hand should be continued in an effort to define the viscous and rarefaction effects more satisfactorily.

5. Except when elastic effects are directly and reversibly related to gas temperature, tests at elevated temperatures need not be conducted.

IX. REFERENCES

1. Cornell, W. G., "Losses in Flow Normal to Plane Screens", Transactions of the ASME 80, p. 791, 1958.

2. Morgan, P. G., "High Speed Flow Through Perforated Plates", Journal of the Royal Aeronautical Society 64, Feb. 1960.

3. Schlichting, H., Boundary Layer Theory, 4th ed., McGraw-Hill Book Co., 1960.

4. Lavier, H. W. S., "Air Permeability of Parachute Cloth", WADC TR 52-283, part II, August 1953.

5. Scheidegger, Adrian E., The Physics of Flow Through Porous Media. University of Toronto Press, 1957.

6. Green, Leon and Duwez, Pol, "Fluid Flow Through Porous Media", J. of Appl. Mech. 18, No. 1, pp. 39-45, March 1951.

7. Lavier, H. W. S. and Boteler, W. C., "Air Permeability of Parachute Cloth", WADC TR 52-283, part V, April 1955.

8. Seshadri, Brown, Backer, Krizik, and Mellen, "Air Flow Characteristics of Parachute Fabrics at Simulated High Altitudes", WADC TR 59-374, August 1959.

9. Klein, Lermond and Platt, "Research Program for the Development of a Design Procedure to Engineer Parachute Fabrics", WADC TR 58-65, May 1958.

10. Bickford, Kuehl, and Rusk, "Study of the Control of Permeability of Nylon Parachute Cloth at High and Low Differential Pressures", WADC TR 54-468, March 1955.

11. Heinrich, Ballinger and Ryan, "Pressure Distribution in Transonic Flow of Ribbon and Guide Surface Parachute Models", WADC TN 59-32, February 1959.

12. Crocco, Luigi, "One-Dimensional Treatment of Steady Gas Dynamics", Fundamentals of Gas Dynamics, H. W. Emmons, editor, Princeton University Press, 1958.

13. Pai, S. I., Viscous Flow Theory, Vol. II, D. Van Nostrand, 1957.

14. A. S. M. E., Fluid Meters.

15. Liepmann, H. W., "A Study of Effusive Flow", Aeronautics and Astronautics. Pergamon Press, 1960.

16. Stearns, Jackson, Johnson, and Larson, Flow Measurement with Orifice Meters. Van Nostrand, 1951.

17. Liepmann, Hans W., "Gaskinetics and Gasdynamics of Orifice Flow", Journal of Fluid Mechanics, Vol. 10, part 1, 1961.

18. Perry, J. A., Jr., "Critical Flow through Sharp-Edged Orifices", Transactions of the ASME, 71, 1949.

19. Marks Mechanical Engineers Handbook, McGraw-Hill Book Co., New York.

20. Morgan, P. G., "High Speed Flow through Wire Gauges", Journal of the Royal Aeronautical Society, Vol. 63, August 1959.

21. Rouse, Hunter, Fluid Mechanics for Hydraulics Engineers, Dover, 1961.

22. Rouse, Hunter, Elementary Mechanics of Fluids, John Wiley, 1947.

23. Gowen, Forrest E. and Perkins, Edward W., "Drag of Circular Cylinders for a Wide Range of Reynolds Numbers and Mach Numbers", NACA TN 2960.

24. Eshbach, editor, Handbook of Engineering Fundamentals. John Wiley, 1952.

25. Kennard, E. H., Kinetic Theory of Gases, McGraw-Hill Book Co., 1938.

APPENDIX I

AN EXTENDED THEORY OF GAS FLOW RATE THROUGH A NOZZLE

A. GENERAL

It is usually assumed that the flow through a convergent-divergent nozzle can be represented quite adequately by treating the fluid as if it were adiabatic and inviscid with uniform properties at each axial location. It has been shown — by experiment and also by more inclusive analysis — that these assumptions are well-substantiated, provided the throat entrance and exit geometries are not too abrupt, the Reynolds number based on throat diameter is not too low, and the throat Knudsen number is not too high. The equations derived under these assumptions are well-known and therefore will not be repeated here. For the purposes of the present investigation, only the equation relating the mass flow and the pressures at the throat and some upstream location is of interest. It is the purpose of the following analysis to determine, if possible, the manner in which this relation must be modified to treat cases for which some of the foregoing assumptions are violated.

B. MODIFICATION FOR REDUCED REYNOLDS NUMBER

Since gases are in fact slightly viscous, reducing the Reynolds number can be expected to produce increasing deviations from the flow rate predicted by the ideal theory. In contrast to the widespread knowledge of the ideal theory result, there appears to be no exact solution for $R_{e_d} << \infty$. Crocco (Ref. 12) examined the situation in some detail but in a rather approximate fashion which, even so, does not permit simple calculation of the ratio of actual mass flow rate to the ideal value, i.e., the discharge coefficient. His analysis shows, however, that the value of C_d is determined almost entirely by events occurring upstream of or at the throat. The exception occurs when the pressure gradient downstream of the throat is unfavorable enough to produce separation upstream of the throat. This situation is discussed in detail later. Schlichting (Ref. 3) and Pai (Ref. 13) discuss theoretical and experimental results for incompressible flow in a straight pipe under both laminar and turbulent flow conditions, and both also give the exact solution for incompressible viscous flow in a converging two-dimensional channel. Unfortunately, while such cases may be similar in many ways to the present one, they are not sufficiently close to warrant inferring from them the quantitative characteristics of compressible nozzle flow.

In the absence of an adequate theoretical treatment one can consult the hydraulics literature for measurements of the discharge characteristics of venturi meters, nozzles and orifices. These are usually limited to incompressible flow, however. One does find (Ref. 14) intimations that the discharge characteristics are the same for a compressible fluid, provided the normalization is carried out using the inviscid compressible flow theory. However, no data was presented to support this conjecture. Also, recent editions of the standard engineering handbooks have tended to regard the earlier measurements as questionable, but because of apparent lack of interest in the nozzle as a standard flow rate measuring device, particularly at low Reynolds numbers, have included little new data. They suggest individual calibration of the device used as the most satisfactory approach.

In view of this situation, it was felt that a detailed calibration of the venturi meter used in this apparatus for metering the higher mass flow would provide some instructive information on the behavior of compressible flow in nozzles at low Reynolds numbers and serve as a standard against which to compare the results of any theory which might be proposed to explain it. The results are shown in Fig. A1. The fact that no measurable change in C_d vs. R_{e_d} was observed when $P_2/P_1 > 0.528$ seems to confirm earlier beliefs in this regard. This might be expected since the maximum Mach number in the converging section is 1.0 and the displacement thickness on a flat plate at least varies but little between $M = 0$ and $M = 1.0$.

After some study, it was found that the experimental results could be explained satisfactorily by the following semi-empirical analysis:

Consider the convergent portion of an axisymmetric nozzle as shown in the sketch

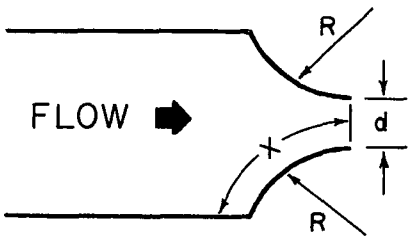

When $10^2 < R_{e_d} < 10^4$, one is probably justified in assuming that the flow at the throat consists of an isentropic core and a laminar boundary layer with displacement thickness δ^*. The discharge coefficient, C_d, can be represented, therefore, by

$$C_d = \left(\frac{d - 2\delta^*}{d}\right)^2 = 1 - \frac{4\delta^*}{d} + \frac{4\delta^{*2}}{d^2} \qquad \text{(A1)}$$

When $2\delta^*/d << 1$,

$$C_d \approx \frac{1}{1 + \frac{4\delta^*}{d}} \qquad \text{(A2)}$$

If one assumes that $\delta^* = \frac{K_1 x}{\sqrt{R_{e_x}}}$, Eq. (A2) becomes

$$C_d = \frac{1}{1 + \frac{4K_1 x}{d\sqrt{R_{e_x}}}} \qquad \text{(A3)}$$

Assumption of such a form for δ^* seems reasonable since one finds this Reynolds number dependence for both a flat plate and a circular cylinder and since it has been shown that two-dimensional boundary layer theory gives good results for flow inside ducts if $\frac{\delta^*}{d} << 1$.

For a given nozzle, x/d = constant, K_2. [It should be noted, however, that if the contraction ratio is > 5 (in terms of diameters), x should probably be measured from the position at which the velocity first becomes significant, i.e., when D/d is first less than 5.] Using the fact that K_2 gives the relation between s and d, one may write

$$\frac{\delta^*}{d} = \frac{K_1\sqrt{K_2}}{\sqrt{Re_d}} \tag{A4}$$

Hence, Eq. (A3) can be written

$$C_d = \frac{1}{1 + \frac{4K_1\sqrt{K_2}}{\sqrt{Re_d}}}$$

or

$$C_d = \frac{1}{1 + \frac{B}{\sqrt{Re_d}}} \tag{A5}$$

The value of K_1, and hence of B, depends upon dP/dx. One may estimate the value of K_1 from the exact analysis of flow over a cylinder. In that analysis

$$\delta^* = \frac{0.8\,R}{\sqrt{\frac{U_\infty\, R}{\nu}}} \tag{A6}$$

at the 90° point. For $R/d = 1.66 \approx K_2$, $B = 4.12$. Tests of a nozzle with this entrance geometry gave $B = 4.0$. The calibration data are shown in Fig. (A1). Dry nitrogen was the test fluid.

Eq. (A5) can be expected to yield reasonable agreement with experiment down to Reynolds number for which the boundary layer completely fills the throat. Continuing the use of the analysis of flow over a cylinder, one has $\delta^*/\delta = 0.3$ at the throat. This result assumes a two-dimensional flow, however. In the three-dimensional case of a nozzle, the pressure gradient is somewhat more favorable and, according to the Karman-Pohlhausen analysis, δ^*/δ is therefore less than 0.3. If one takes $\delta^*/\delta = 0.27$ then one has $C_d = 0.65$ which agrees with experiment.

As the Reynolds number is decreased below this point, the flow velocity at the throat decreases. This comes about because the pressure at the throat does not decrease - as near as can be determined experimentally - compared with the upstream pressure while the viscous dissipation continues to increase. Because the velocity decreases and the dissipation results in increased temperature, the entire flow soon becomes nearly isothermal. For such flows, the discharge is the same as for incompressible, viscous flow for which $\dot{m} \sim \Delta P$ in a straight pipe. Isentropic nozzle theory, however, gives $\dot{m} \sim \sqrt{\Delta P}$ for constant P_2 so that in a slowly contracting channel $\dot{m}/\dot{m}_{inviscid} \sim \sqrt{R_e}$. Thus,

$$C_d = \frac{\sqrt{R_{e_d}}}{C} \qquad \text{(A7)}$$

The value of C depends, of course on dP/dx. If one assumes that for a unit length of straight pipe $\Delta P = .472P_1$, then from the viscous pipe flow equation and isentropic nozzle equation, one obtains a value for C = 7.14 for nitrogen. It would seem reasonable to assume that in a rapidly converging channel there is more dissipation and hence the value of C is greater. The data in Fig. A1 indicates that 11.4 may be a good value for C. This is 2.86 times B for the same nozzle. A check of two sets of data in the literature on C_d vs. R_{e_d} (for incompressible flow, however) indicates that this ratio may be quite universal (see Fig. A2). If this is the case, then one may describe the discharge characteristics of a given nozzle in terms of a single constant which depends on geometry:

$$C_d = \frac{1}{1 + \frac{B}{\sqrt{R_{e_d}}}} \text{ for } C_d \geq 0.65; \quad C_d = \frac{\sqrt{R_{e_d}}}{2.86\,B} \text{ for } C_d \leq 0.65 \qquad \text{(A8)}$$

Since the Reynolds number is based properly on the actual mass flow, it is necessary to do some rearranging in order to find the actual mass flow in terms of that given by inviscid theory. This procedure is shown below.

$$\frac{\dot{m}}{\dot{m}_{\text{inviscid}}} = C_d = \frac{1}{1 + \frac{B}{\sqrt{\frac{4\dot{m}}{\pi\mu_2 d}}}} \qquad \text{(A9)}$$

$$\dot{m} + \frac{B\dot{m}}{\sqrt{\frac{4\dot{m}}{\pi\mu_2 d}}} = \dot{m}_i$$

$$\dot{m}_i - \dot{m} = 0.886\, B\sqrt{\mu_2 d\dot{m}}$$

$$\dot{m}_i^2 - 2\dot{m}\dot{m}_i + \dot{m}^2 = 0.7854\, B^2 \mu_2\, d\dot{m}$$

$$\dot{m}^2 - (2\dot{m}_i + .7854\, B^2 \mu_2 d)\, \dot{m} + \dot{m}_i^2 = 0$$

$$\dot{m} = \dot{m}_i + .3927\, B^2 \mu_2 d \pm 1/2 \sqrt{4\dot{m}_i^2 \pm 4\dot{m}_i B^2 \mu_2 d(.7854) + \left[.7854\, B^2 \mu_2 d\right]^2 - 4\dot{m}_i^2}$$

$$\dot{m} = \dot{m}_i + .3927\, B^2 \mu_2 d \left[1 - \sqrt{1 + \frac{\dot{m}_i}{.1964\, B^2 \mu_2 d}}\right]$$

for $C_d \geq 0.65$ (A10)

$$C_d = \frac{\sqrt{\frac{4\dot{m}}{\pi\mu_2 d}}}{2.86\, B} = \frac{\dot{m}}{\dot{m}_i} \qquad \text{(A11)}$$

$$\frac{\dot{m}^2}{\dot{m}_i^2} = \frac{4\dot{m}}{\pi\mu_2 d(8.2) B^2}$$

$$\dot{m} = \frac{\dot{m}_i^2}{6.44\, B^2 \mu_2 d} \quad \text{for } C_d \leq 0.65 \qquad \text{(A12)}$$

The inviscid mass flow above which one uses Eq. (A10) is from Eq. (A12)

$$\dot{m}_{i_{C_d = .65}} = 4.18\, B^2 \mu_2 d \qquad \text{(A13)}$$

Substitution of suitable expressions for μ_2 and $\dot{m}_i$ in terms of γ, A_2, A_2/A_1, P_1, P_2, and T_s into Eqs. (A10), (A12), and (A13) then yields general expressions for compressible, viscous flow through a nozzle (or venturi meter) in terms of quantities which may be measured directly. The results are given below:

$$\dot{m} = P_1 \frac{A}{\sqrt{T_s}} \left(1 - \frac{\Delta P}{P_1}\right)^{\frac{1}{\gamma}} \frac{\sqrt{\frac{2\gamma}{(\gamma-1)R}\left[1-\left(1-\frac{\Delta P}{P_1}\right)^{\frac{\gamma-1}{\gamma}}\right]\left[1-\left(\frac{A_2}{A_1}\right)^2\left(1-\frac{\Delta P}{P_1}\right)^{\frac{\gamma+1}{\gamma}}\right]}}{1-\left(\frac{A_2}{A_1}\right)^2\left(1-\frac{\Delta P}{P_1}\right)^{\frac{2}{\gamma}}}$$

$$+ .3927 B^2 d \mu_o \left[\frac{T_s}{T_o} \frac{\left(1-\frac{\Delta P}{P_1}\right)^{\frac{\gamma-1}{\gamma}} - \left(\frac{A_2}{A_1}\right)^2\left(1-\frac{\Delta P}{P_1}\right)^{\frac{\gamma+1}{\gamma}}}{1-\left(\frac{A_2}{A_1}\right)^2\left(1-\frac{\Delta P}{P_1}\right)^{\frac{\gamma+1}{\gamma}}}\right]^n$$

$$\left[1-\sqrt{1+\frac{P_1 A_2}{\sqrt{T_s}}\left(1-\frac{\Delta P}{P_1}\right)^{\frac{1}{\gamma}} \frac{\sqrt{\frac{2\gamma}{(\gamma-1)R}}\left[1-\left(1-\frac{\Delta P}{P_1}\right)^{\frac{\gamma-1}{\gamma}}\right]\left[1-\left(\frac{A_2}{A_1}\right)^2\left(1-\frac{\Delta P}{P_1}\right)^{\frac{\gamma+1}{\gamma}}\right]^{2n+1}}{.1964 B^2 d \mu_o \left\{\frac{T_s}{T_o}\left[\left(1-\frac{\Delta P}{P_1}\right)^{\frac{\gamma-1}{\gamma}} - \left(\frac{A_2}{A_1}\right)^2\left(1-\frac{\Delta P}{P_1}\right)^{\frac{\gamma-1}{\gamma}}\right]\right\}^n \left[1-\left(\frac{A_2}{A_1}\right)\left(1-\frac{\Delta P}{P_1}\right)^{\frac{2}{\gamma}}\right]}}\right] \quad (A14)$$

NOMENCLATURE

$\dot{m}$ = mass flow per unit time
P_1 = absolute pressure at upstream source
A_2 = throat area
T_s = stagnation temperature
ΔP = pressure difference between throat source and upstream source
d = throat diameter
γ = ratio of specific heats
R = gas constant
A_1 = upstream area
μ_o = standard value of dynamic viscosity
T_o = temperature (absolute) for μ_o
n = exponent in viscosity-temperature law
B = a constant determined by the geometry

$$\dot{m} = \frac{P_1^2 A_2^2 \left(1-\frac{\Delta P}{P_1}\right)^{\frac{2}{\gamma}} \frac{2\gamma}{(\gamma-1)R}\left[1-\left(1-\frac{\Delta P}{P_1}\right)^{\frac{\gamma-1}{\gamma}}\right]\left[1-\left(\frac{A_2}{A_1}\right)^2\left(1-\frac{\Delta P}{P_1}\right)^{\frac{\gamma+1}{\gamma}}\right]}{6.44 B \mu_0 d T_s \left[\frac{T_s}{T_0}\,\frac{\left(1-\frac{\Delta P}{P_1}\right)^{\frac{\gamma-1}{\gamma}} - \left(\frac{A_2}{A_1}\right)^2\left(1-\frac{\Delta P}{P_1}\right)^{\frac{\gamma+1}{\gamma}}}{1-\left(\frac{A_2}{A_1}\right)^2\left(1-\frac{\Delta P}{P_1}\right)^{\frac{\gamma+1}{\gamma}}}\right]^n \left[1-\left(\frac{A_2}{A_1}\right)^2\left(1-\frac{\Delta P}{P_1}\right)^{\frac{2}{\gamma}}\right]^2} \qquad \text{(A15)}$$

for $C_d \leq 0.65$

$$\dot{m}_{i_{C_d=0.65}} = 4.18\, B^2 d/\mu_0 \left[\frac{T_s}{T_0}\,\frac{\left(1-\frac{\Delta P}{P_1}\right)^{\frac{\gamma-1}{\gamma}} - \left(\frac{A_2}{A_1}\right)^2\left(1-\frac{\Delta P}{P_1}\right)^{\frac{\gamma+1}{\gamma}}}{1-\left(\frac{A_2}{A_1}\right)^2\left(1-\frac{\Delta P}{P_1}\right)^{\frac{\gamma+1}{\gamma}}}\right]^n \qquad \text{(A16)}$$

Implicit in these equations are the assumptions that

1. The gas flow is steady and adiabatic.
2. The pressure is constant across the nozzle at the stations where it is measured.
3. The gas is perfect.

In c. g. s. units, $R = 2.97 \times 10^6$ ergs/gm $^\circ$K for N_2; $P = h(13,340$ dynes/cm$^3)$ where h is the heigth of the manometer in cm of Hg; $\dot{m}$ is in gm/sec; A is in cm^2; μ_o in poise; T_s in $^\circ$K.

n may be taken as = 0.76 if $T_s \approx 300^\circ$K.

C. MODIFICATION FOR INCREASED KNUDSEN NUMBER

In the preceding section, the effect of reduced Reynolds number on the mass flow through a nozzle with no upstream separation was considered. It was indicated that at very low Reynolds numbers the discharge coefficient varies as $R_{e_d}{}^{1/2}$. No lower limit was given for C_d, implying that $C_d \longrightarrow 0$ as $R_{e_d}{}^{1/2} \longrightarrow 0$. For a particular liquid, this probably is true since one can reduce R_{e_d} only by reducing u or d; neither action affects the basic assumptions. For a gas, however, one may also reduce the Reynolds number by reducing the density. This tends to increase molecular mean free path lengths in the gas. At a sufficiently low density the mean free path lengths is a significant function of the nozzle diameter and the flow may no longer be regarded as a continuum. Deviation from continuum theory results have been found to occur when this dimensionless ratio, known as the Knudsen Number, exceeds 0.01. For Knudsen numbers larger than 3.0, the flow can be analyzed by free molecule theory. At intermediate values of Knudsen number, however, there is as yet no satisfactory theoretical description of the flow characteristics.

Whereas the continuum theory indicates that $C_d \longrightarrow 0$ as $R_{e_d} \longrightarrow 0$, free molecule theory indicates that $C_d \longrightarrow$ a constant $\neq 0$ as $R_{e_d} \longrightarrow 0$ if R_{e_d} is reduced by reducing the gas density. This constant is a function of the nozzle geometry and has not been calculated

except in the case of an orifice for which it has the value 0.697 (Ref. 15). One may, however, estimate the value for a nozzle from the theoretical results for free molecule flow in a pipe (Ref. 25). Taking the pipe length equal to its diameter and $P_2/P_1 = 0$ gives

$$C_{d_{min}} \approx 0.28$$

The actual value may be more or less depending upon the entry geometry and pressure ratio. Gradual entry shapes would be expected to have lower values of $C_{d_{min}}$. For the nozzle shown in Fig. A1, $C_{d_{min}}$ is probably about 0.10 when $P_2/P_1 = 0.528$. One would expect that the data would begin to show evidence of the rarefaction effect for $P_1 < 100\,\mu$ Hg, the pressures for which the Knudsen number is greater than 0.01. It is to be expected that $C_{d_{min}}$ will be reached when $P_1 < 1\,\mu$ Hg. For nozzles with smaller throats, these rarefaction effects will be encountered at higher pressures. For example, if the throat diameter is 0.01" (0.25 mm), one would expect that deviations from continuum results would begin for $P_1 < 4$ mm Hg.

Although there is at present no experimental verification, it seems reasonable to expect that one could account for rarefaction effects by adding to Eq. (A7) the term

$$E \tanh\left(\frac{F\lambda}{d}\right) \qquad \text{(A17)}$$

where E and F are constants depending on the nozzle geometry. For the

nozzle shown in Fig. A1, values of 0.1 and 3, respectively, seem to be appropriate. However, since Eq. (A17) is largely speculative, it does not appear worthwhile to include this effect in the derivation of Eq. (A15). It would be well, nevertheless, to add the restriction to Eq. (A15) that it be used only for $\lambda/d < 0.01$.

D. MODIFICATIONS FOR CHANGES IN INLET GEOMETRY

As indicated above, the one-dimensional flow equations are based on the assumption that pressure gradients across the flow at the station of measurement are negligible. This is approximately true for gradual entry nozzles. For abrupt-entry nozzles with short throats this is patently false. It is common practice, however, to continue the use of the one-dimensional equations and to account for this effect by means of an expansion factor, a part of the gross discharge coefficient. The expansion factor is that part which depends on pressure ratio but not on Reynolds number. It can be written

$$Y = \frac{C_d}{C_{d_{viscous}}} \tag{A18}$$

Because of the difficulty in obtaining exact theoretical solutions for flow in channels which permit changes in C_d with pressure ratio, Y is generally determined empirically. A theoretical solution was recently obtained for inviscid flow through a two-dimensional slit, and the results

were found to agree closely with experimental data on flow through a sharp-edged orifice at high Reynolds numbers. The interesting feature of the theoretical solution (Liepmann, Ref. 17, discusses this at some length) is that the maximum mass flow is not reached until $P_2/P_1 < 0.05$. This result is a consequence of the fact that in the orifice, the centerline pressure is greater than that near the edge. The centerline flow has, therefore, a higher signal speed. Not until the edge flow has accelerated through a 45° angle does the signal from it propagate rapidly enough toward the centerline to halt the influence of lowered downstream pressure on the flow. Perry (Ref. 18) found that he could fit his experimental results with the relations

$$Y = 0.227 \left[\frac{1 - \left(\frac{P_2}{P_1}\right)^2}{\left(\frac{P_2}{P_1}\right)^{1.43} \left(1 - \left[\frac{P_2}{P_1}\right]^{2/7}\right)} \right] \qquad \text{for } P_2/P_1 \geq 0.528 \tag{A19}$$

and

$$Y = \left[0.848 + 0.455 \frac{P_2}{P_1}\right] \sqrt{1 - \frac{P_2}{P_1}} \qquad \text{for } P_2/P_1 \leq 0.528 \tag{A20}$$

if $d/D \leq 0.2$ and $C_{d_{viscous}} = 1.0$. One would expect some changes in Y if $d/D > 0.2$, but no data exists on this question.

Examination of Liepmann's results (Ref. 17) indicates that for $P_2/P_1 = 0.001$ and $d/D \ll 1$, the variation in $C_{d_{viscous}}$ with Reynolds number is about the same as given in the handbooks for $P_2/P_1 \approx 1.0$. It would seem, therefore, that the viscous and expansion effects can be treated separately. Liepmann plans additional tests to cast more light on this point, however.

For the present, if one assumes that such separation is possible, one may make use of the vast quantity of data available in the literature on the discharge characteristics of various geometries measured using water or air with $\Delta P/P_1 \ll 1$. From these data, it may be concluded that a relation of the type given by Eq. (A5) will be valid for $R/d > 0.25$. When $R/d < 0.25$, apparently the flow will separate from the wall at high Reynolds numbers and $C_d \longrightarrow 0.61$ as $R_{e_d} \longrightarrow \infty$. Ref. 19 indicates that the expression

$$C_{d_{R_e=\infty}} = 0.61 + 1.9\, R/d \qquad \text{(A21)}$$

may be used for $R/d \leq 0.1$. When $d/D > 0.2$, $C_{d_{R_e=\infty}}$ increases. For example, when $d/D = .4$, $C_{d_{R_e=\infty}} = .62$; when $d/D = .6$, $C_{d_{R_e=\infty}} = 0.65$; when $d/D = 0.8$, $C_{d_{R_e=\infty}} = 0.78$. The dependence of C_d on diameter ratio persists down to a Reynolds number of about 10, below which the curves are identical. These results apply when the throat is shorter than 2 throat diameters. For longer throats, the viscous

effects and the expansion effects are somewhat different, but they will not be discussed further because such geometries have less application to the present study.

It is, of course, possible to fit empirical formulae to each of these discharge curves or to the family as a whole. For example, when $d/D \leq 0.2$ and $R/d = 0$,

$$C_d = \sqrt{\frac{R_{e_d}(R_{e_d} + 800)}{1950\, R_{e_d} + 2.75\,(R_{e_d} - 100)^2}} \qquad (A22)$$

fits the experimental data generally to within 4% or less. This relation, however, does not lend itself to simplification or rearrangement as did Eq.(A5). Even if one were to attempt a two segment fit such as was done with Eq.(A8), inclusion of diameter ratio and leading edge ratio effects would hopelessly complicate the expressions. For this reason, it would appear that for simplicity one should rely on graphical presentations of the characteristics of a particular device to determine the mass flow represented by a given P_1, P_2, and T_s when $R/d < 0.25$.

E. MODIFICATIONS FOR EXCESSIVE UNFAVORABLE PRESSURE GRADIENTS DOWNSTREAM OF THE THROAT

When a nozzle diverges rapidly downstream of the throat, a large unfavorable pressure gradient must be overcome if a subsonic flow is to adhere to the walls. If the gradient is too large, the flow will separate from the nozzle wall. The separation point depends upon the particular

geometry. Instantaneous increases in nozzle area fix the separation point for all Reynolds numbers and thus do not modify the results obtained in Subsection A. For certain relations of the expansion angle to the throat diameter and length, however, the wall exerts an influence on the separation point. As a result, the separation point and the general flow pattern can be expected to respond to changes in Reynolds number. The functional dependence of $\dot{m}$ on R_e is therefore quite different from that treated in Subsection A. There are, of course, many possible variations in geometry which could be considered; only one will be considered here. Because of its relation to the flow through screens - and possibly, therefore, also to flow through cloth - the flow studied will be that over circular cylinders.

From the drag characteristics of a cylinder, it appears that as the Reynolds number is increased from very low values, the separation point moves further from the stagnation point to about the 70° location, reaching this at a Reynolds number of about 10^3. It remains there for all higher Reynolds numbers for which the flow is laminar. This shift in separation point is accompanied by a decrease in the width of the wake.

If one were to assume a nozzle to be made from the region between two noninteracting cylinders, one can determine the discharge characteristics from the experimental drag coefficients of a single cylinder as indicated in Section II. To perform a quantitative calculation, three additional assumptions are required:

(1) The downstream pressure in the region where the flow is again uniform is the same as or at least related in some explicit manner to the pressure in the minimum area.

(2) The pressure, velocity, and density in the minimum area are those which would exist if the flow were one-dimensional.

(3) The reference Mach number and Reynolds number are based on these flow conditions.

The force on an evenly-spaced group of cylinders lying in a plane normal to the direction of flow in a constant area channel is then

$$A\Delta P = C_D n q_2 d' \ell \tag{A23}$$

But

$$n d' \ell = sA \tag{A24}$$

and

$$\rho_1 u_1 A = \rho_2 u_2 (1 - s) A \tag{A25}$$

so that

$$\frac{\dot{m}}{A} = \frac{1 - s}{\sqrt{s}} \sqrt{\frac{2 \rho_2 \Delta P}{C_D(R_e, M)}} \quad \text{for } P_2/P_1 \geq 0.528 \tag{A26}$$

This equation may also be written

$$\frac{\dot{m}}{A} = \frac{P_1 A_2/A}{\sqrt{1 - \frac{A2}{A}}} \sqrt{\frac{\frac{2}{R T_s} \left(\frac{P_2}{P_1}\right)^{\frac{1}{\gamma}} \left(1 - \frac{P_2}{P_1}\right) \left(\frac{P_s}{P_1}\right)^{\frac{\gamma - 1}{\gamma}}}{C_D(R_e, M)}} \tag{A27}$$

If one takes the drag coefficients for $M \leq 1.0$, $R_e > 10^3$ given in the literature, one may compute $\dot{m}/A$ for various ΔP's and P_2's. If the results are graphed, it will be seen that for $R_e \geq 10^3$ the curve has the same appearance as that for an isentropic nozzle. In view of the close similarity between Eqs. (A27) and (A14), this is not surprising; particularly since variation in C_D with M appears to have the proper form to account for the difference. This leads one to speculate that the flow in region between two cylinders can be represented by the isentropic nozzle function multiplied by a discharge coefficient derived from the inverse square root of the drag coefficient of a cylinder:

$$\dot{m} = C_d \frac{P_1 A_2}{\sqrt{T_s}} \left(1-\frac{\Delta P}{P_1}\right)^{\frac{1}{\gamma}} \frac{\sqrt{\frac{2\gamma}{(\gamma-1)\mathcal{R}}\left[1-\left(1-\frac{\Delta P}{P_1}\right)^{\frac{\gamma-1}{\gamma}}\right]\left[1-\left(\frac{A_2}{A_1}\right)^2\left(1-\frac{\Delta P}{P_1}\right)^{\frac{\gamma+1}{\gamma}}\right]}}{1-\left(\frac{A_2}{A_1}\right)^2\left(1-\frac{\Delta P}{P_1}\right)^{\frac{2}{\gamma}}} \qquad \text{(A28)}$$

C_d as a function of Reynolds number is shown in Fig. A3. For comparison purposes, the C_d for a unseparated nozzle and an orifice are also included. It will be noted that the change in slope of C_d vs. R_e extends over several orders of magnitude more for the two cylinder nozzle than it does for an unseparated nozzle or an orifice. This situation, reflecting as it does changes in a separated flow, makes it very difficult, if not impossible, to devise a semitheoretical description in the manner of Eqs. (A8). One must, therefore, use the curve in Fig. A3 in computing $\dot{m}$. It is possible, however, to approximate this curve with the functions.

$$C_d = 0.31\, R_e^{0.33} \qquad R_e < 10 \tag{A29}$$

$$C_d = 0.43\, R_e^{0.122} \qquad 10 \leq R_e \leq 10^3 \tag{A30}$$

$$C_d = 1.0 \qquad R_e > 10^3 \tag{A31}$$

with fair accuracy. Since

$$R_e = \frac{\dot{m}\, d'}{(1 - s)\, A \mu_2} \tag{A32}$$

in this case, the actual mass flow can be written in terms of the ideal as follows

$$\dot{m} = \left[0.31\, \dot{m}_i \left(\frac{d'}{[1 - s]\, A \mu_2} \right)^{.33} \right]^{1.5} \qquad R_e < 10 \tag{A33}$$

$$\dot{m} = \left[0.43\, \dot{m}_i \left(\frac{d'}{[1 - s]\, A \mu_2} \right)^{0.122} \right]^{1.22} \qquad 10 \leq R_e \leq 10^3 \tag{A34}$$

$$\dot{m} = \dot{m}_i \qquad R_e > 10^3 \tag{A35}$$

It is to be expected that these relations will be valid only in the limit as $s \longrightarrow 0$. As s increases, interaction should also increase, particularly at very low Reynolds numbers. It is interesting to compare, however, the coefficient in Eq. (5) which is $6/R_e^{1/3}$ with $(1/(.43)R_e^{.122})^2 = 5.4/R_e^{.244}$ from Eq. (A30). This indicates that for $R_e > 60$, the interaction effects are quite small. On the other hand, the right hand side of Eq. (6) is considerably different from $(10/R_e^{2/3})\, s/(1-s)^2$, indicating that for $R_e < 20$ interaction effects make the use of the two-cylinder model less useful.

F. CONCLUDING REMARKS

It has been shown above that it is possible to include, without undue complication and with good accuracy, the effects of viscosity in the expressions for flow through a smooth entry nozzle. For those geometries which produce flow separation (i.e., sharp-edged orifices) no general analytical description is known, nor are the empirical equations sufficiently simple for common use. The effects of reduced gas density are at present also poorly understood and little experimental data exists to ameliorate the condition. Thus, the conclusion may be drawn that while it is possible to account for some of the deviations from the ideal in nozzle flow, reliance must continue for the most part on calibration under actual test conditions.

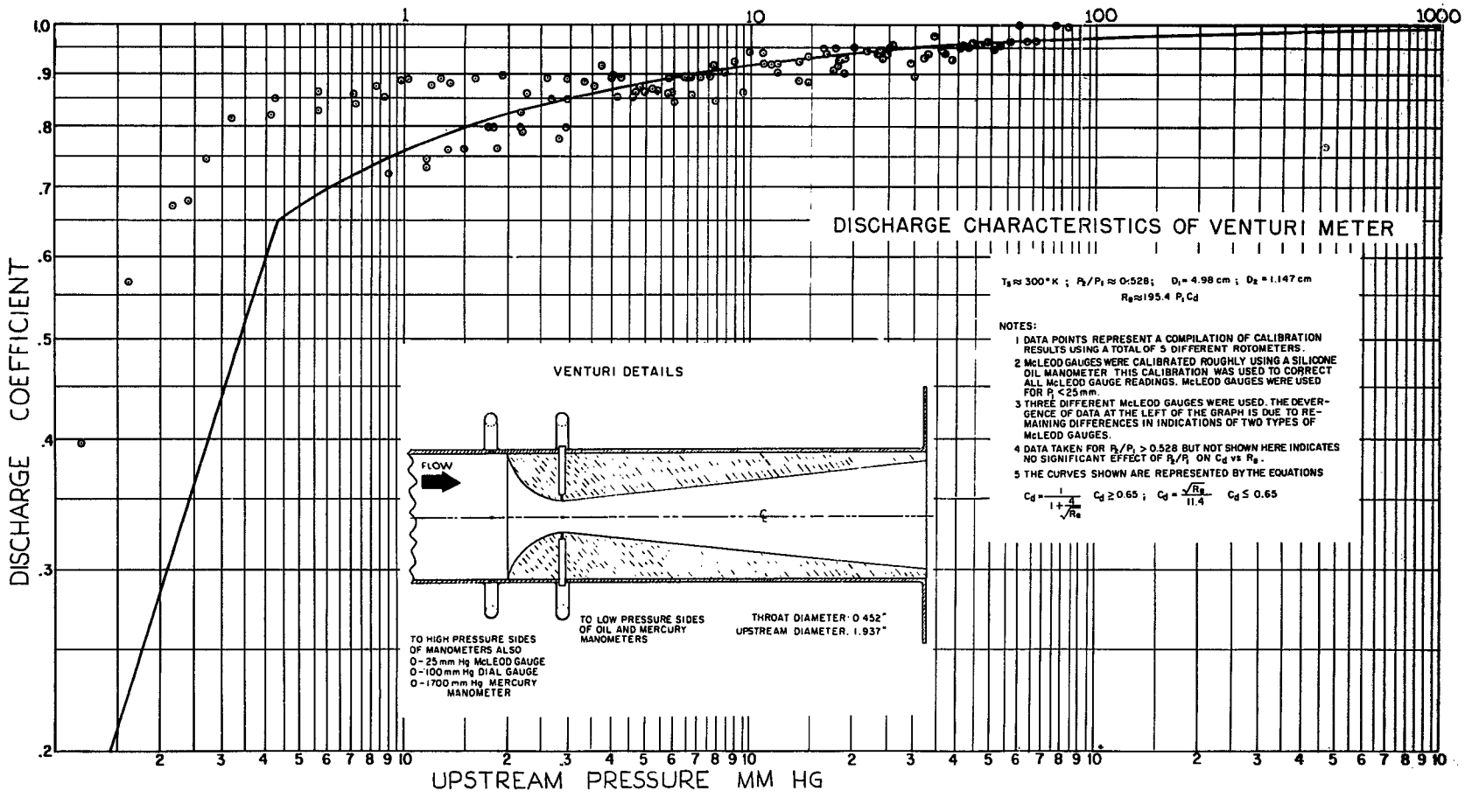
DISCHARGE CHARACTERISTICS OF VENTURI METER
DISCHARGE COEFFICIENT
UPSTREAM PRESSURE MM HG
1.0
.9
.8
.7
.6
.5
.4
.3
.2
1
10
100
1000
$T_0 \approx 300°K$; $P_2/P_1 \approx 0.528$; $D_1 = 4.98$ cm ; $D_2 = 1.147$ cm
$R_e \approx 195.4\ P_1 C_d$
NOTES:
1 DATA POINTS REPRESENT A COMPILATION OF CALIBRATION RESULTS USING A TOTAL OF 5 DIFFERENT ROTOMETERS.
2 McLEOD GAUGES WERE CALIBRATED ROUGHLY USING A SILICONE OIL MANOMETER THIS CALIBRATION WAS USED TO CORRECT ALL McLEOD GAUGE READINGS. McLEOD GAUGES WERE USED FOR $P_1 < 25$ mm.
3 THREE DIFFERENT McLEOD GAUGES WERE USED. THE DEVERGENCE OF DATA AT THE LEFT OF THE GRAPH IS DUE TO REMAINING DIFFERENCES IN INDICATIONS OF TWO TYPES OF McLEOD GAUGES.
4 DATA TAKEN FOR $P_2/P_1 > 0.528$ BUT NOT SHOWN HERE INDICATES NO SIGNIFICANT EFFECT OF P_2/P_1 ON C_d vs R_e.
5 THE CURVES SHOWN ARE REPRESENTED BY THE EQUATIONS
$C_d = \frac{1}{1+\frac{4}{\sqrt{R_e}}}$ $C_d \geq 0.65$; $C_d = \frac{\sqrt{R_e}}{11.4}$ $C_d \leq 0.65$
VENTURI DETAILS
FLOW
TO HIGH PRESSURE SIDES OF MANOMETERS ALSO
0 - 25 mm Hg McLEOD GAUGE
0 - 100 mm Hg DIAL GAUGE
0 - 1700 mm Hg MERCURY MANOMETER
TO LOW PRESSURE SIDES OF OIL AND MERCURY MANOMETERS
THROAT DIAMETER: 0.452"
UPSTREAM DIAMETER: 1.937"

FIGURE A1

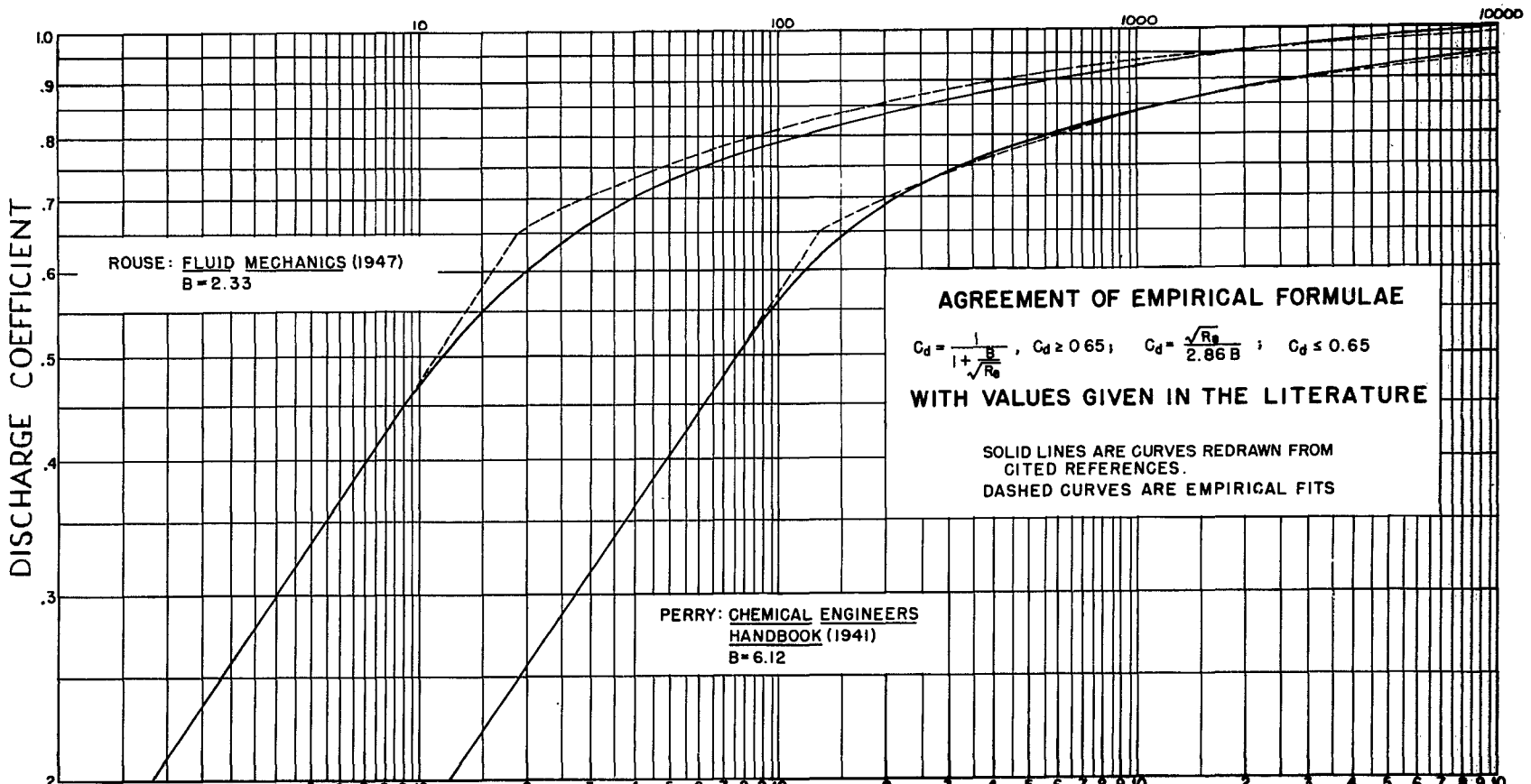
DISCHARGE COEFFICIENT
REYNOLDS NUMBER
1.0
.9
.8
.7
.6
.5
.4
.3
.2
10
100
1000
10000
2 3 4 5 6 7 8 9 10
ROUSE: FLUID MECHANICS (1947)
B = 2.33
AGREEMENT OF EMPIRICAL FORMULAE
$C_d = \frac{1}{1+\frac{B}{\sqrt{R_e}}}$, $C_d \geq 0.65$; $C_d = \frac{\sqrt{R_e}}{2.86\,B}$; $C_d \leq 0.65$
WITH VALUES GIVEN IN THE LITERATURE
SOLID LINES ARE CURVES REDRAWN FROM CITED REFERENCES.
DASHED CURVES ARE EMPIRICAL FITS
PERRY: CHEMICAL ENGINEERS HANDBOOK (1941)
B = 6.12

FIGURE A2

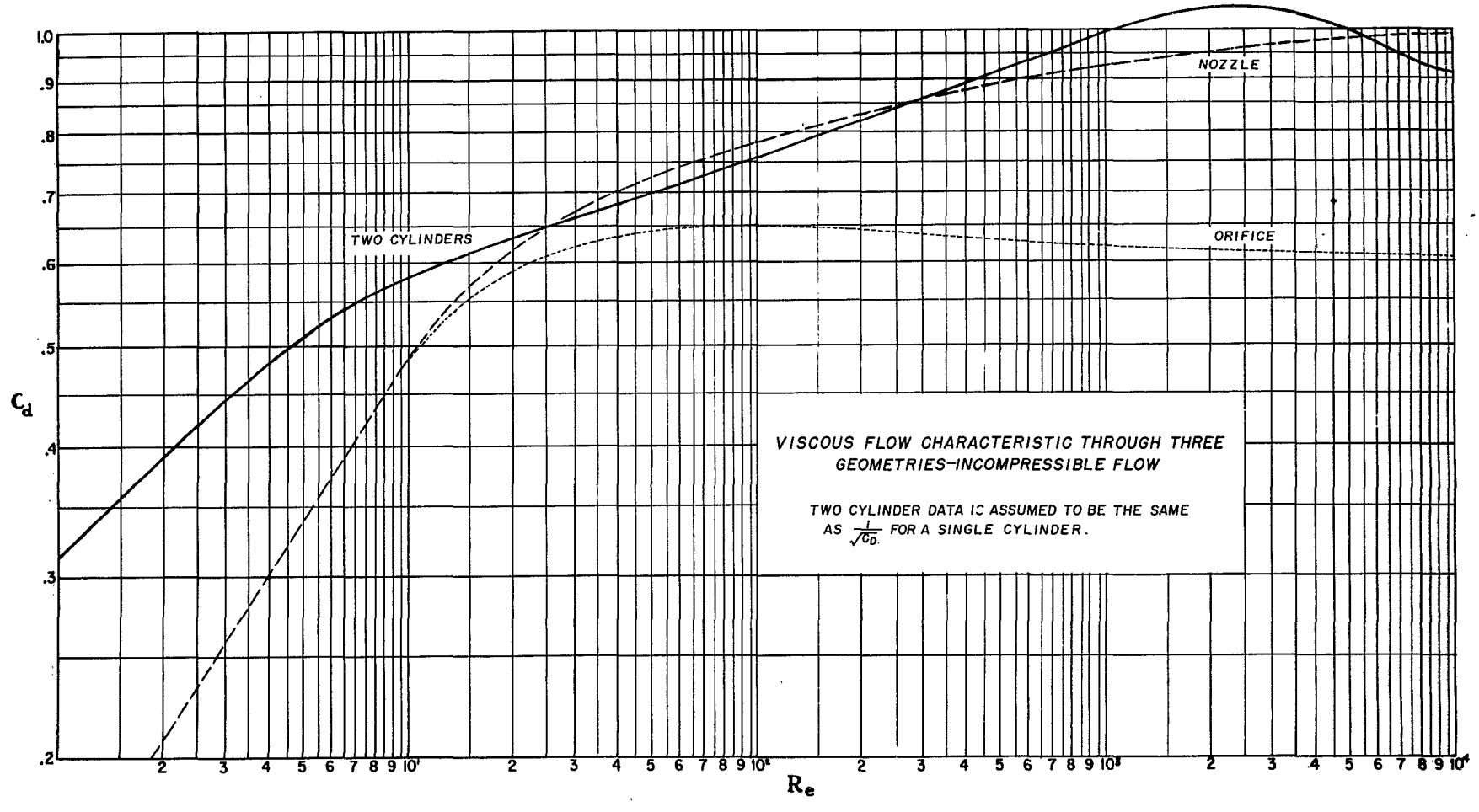
1.0
.9
.8
.7
.6
.5
.4
.3
.2
C_d
TWO CYLINDERS
NOZZLE
ORIFICE
VISCOUS FLOW CHARACTERISTIC THROUGH THREE GEOMETRIES–INCOMPRESSIBLE FLOW
TWO CYLINDER DATA IS ASSUMED TO BE THE SAME AS $\frac{1}{\sqrt{C_D}}$ FOR A SINGLE CYLINDER.
2 3 4 5 6 7 8 9 10^1 2 3 4 5 6 7 8 9 10^2 2 3 4 5 6 7 8 9 10^3 2 3 4 5 6 7 8 9 10^4
R_e

FIGURE A3

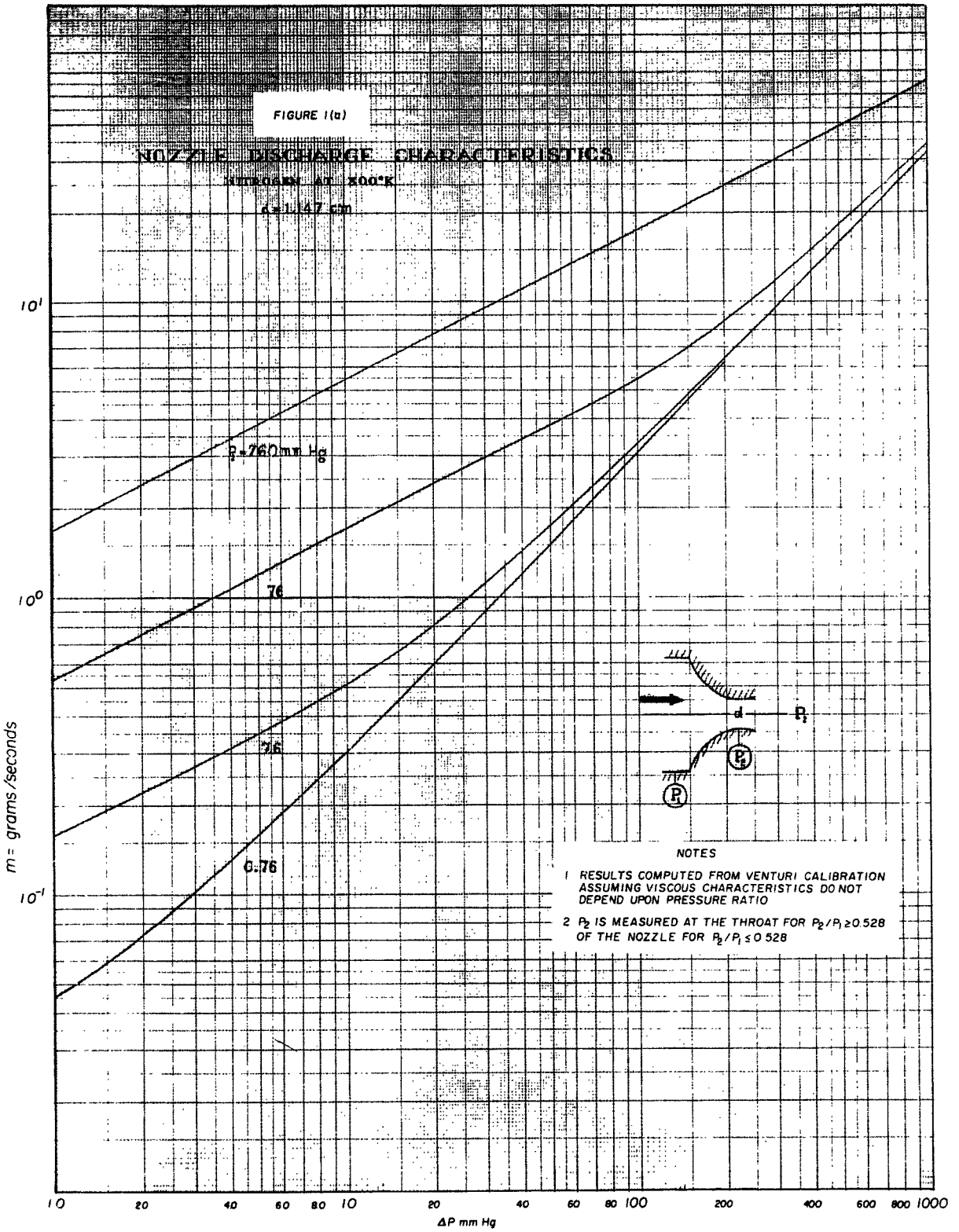
FIGURE 1(a)
NOZZLE DISCHARGE CHARACTERISTICS
Nitrogen at 300°K
d = 1.147 cm
P_1 = 760 mm Hg
76
7.6
0.76
10^1
10^0
10^{-1}
m = grams/seconds
10
20
40
60
80
10
20
40
60
80
100
200
400
600
800
1000
ΔP mm Hg
NOTES
1 RESULTS COMPUTED FROM VENTURI CALIBRATION ASSUMING VISCOUS CHARACTERISTICS DO NOT DEPEND UPON PRESSURE RATIO
2 P_2 IS MEASURED AT THE THROAT FOR $P_2/P_1 \geq 0.528$ OF THE NOZZLE FOR $P_2/P_1 \leq 0.528$
d
P_1
P_2
P_1

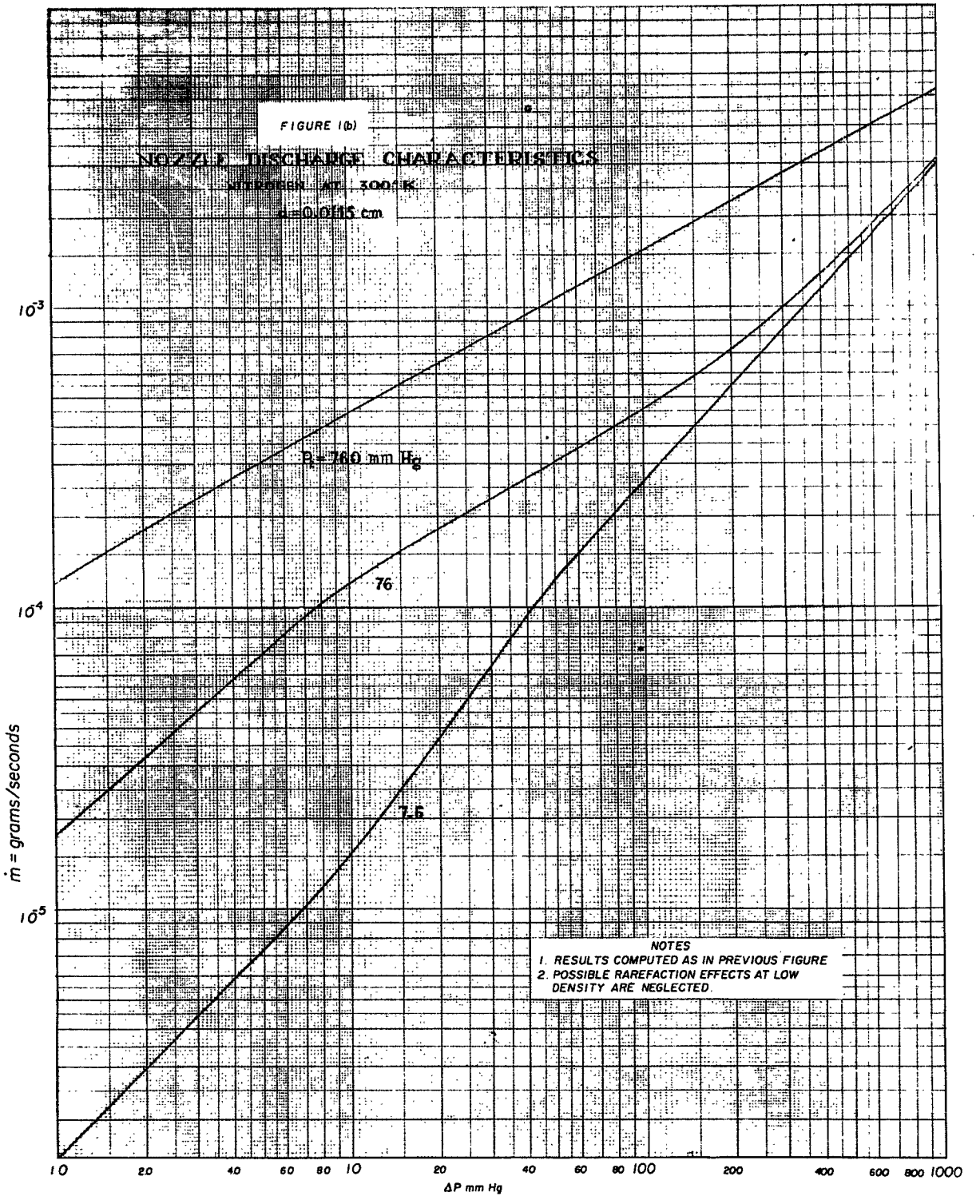
FIGURE 1(b)
NOZZLE DISCHARGE CHARACTERISTICS
NITROGEN AT 300°K
a=0.0015 cm
P_t = 760 mm Hg
76
7.6
10^{-3}
10^{-4}
10^{-5}
$\dot{m}$ = grams/seconds
10 20 40 60 80 10 20 40 60 80 100 200 400 600 800 1000
ΔP mm Hg
NOTES
1. RESULTS COMPUTED AS IN PREVIOUS FIGURE
2. POSSIBLE RAREFACTION EFFECTS AT LOW DENSITY ARE NEGLECTED.

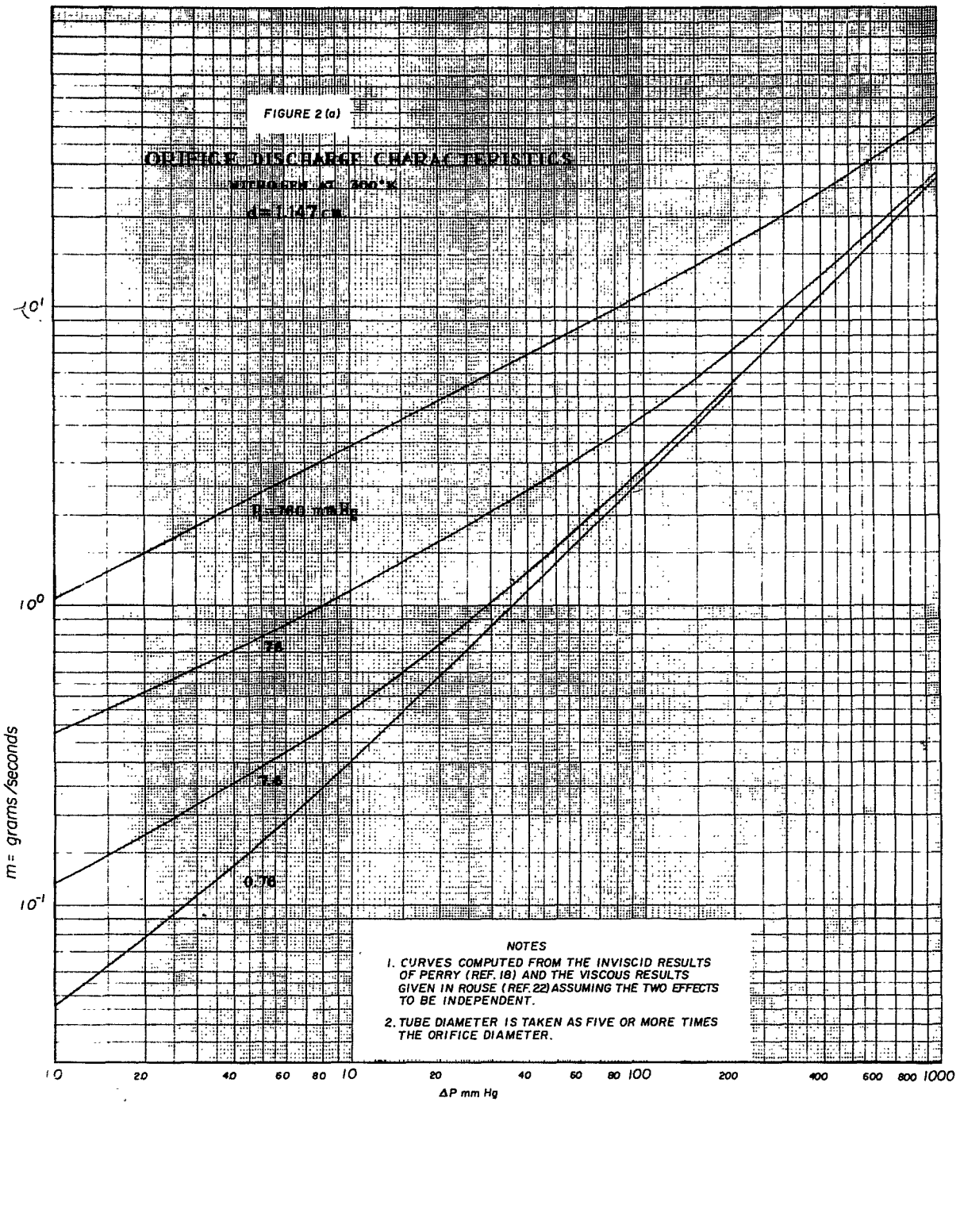
FIGURE 2 (a)
ORIFICE DISCHARGE CHARACTERISTICS
NITROGEN AT 300°K
d = 1.147 cm
10^1
10^0
10^{-1}
m = grams/seconds
P_1 = 760 mm Hg
76
7.6
0.76
NOTES
1. CURVES COMPUTED FROM THE INVISCID RESULTS OF PERRY (REF. 18) AND THE VISCOUS RESULTS GIVEN IN ROUSE (REF. 22) ASSUMING THE TWO EFFECTS TO BE INDEPENDENT.
2. TUBE DIAMETER IS TAKEN AS FIVE OR MORE TIMES THE ORIFICE DIAMETER.
10 20 40 60 80 10 20 40 60 80 100 200 400 600 800 1000
ΔP mm Hg

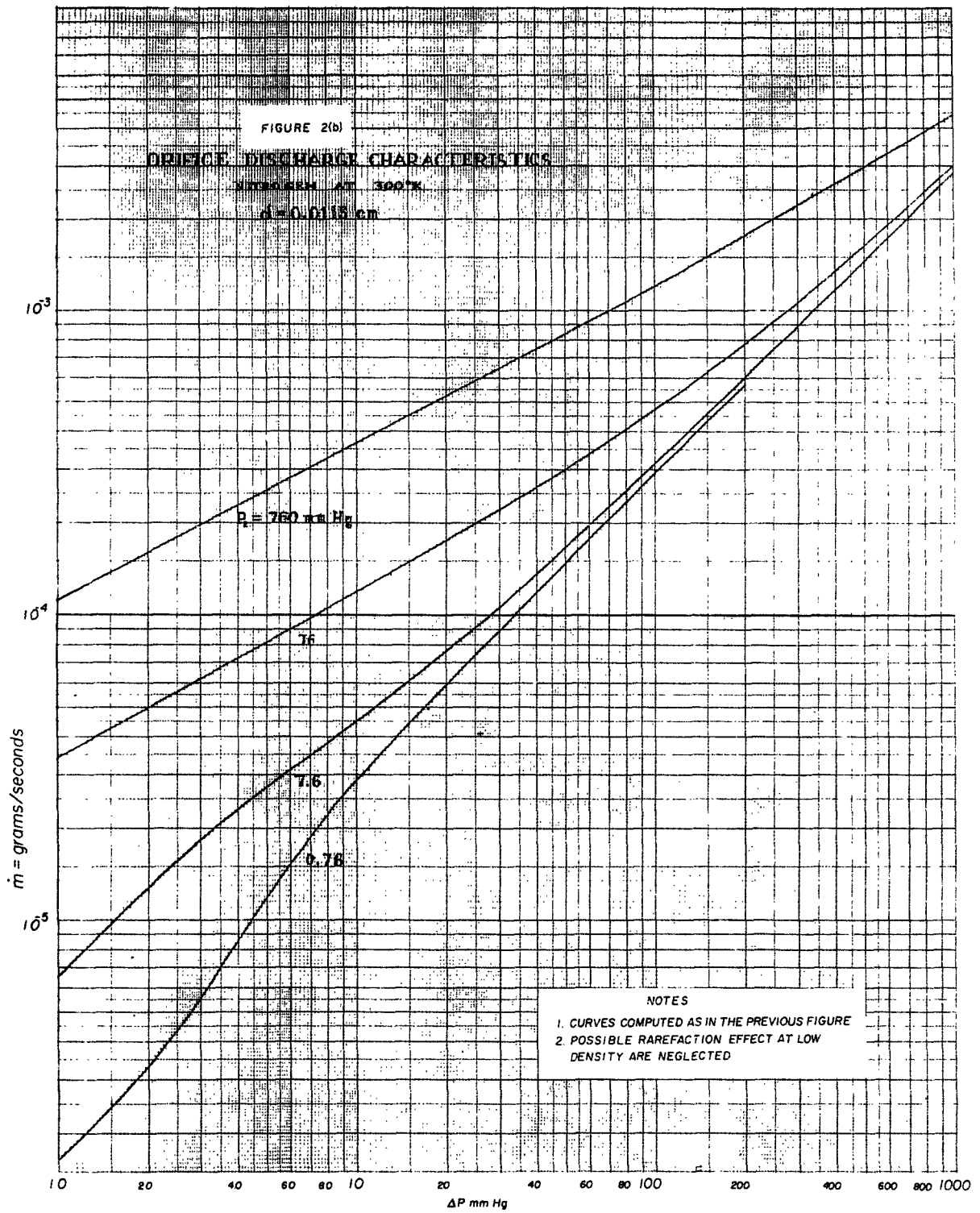
FIGURE 2(b)
ORIFICE DISCHARGE CHARACTERISTICS
NITROGEN AT 300°K
d = 0.0115 cm
10^{-3}
10^{-4}
10^{-5}
P_t = 760 mm Hg
76
7.6
0.76
$\dot{m}$ = grams/seconds
NOTES
1. CURVES COMPUTED AS IN THE PREVIOUS FIGURE
2. POSSIBLE RAREFACTION EFFECT AT LOW DENSITY ARE NEGLECTED
10 20 40 60 80 10 20 40 60 80 100 200 400 600 800 1000
ΔP mm Hg

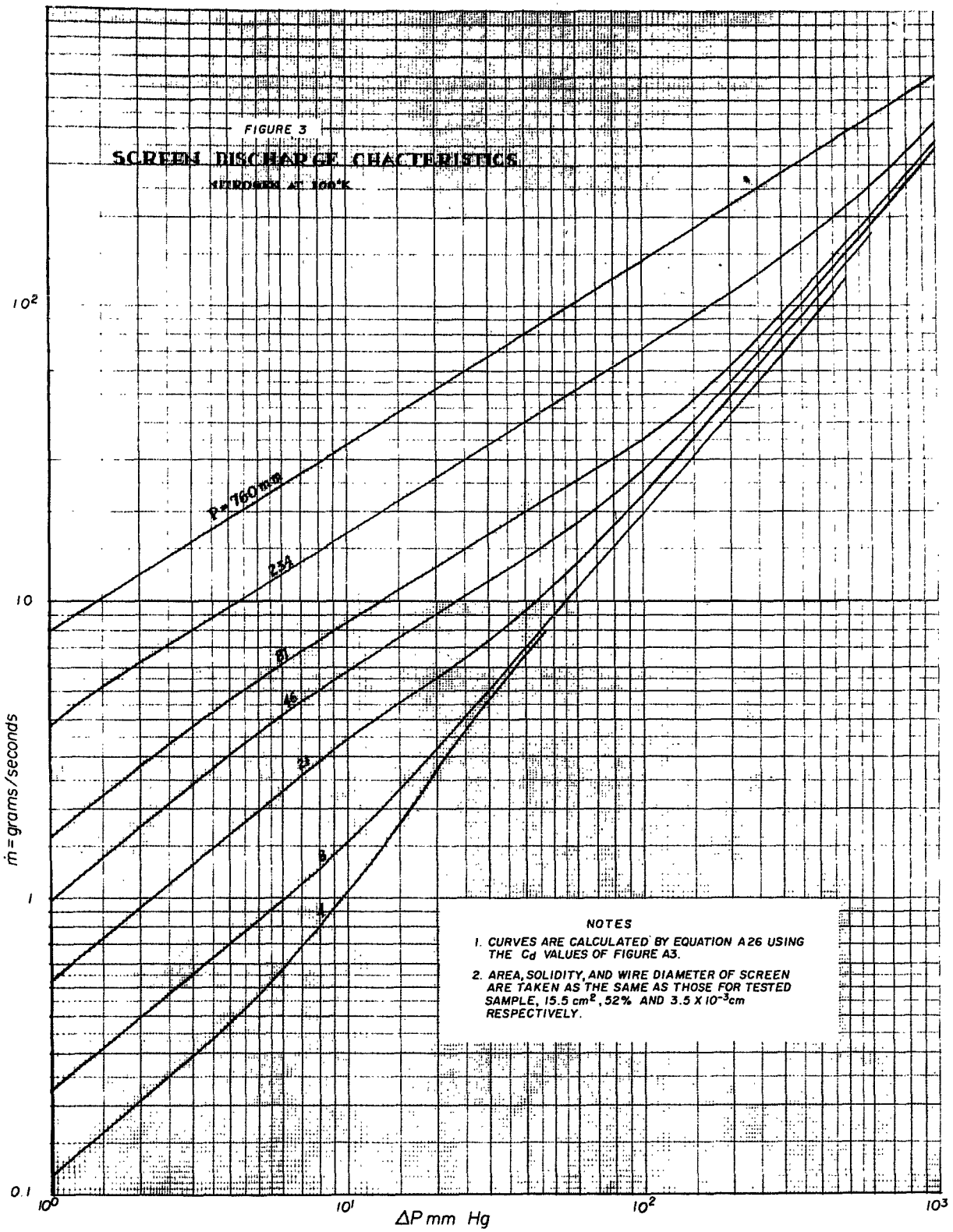
FIGURE 3
SCREEN DISCHARGE CHACTERISTICS
NITROGEN AT 100°K
10^2
10
1
0.1
$\dot{m}$ = grams/seconds
P = 760 mm
254
81
46
23
8
4
NOTES
1. CURVES ARE CALCULATED BY EQUATION A26 USING THE C_d VALUES OF FIGURE A3.
2. AREA, SOLIDITY, AND WIRE DIAMETER OF SCREEN ARE TAKEN AS THE SAME AS THOSE FOR TESTED SAMPLE, 15.5 cm^2, 52% AND 3.5 X 10^{-3}cm RESPECTIVELY.
10^0
10^1
10^2
10^3
ΔP mm Hg

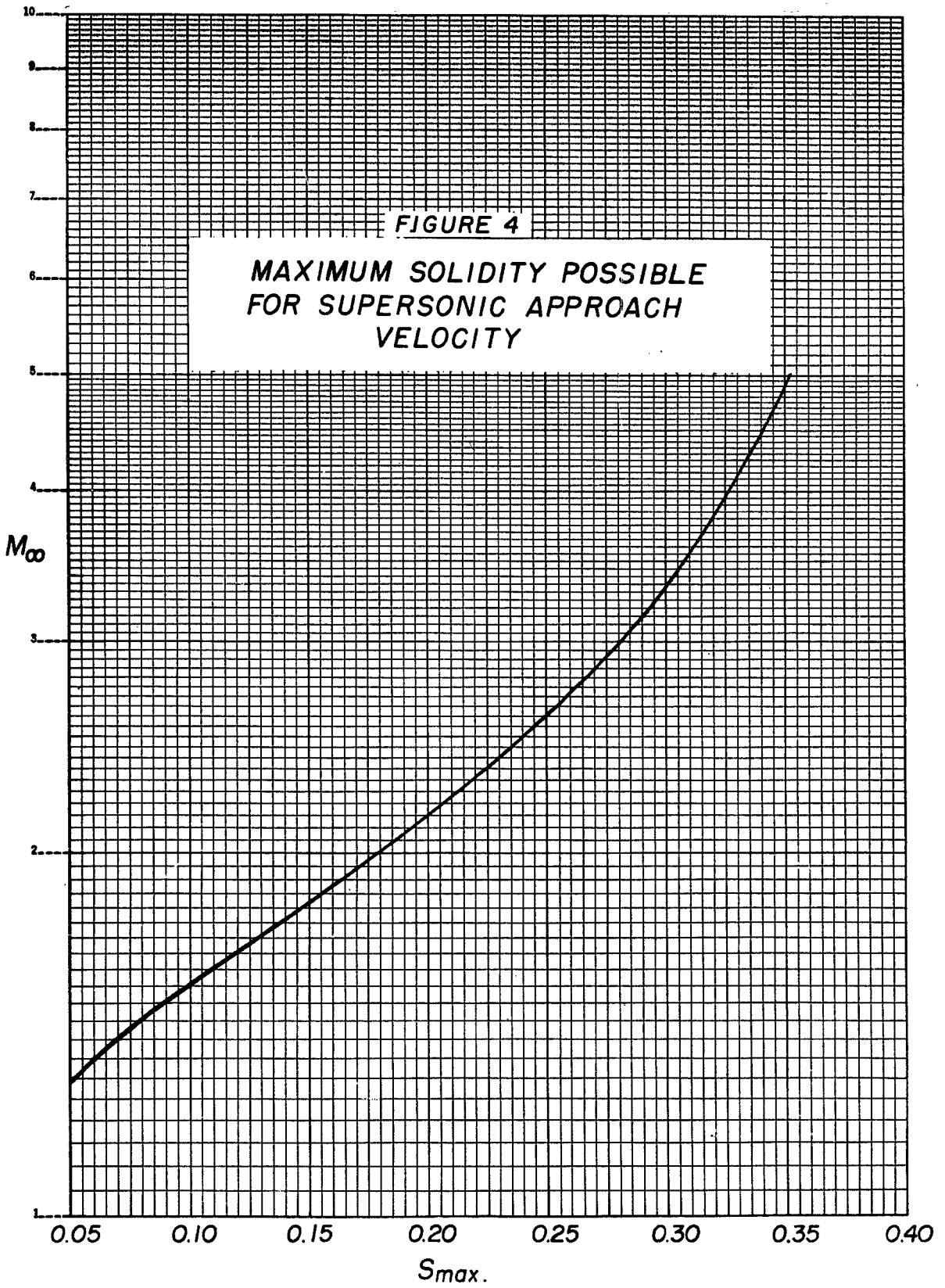
FIGURE 4
MAXIMUM SOLIDITY POSSIBLE FOR SUPERSONIC APPROACH VELOCITY
M_∞
10
9
8
7
6
5
4
3
2
1
0.05
0.10
0.15
0.20
0.25
0.30
0.35
0.40
$S_{max.}$

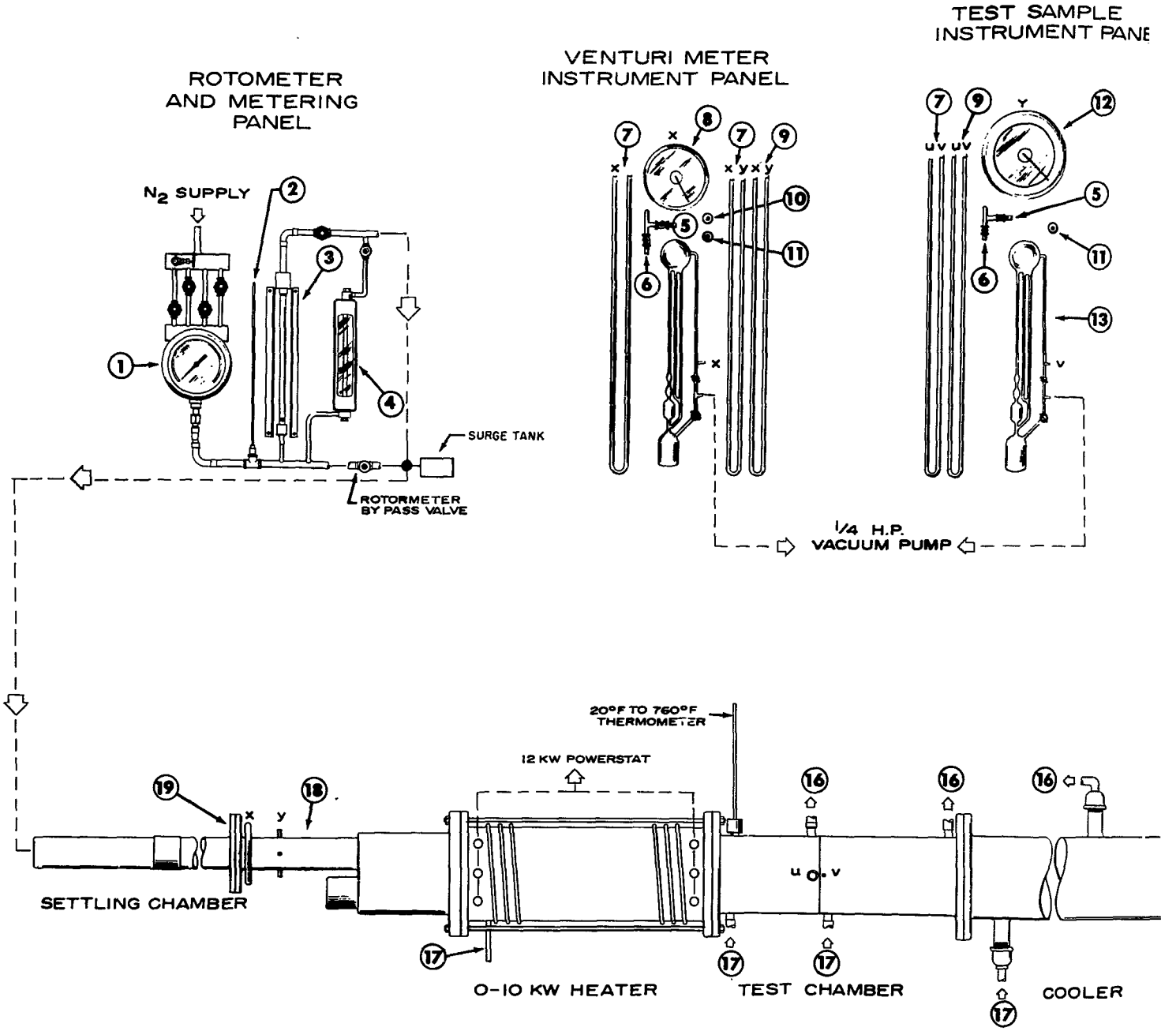

FIGURE 5. LOW PRESSURE HIGH TEMPERATURE PERMEABILITY A

NOMENCLATURE	
1	ASHCROFT 0-30 PSI TEST GAUGE
2	54-101°F THERMOMETER
3	3/8-INCH MANOSTAT FLOWRATER
4	1/8-INCH FISCHER AND PORTER FLOWRATER
5	VENT COCK
6	OIL MANOMETER DISCONNECT
7	MANOMETER U-TUBE
8	0-100MM WALLACE AND TIERNAN GAUGE
9	SILICONE OIL U-TUBE
10	GAUGE SEAL OFF
11	McLEOD GAUGE SEAL OFF VALVE
12	0-800 MM WALLACE AND TIERNAN GAUGE (1 MM DIV)
13	McLEOD GAUGE
14	1/4-INCH FINE METERING VALVE
15	2-INCH COARSE METERING VALVE
16	WATER OUTLET
17	COOLING WATER INLET
18	VENTURI METER
19	ACCESS FLANGE

VENTURI METER
INSTRUMENT PANEL

TEST SAMPLE
INSTRUMENT PANEL

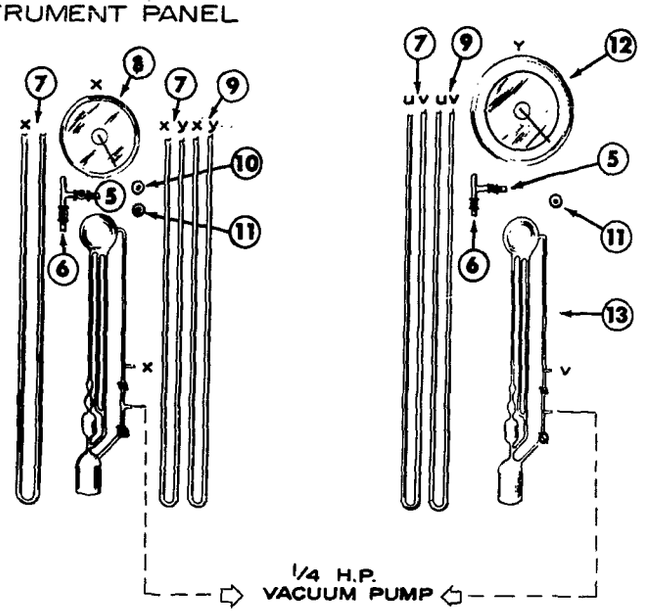

2

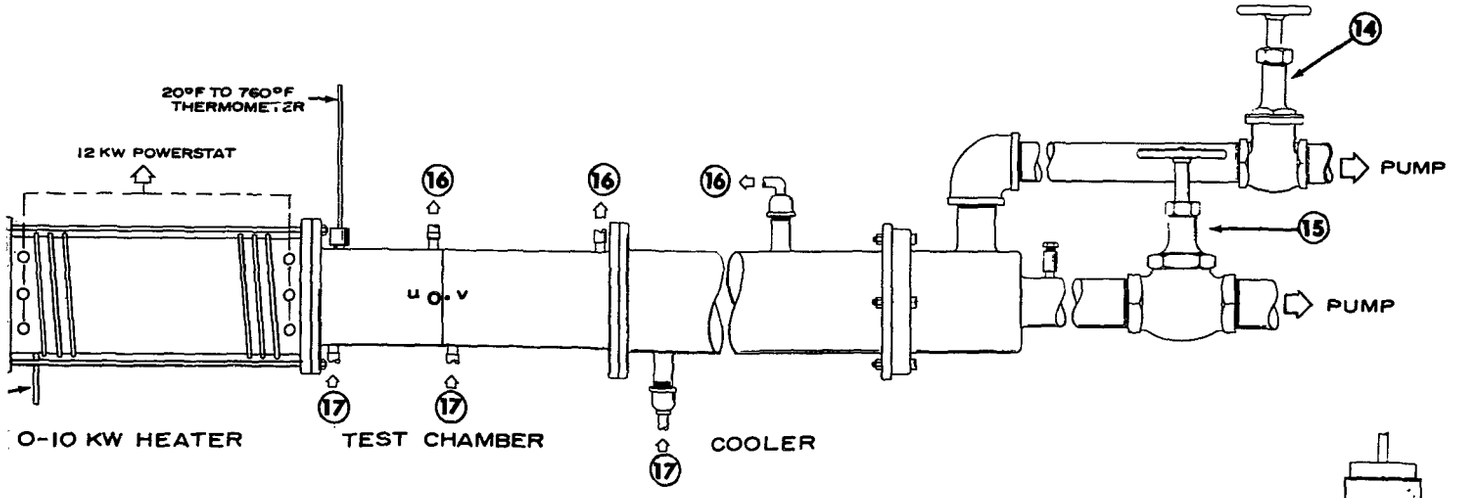

NOTE TUNNEL COMPONENTS SHOWN TO SCALE, OTHERS SHOWN SCHEMATICALLY

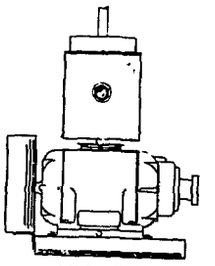

130 CFM
VACUUM PUMP

PRESSURE HIGH TEMPERATURE PERMEABILITY APPARATUS

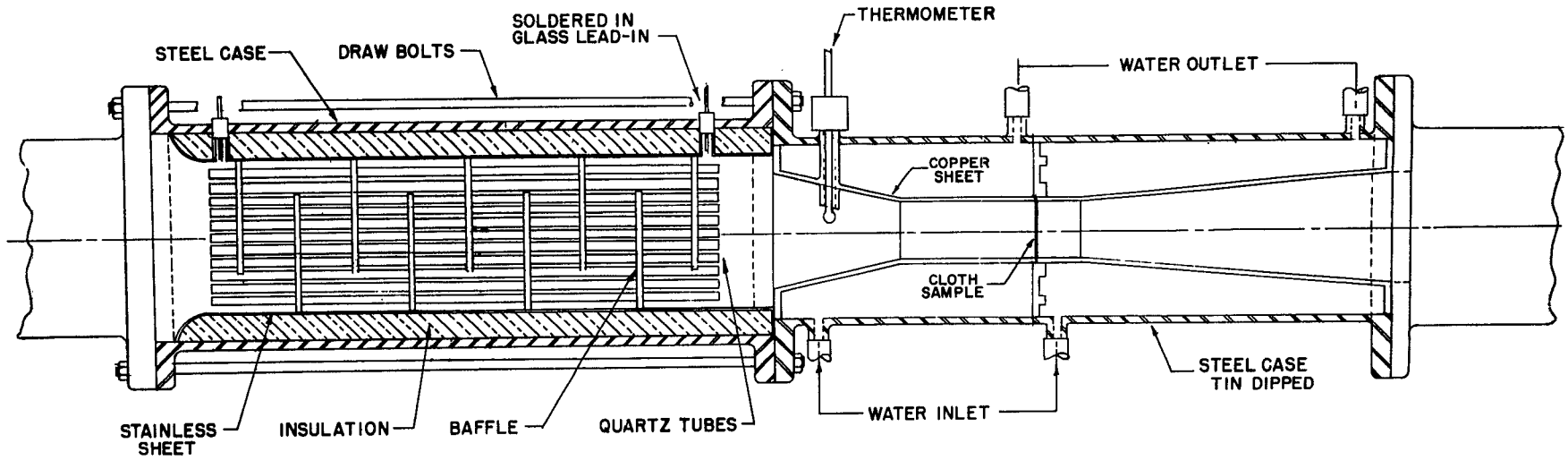

FIGURE 6 APPARATUS DETAILS

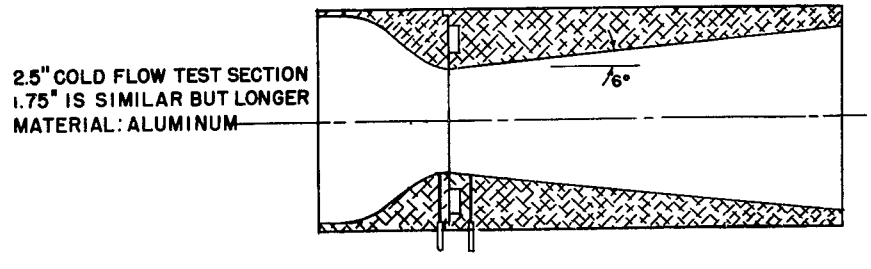

FIGURE 7 APPARATUS DETAILS

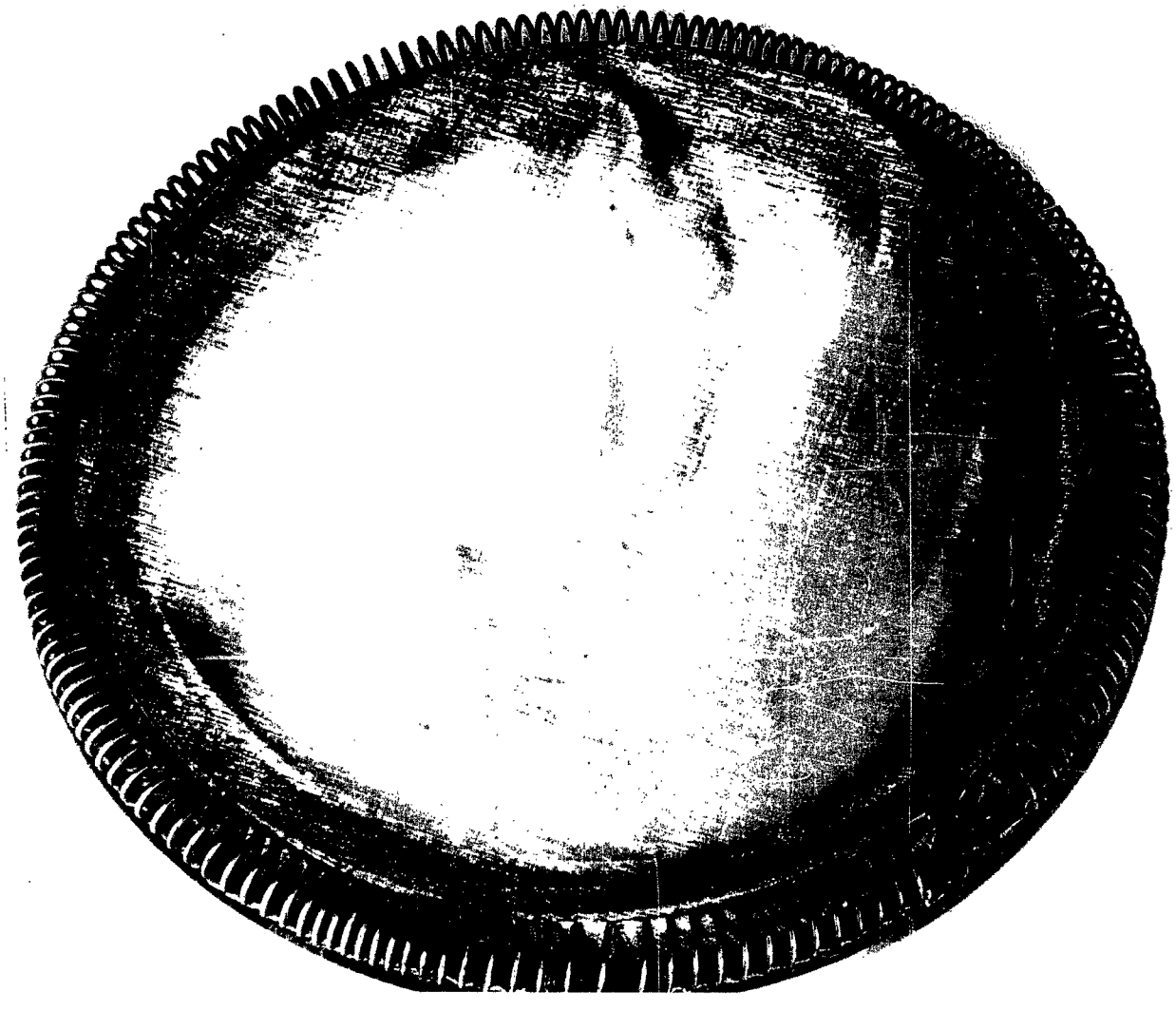

FIGURE 8 SAMPLE HOLDER (SHOWN WITH STAINLESS STEEL FABRIC) DIAMETER 3.5"

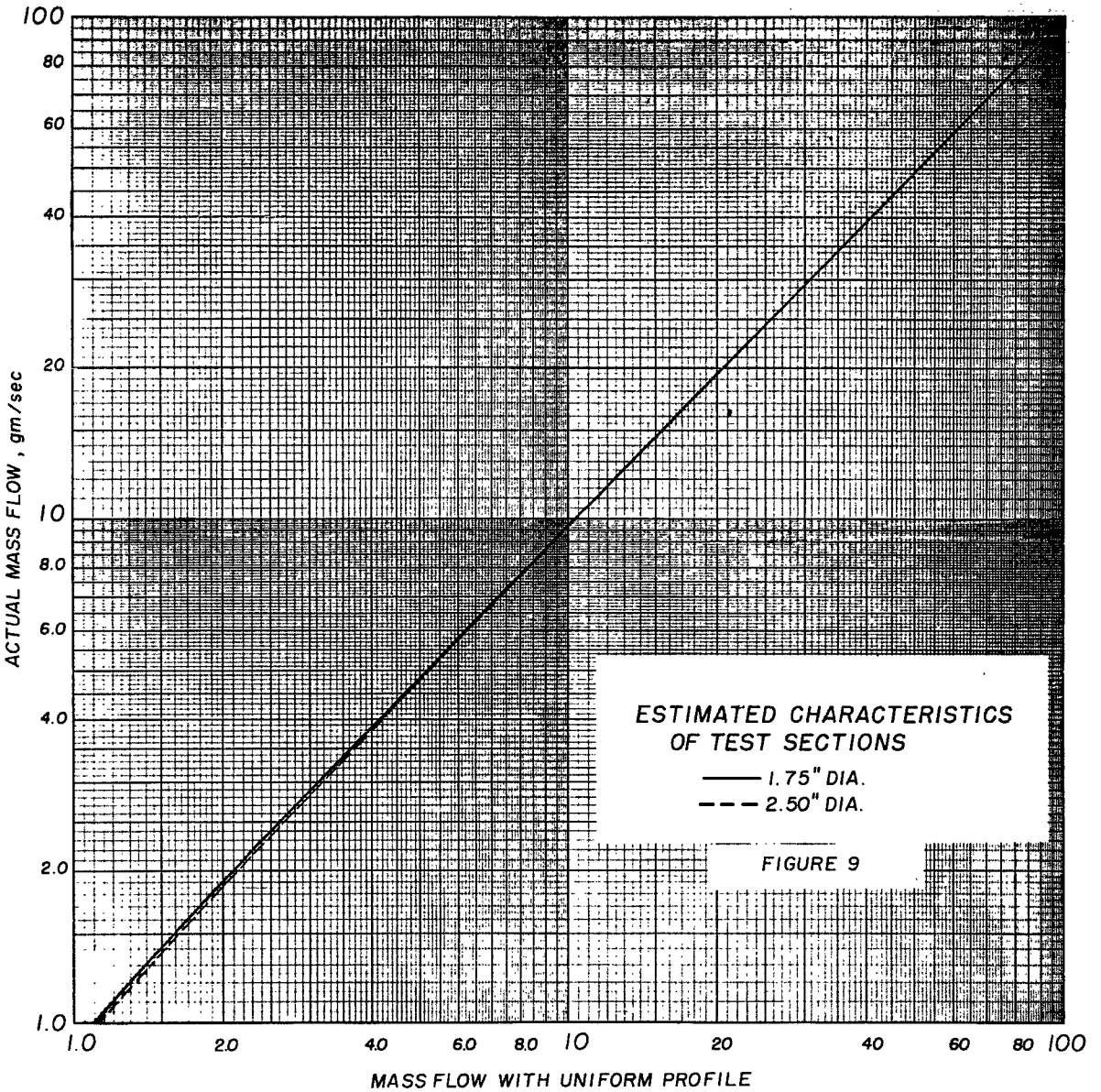
100
80
60
40
20
10
8.0
6.0
4.0
2.0
1.0
ACTUAL MASS FLOW , gm/sec
1.0
2.0
4.0
6.0
8.0
10
20
40
60
80
100
MASS FLOW WITH UNIFORM PROFILE
ESTIMATED CHARACTERISTICS
OF TEST SECTIONS
1.75" DIA.
2.50" DIA.

FIGURE 9

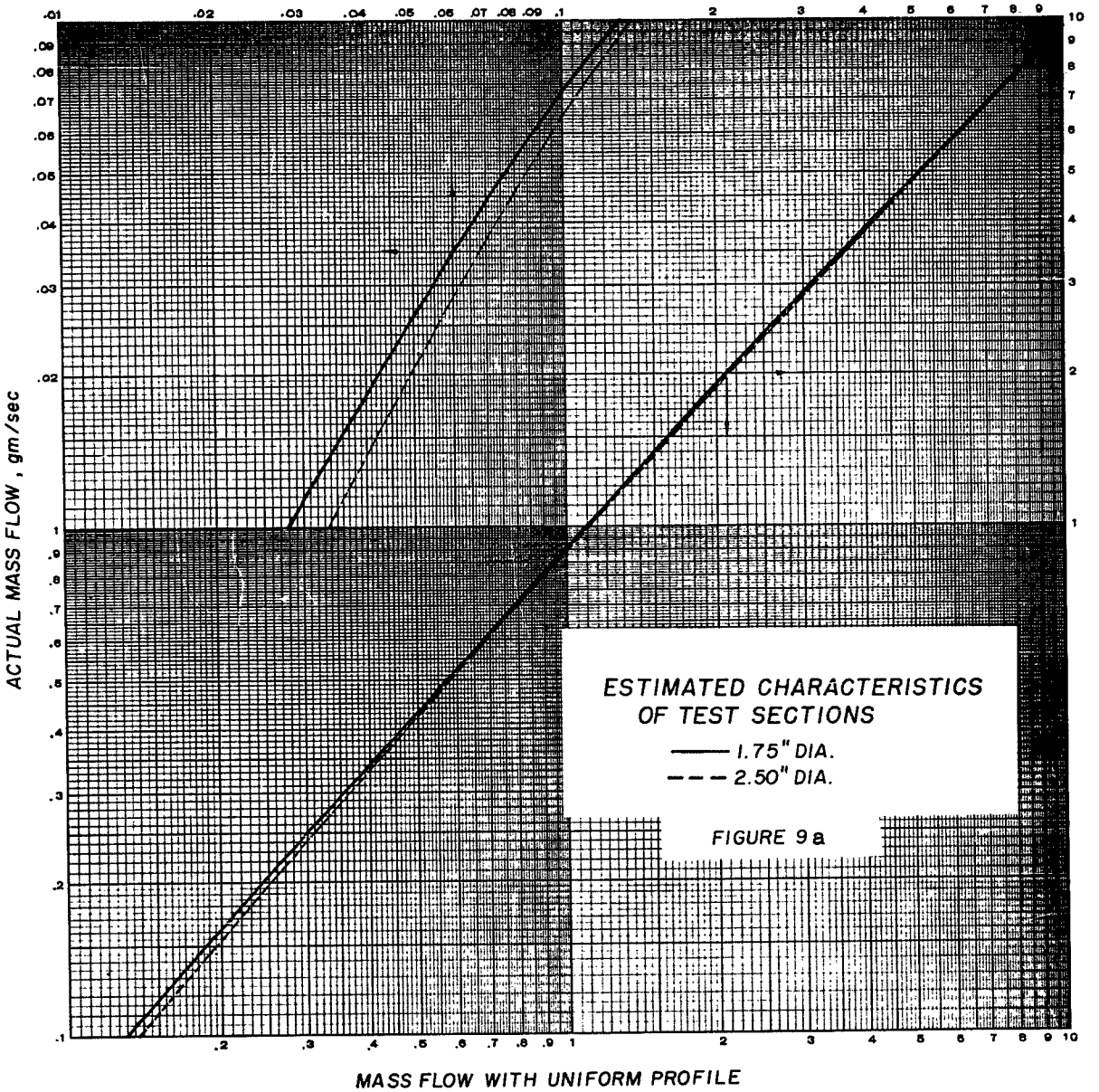
ACTUAL MASS FLOW , gm/sec
MASS FLOW WITH UNIFORM PROFILE
ESTIMATED CHARACTERISTICS
OF TEST SECTIONS
1.75" DIA.
2.50" DIA.

FIGURE 9a

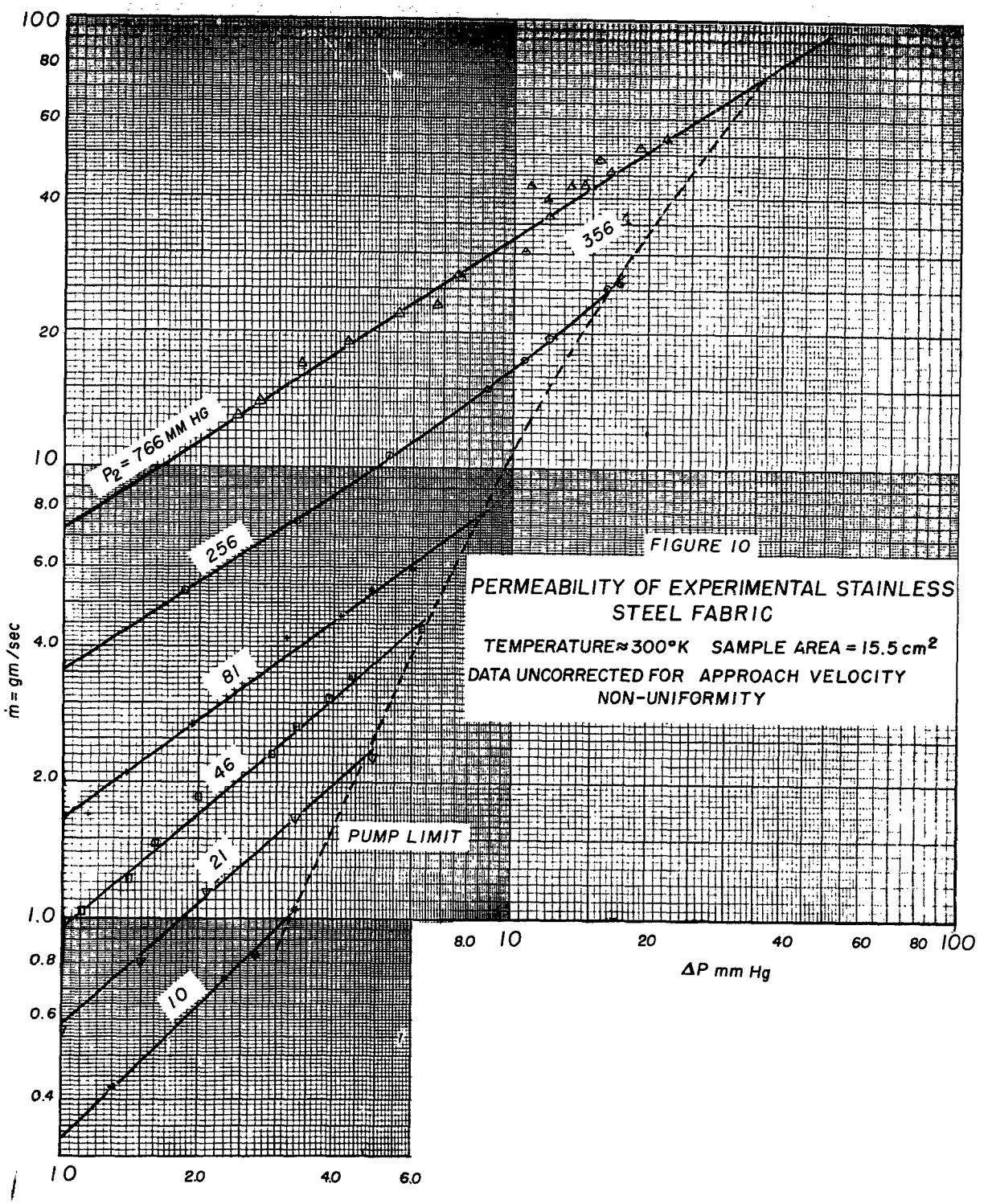

FIGURE 10

PERMEABILITY OF EXPERIMENTAL STAINLESS STEEL FABRIC

TEMPERATURE≈300°K SAMPLE AREA = 15.5 cm^2

DATA UNCORRECTED FOR APPROACH VELOCITY NON-UNIFORMITY

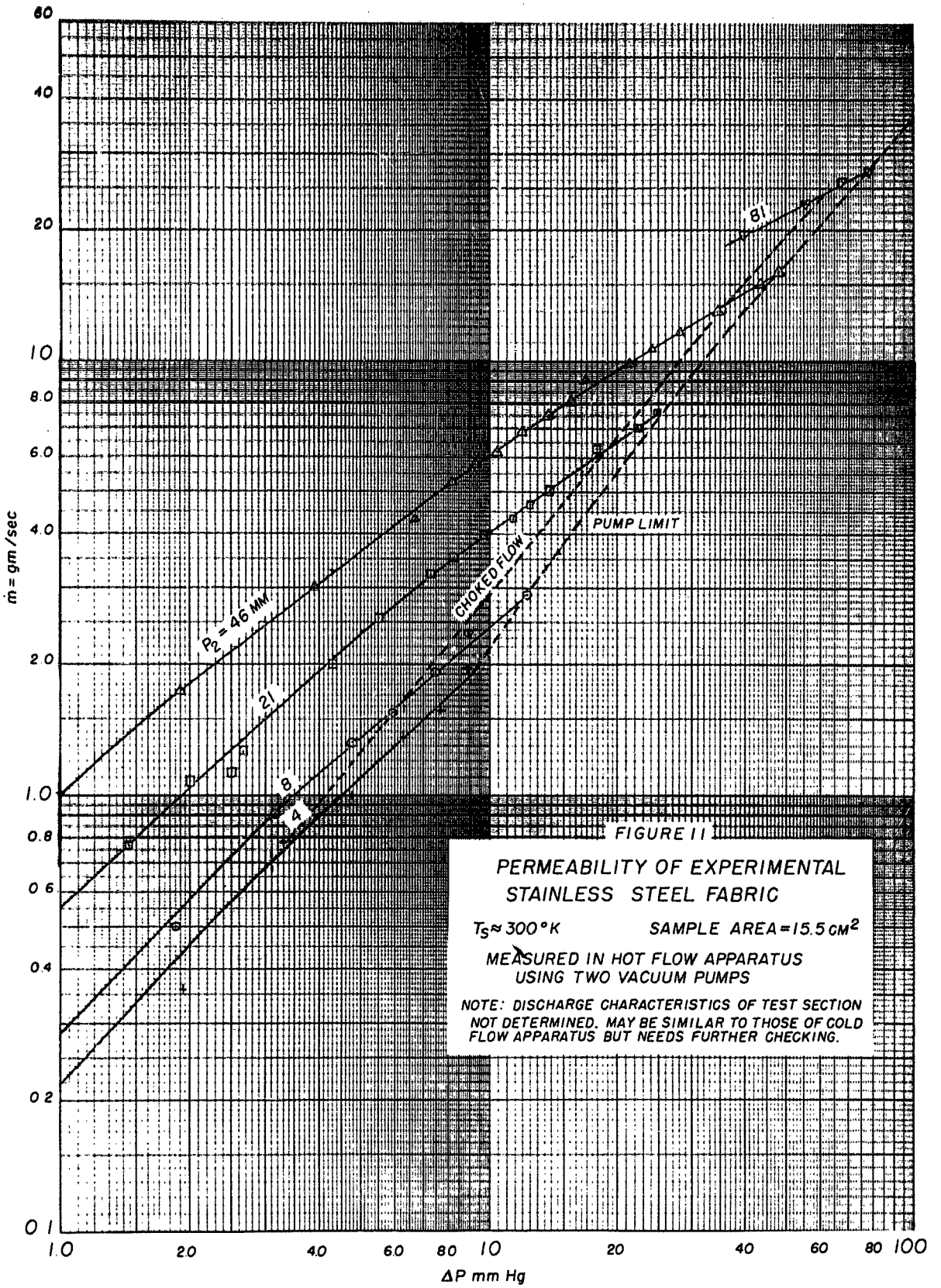

FIGURE 11

PERMEABILITY OF EXPERIMENTAL STAINLESS STEEL FABRIC

$T_S \approx 300°K$ SAMPLE AREA = 15.5 CM^2

MEASURED IN HOT FLOW APPARATUS USING TWO VACUUM PUMPS

NOTE: DISCHARGE CHARACTERISTICS OF TEST SECTION NOT DETERMINED. MAY BE SIMILAR TO THOSE OF COLD FLOW APPARATUS BUT NEEDS FURTHER CHECKING.

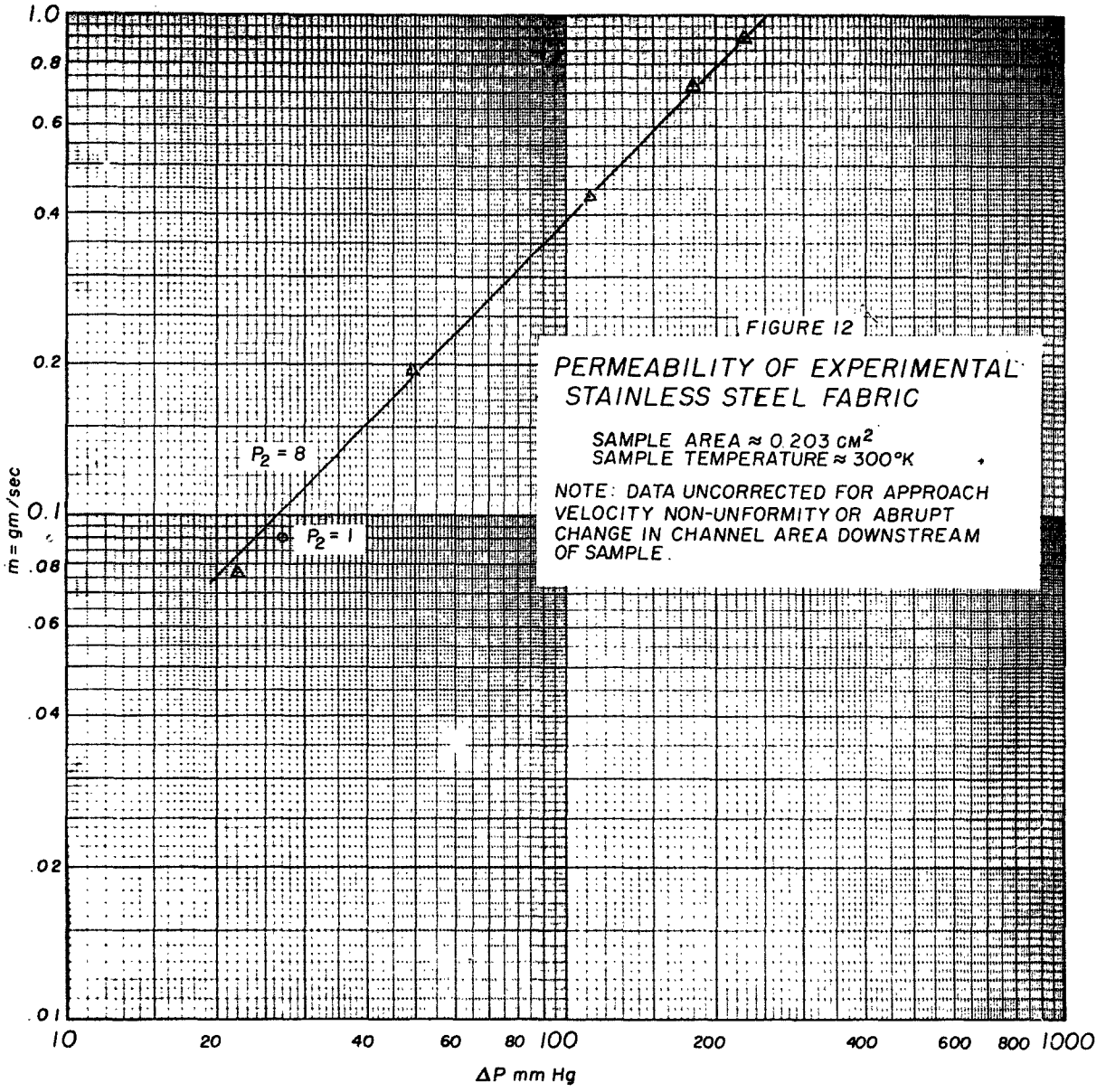

FIGURE 12

PERMEABILITY OF EXPERIMENTAL STAINLESS STEEL FABRIC

SAMPLE AREA ≈ 0.203 cm^2
SAMPLE TEMPERATURE ≈ 300°K

NOTE: DATA UNCORRECTED FOR APPROACH VELOCITY NON-UNFORMITY OR ABRUPT CHANGE IN CHANNEL AREA DOWNSTREAM OF SAMPLE.

FIGURE 13

PERMEABILITY OF MIL-C-7

SAMPLE AREA = 15.5 cm² SAMPLE

DATA UNCORRECTED FOR APPROACH V

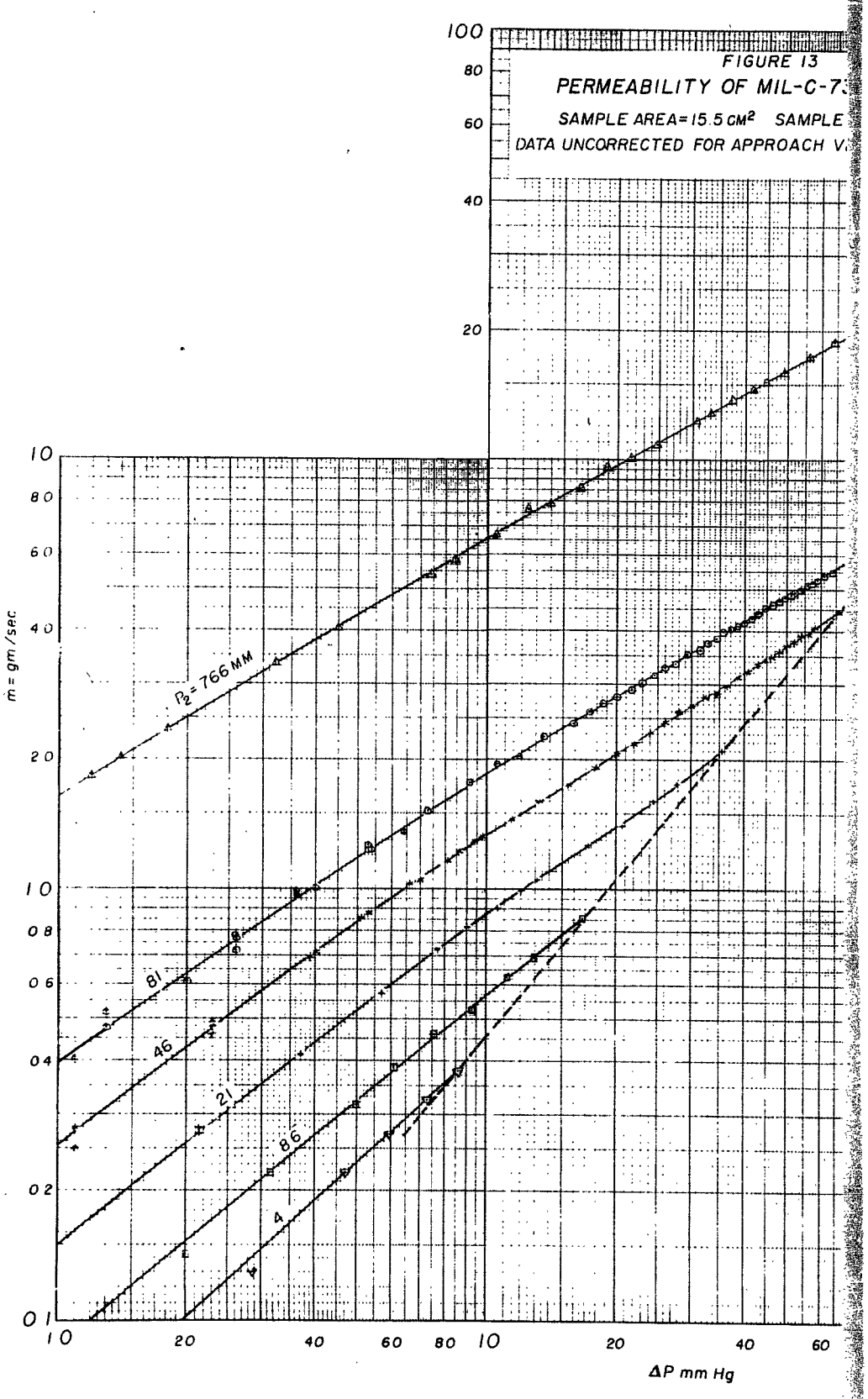

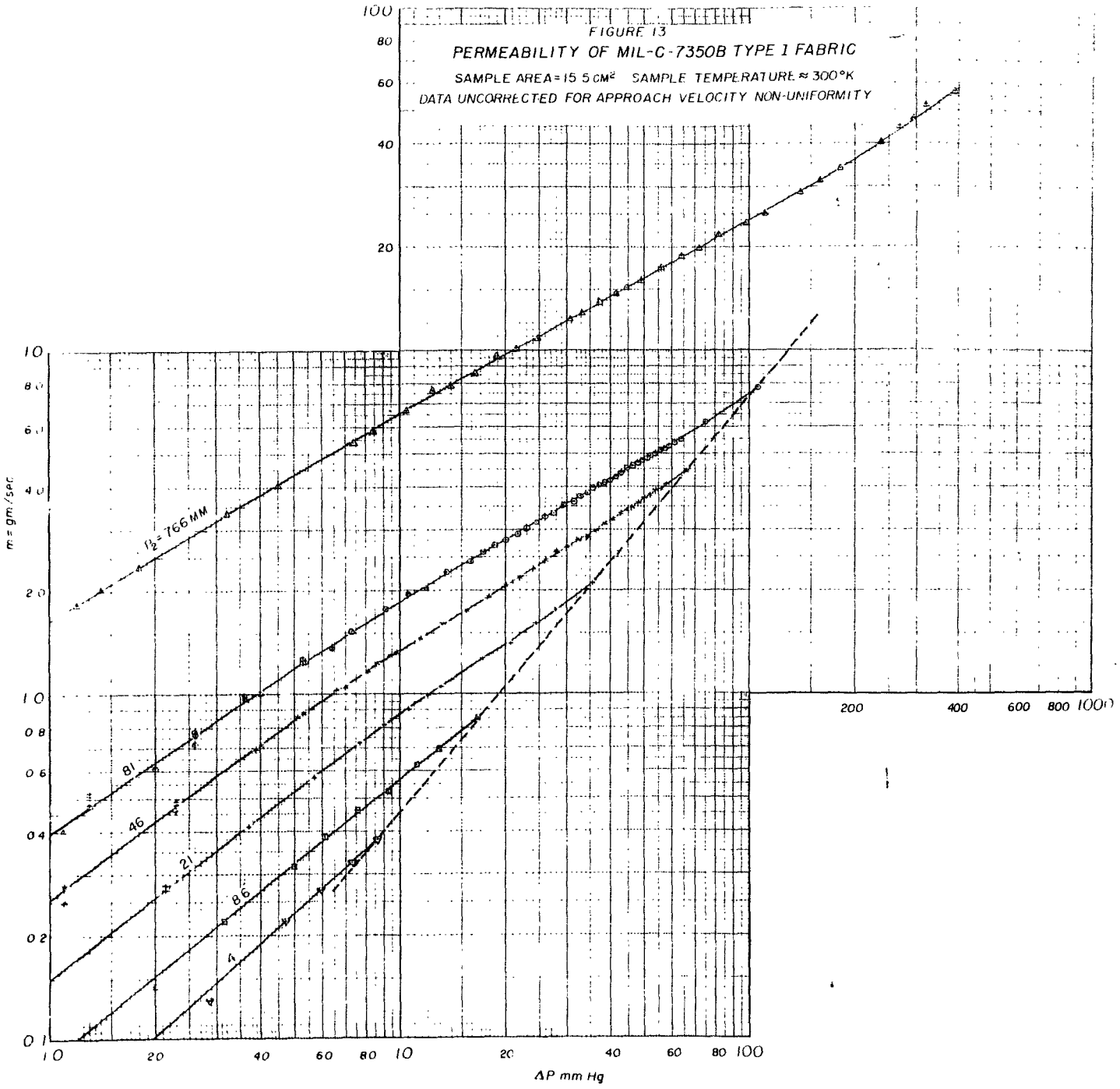
FIGURE 13
PERMEABILITY OF MIL-C-7350B TYPE I FABRIC
SAMPLE AREA = 15.5 CM² SAMPLE TEMPERATURE ≈ 300°K
DATA UNCORRECTED FOR APPROACH VELOCITY NON-UNIFORMITY
m = gm/sec
ΔP mm Hg
P₂ = 766 MM
81
46
21
8.6
4

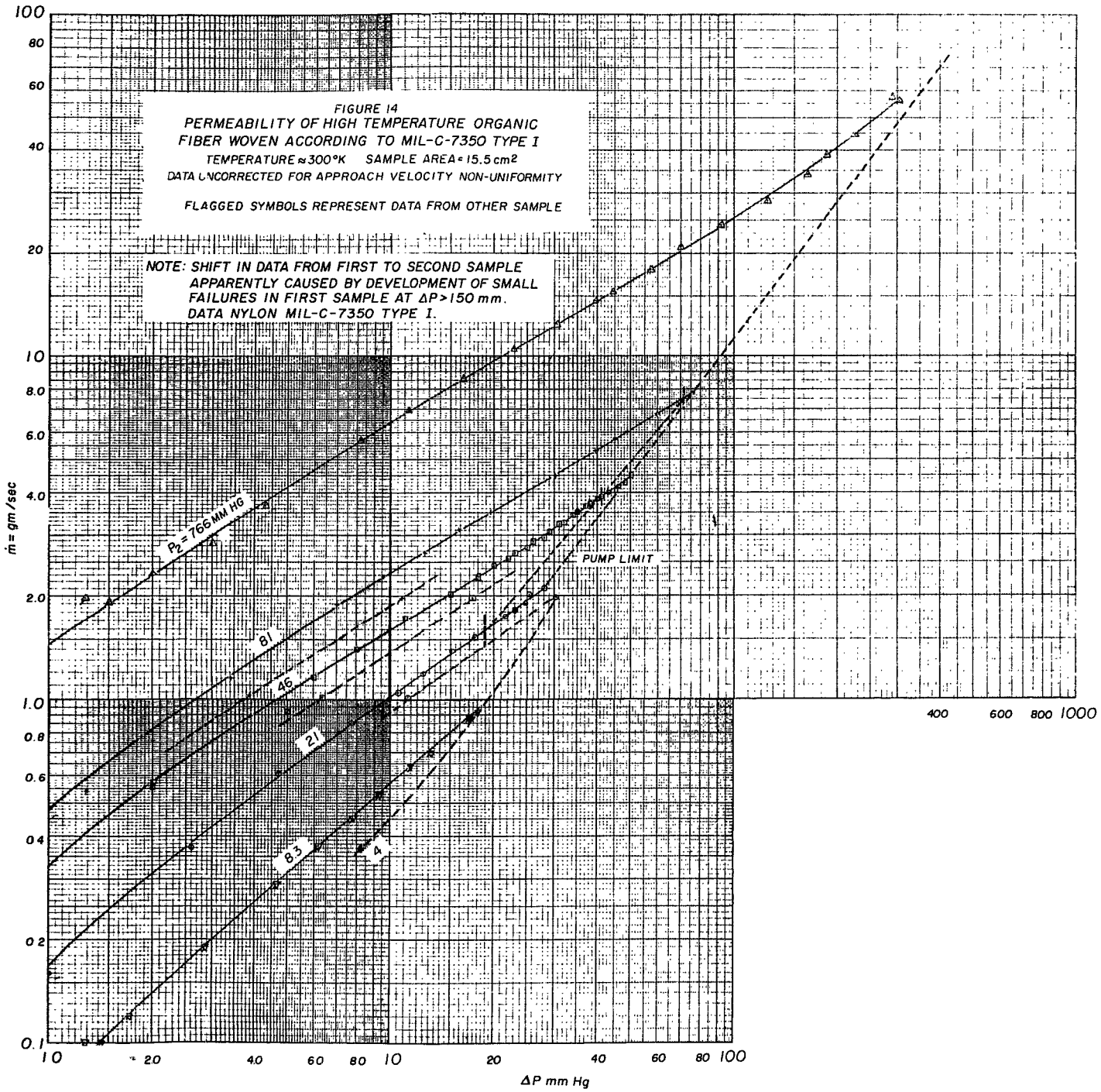
FIGURE 14
PERMEABILITY OF HIGH TEMPERATURE ORGANIC FIBER WOVEN ACCORDING TO MIL-C-7350 TYPE I
TEMPERATURE ≈ 300°K SAMPLE AREA = 15.5 cm2
DATA UNCORRECTED FOR APPROACH VELOCITY NON-UNIFORMITY
FLAGGED SYMBOLS REPRESENT DATA FROM OTHER SAMPLE
NOTE: SHIFT IN DATA FROM FIRST TO SECOND SAMPLE APPARENTLY CAUSED BY DEVELOPMENT OF SMALL FAILURES IN FIRST SAMPLE AT ΔP > 150 mm.
DATA NYLON MIL-C-7350 TYPE I.
Pz = 766 MM HG
PUMP LIMIT
81
46
21
83
4
ṁ = gm/sec
ΔP mm Hg
100
80
60
40
20
10
8.0
6.0
4.0
2.0
1.0
0.8
0.6
0.4
0.2
0.1
10
20
40
60
80
100
200
400
600
800
1000

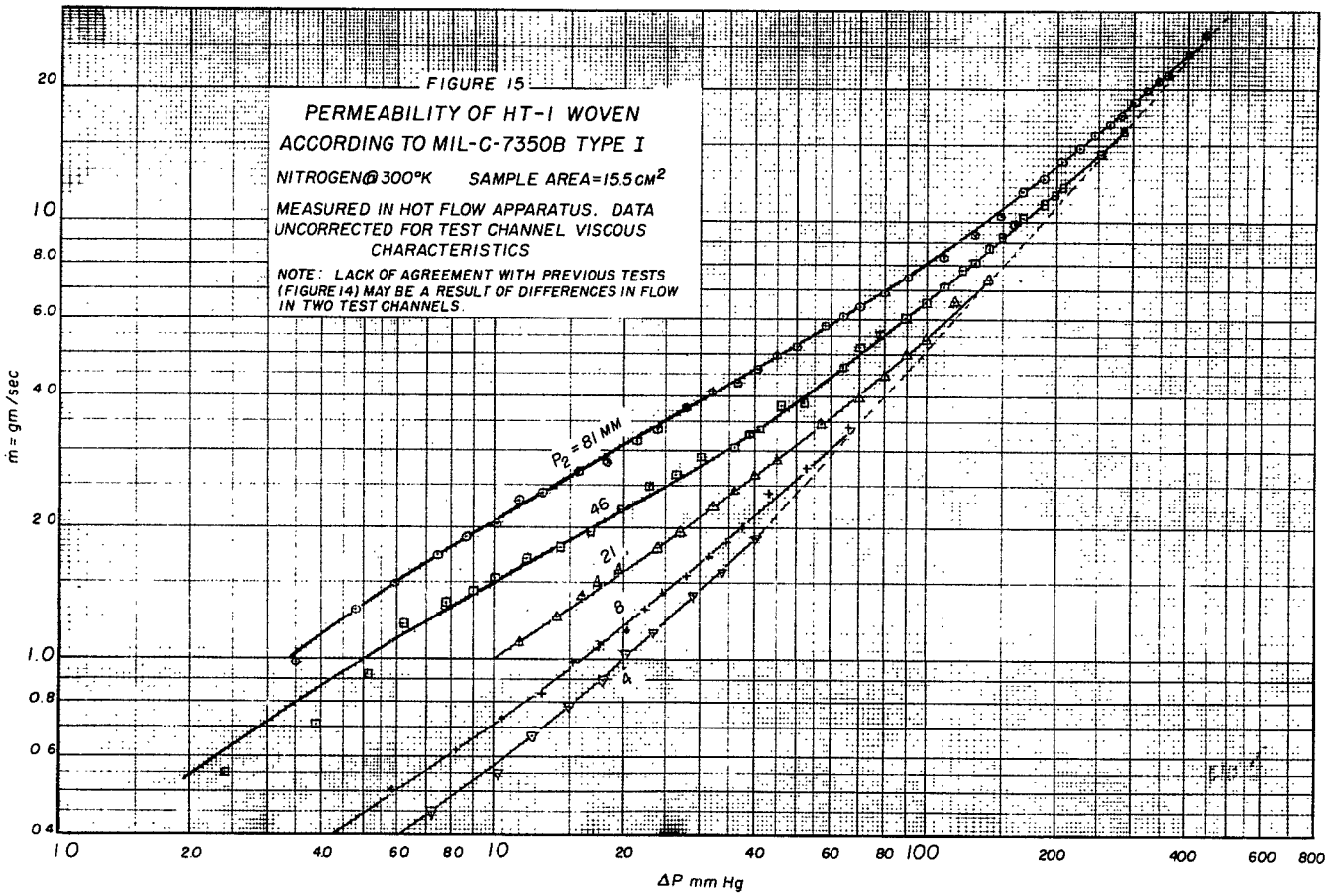
FIGURE 15
PERMEABILITY OF HT-1 WOVEN
ACCORDING TO MIL-C-7350B TYPE I
NITROGEN @ 300°K SAMPLE AREA=15.5 cm²
MEASURED IN HOT FLOW APPARATUS. DATA
UNCORRECTED FOR TEST CHANNEL VISCOUS
CHARACTERISTICS
NOTE: LACK OF AGREEMENT WITH PREVIOUS TESTS
(FIGURE 14) MAY BE A RESULT OF DIFFERENCES IN FLOW
IN TWO TEST CHANNELS.
P_2 = 81 MM
46
21
8
4
ṁ = gm/sec
ΔP mm Hg
20
10
8.0
6.0
4.0
2.0
1.0
0.8
0.6
0.4
10
20
40
60
80
100
200
400
600
800

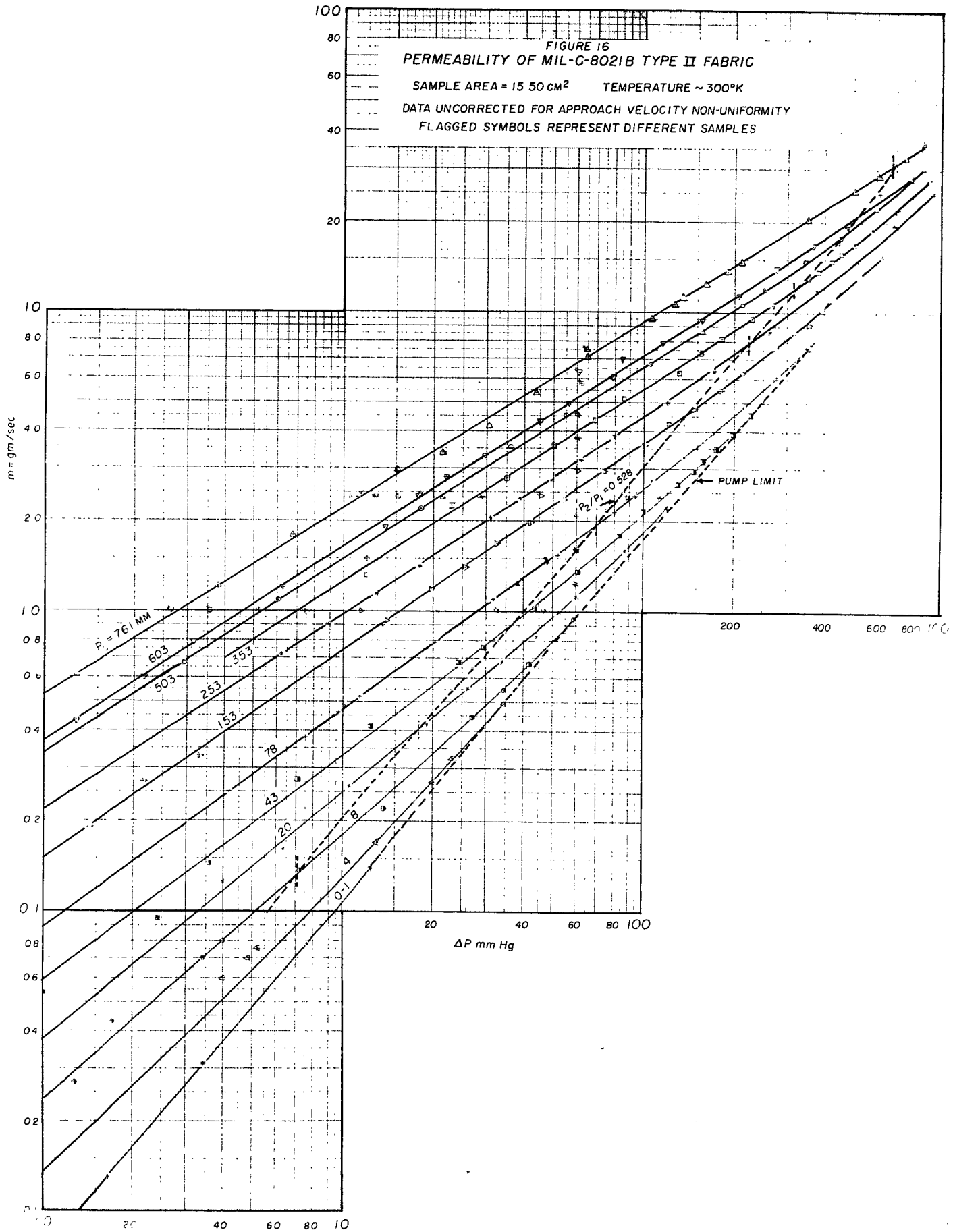
FIGURE 16
PERMEABILITY OF MIL-C-8021B TYPE II FABRIC
SAMPLE AREA = 15 50 cm²
TEMPERATURE ~ 300°K
DATA UNCORRECTED FOR APPROACH VELOCITY NON-UNIFORMITY
FLAGGED SYMBOLS REPRESENT DIFFERENT SAMPLES
m = gm/sec
ΔP mm Hg
P₁ = 761 MM
603
503
353
253
153
78
43
20
8
4
0-1
P₂/P₁ = 0 528
PUMP LIMIT

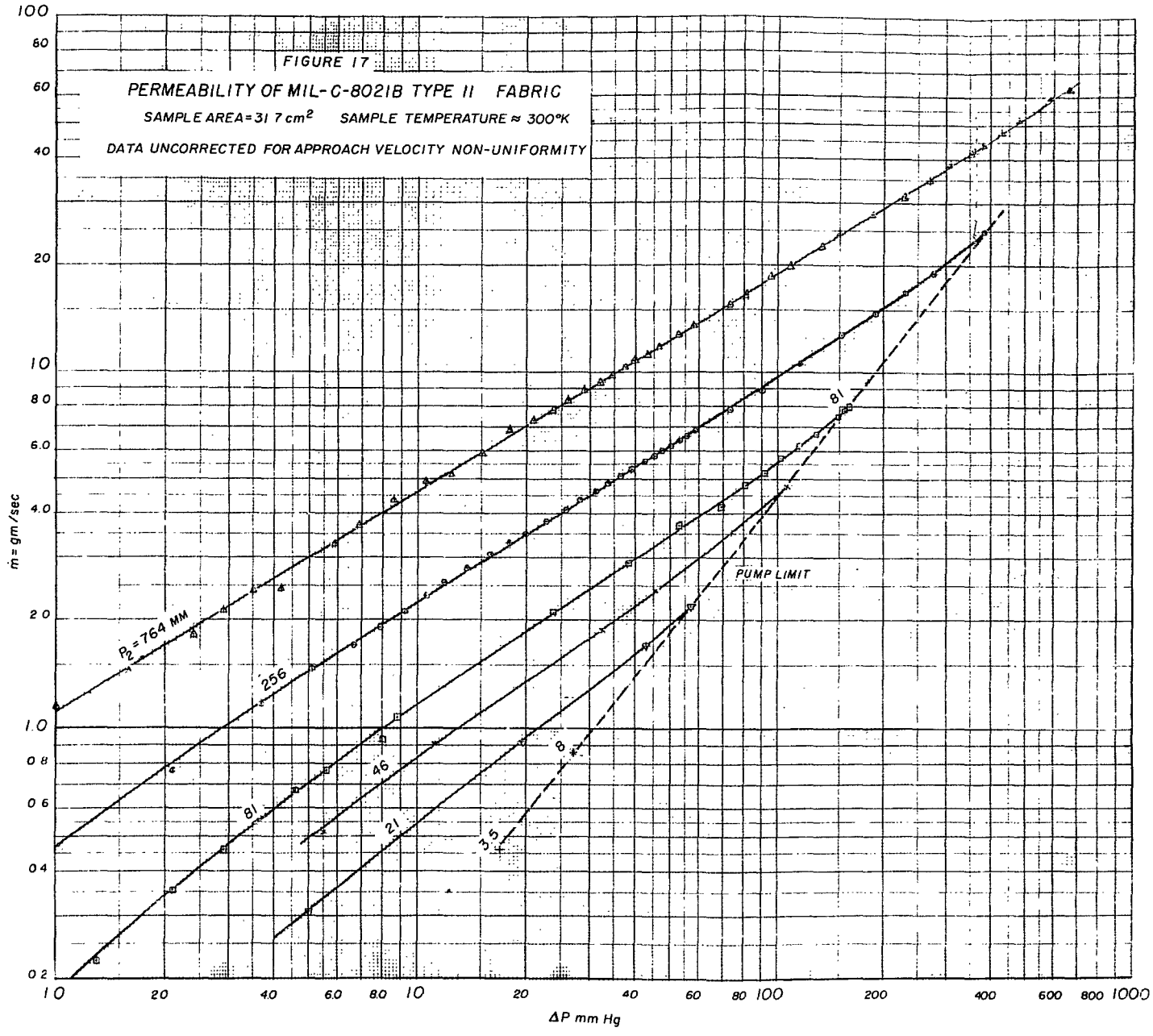
FIGURE 17
PERMEABILITY OF MIL-C-8021B TYPE II FABRIC
SAMPLE AREA = 31.7 cm² SAMPLE TEMPERATURE ≈ 300°K
DATA UNCORRECTED FOR APPROACH VELOCITY NON-UNIFORMITY
ṁ = gm/sec
ΔP mm Hg
P₂ = 764 MM
256
81
46
21
8
3.5
PUMP LIMIT
100
60
60
40
20
10
8.0
6.0
4.0
2.0
1.0
0.8
0.6
0.4
0.2
10
20
40
6.0
8.0
10
20
40
60
80
100
200
400
600
800
1000

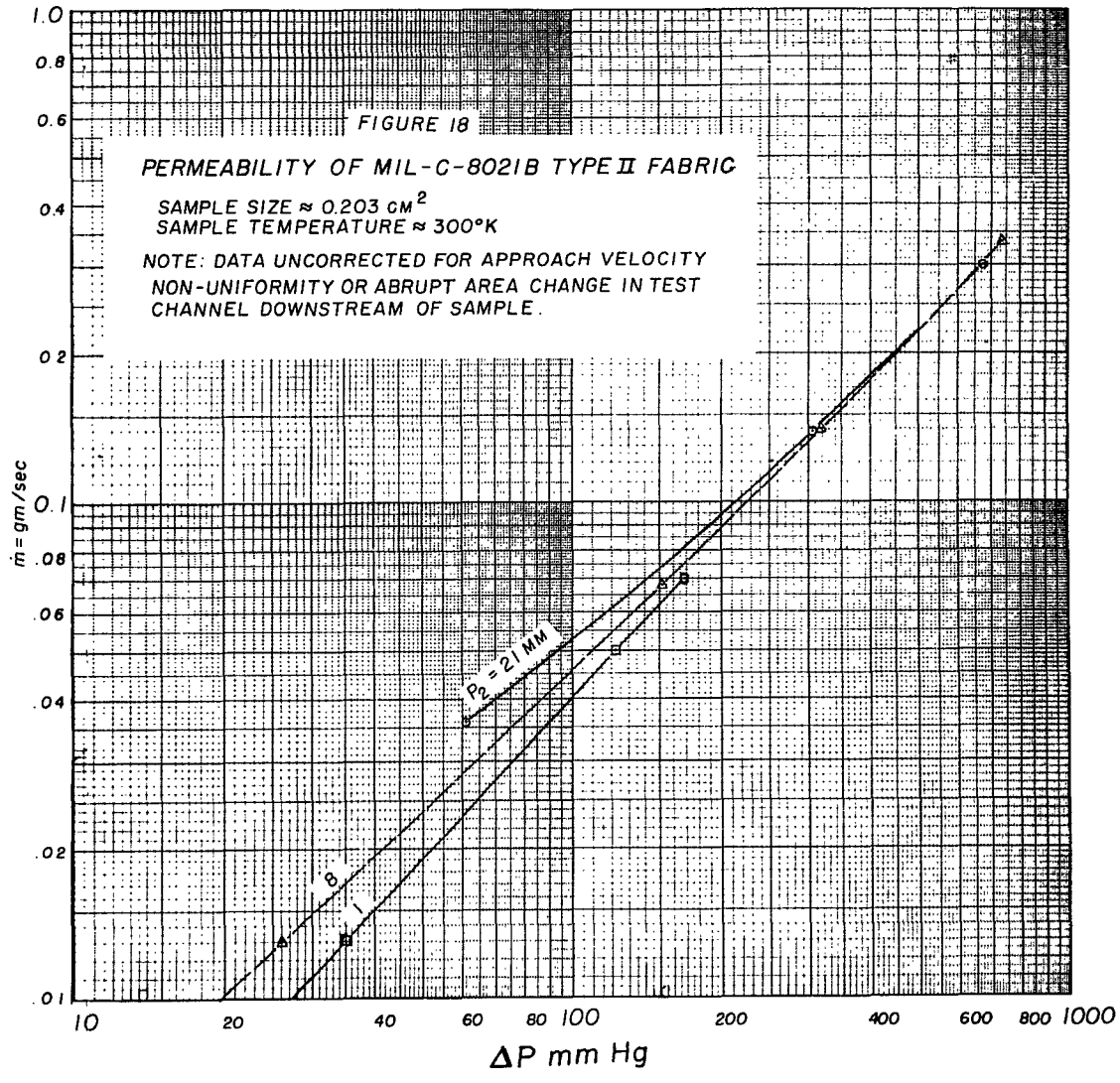
FIGURE 18
PERMEABILITY OF MIL-C-8021B TYPE II FABRIC
SAMPLE SIZE ≈ 0.203 cm²
SAMPLE TEMPERATURE ≈ 300°K
NOTE: DATA UNCORRECTED FOR APPROACH VELOCITY NON-UNIFORMITY OR ABRUPT AREA CHANGE IN TEST CHANNEL DOWNSTREAM OF SAMPLE.
ṁ = gm/sec
1.0
0.8
0.6
0.4
0.2
0.1
.08
.06
.04
.02
.01
10
20
40
60
80
100
200
400
600
800
1000
ΔP mm Hg
P2 = 21 MM
8
1

FIGURE 19

PERMEABILITY OF MIL-F-9084A TYPE VIII FABRIC

SAMPLE AREA = 15.5 cm² SAMPLE TEMPERATURE ≈ 300°K

DATA UNCORRECTED FOR APPROACH VELOCITY NON-UNIFORMITY

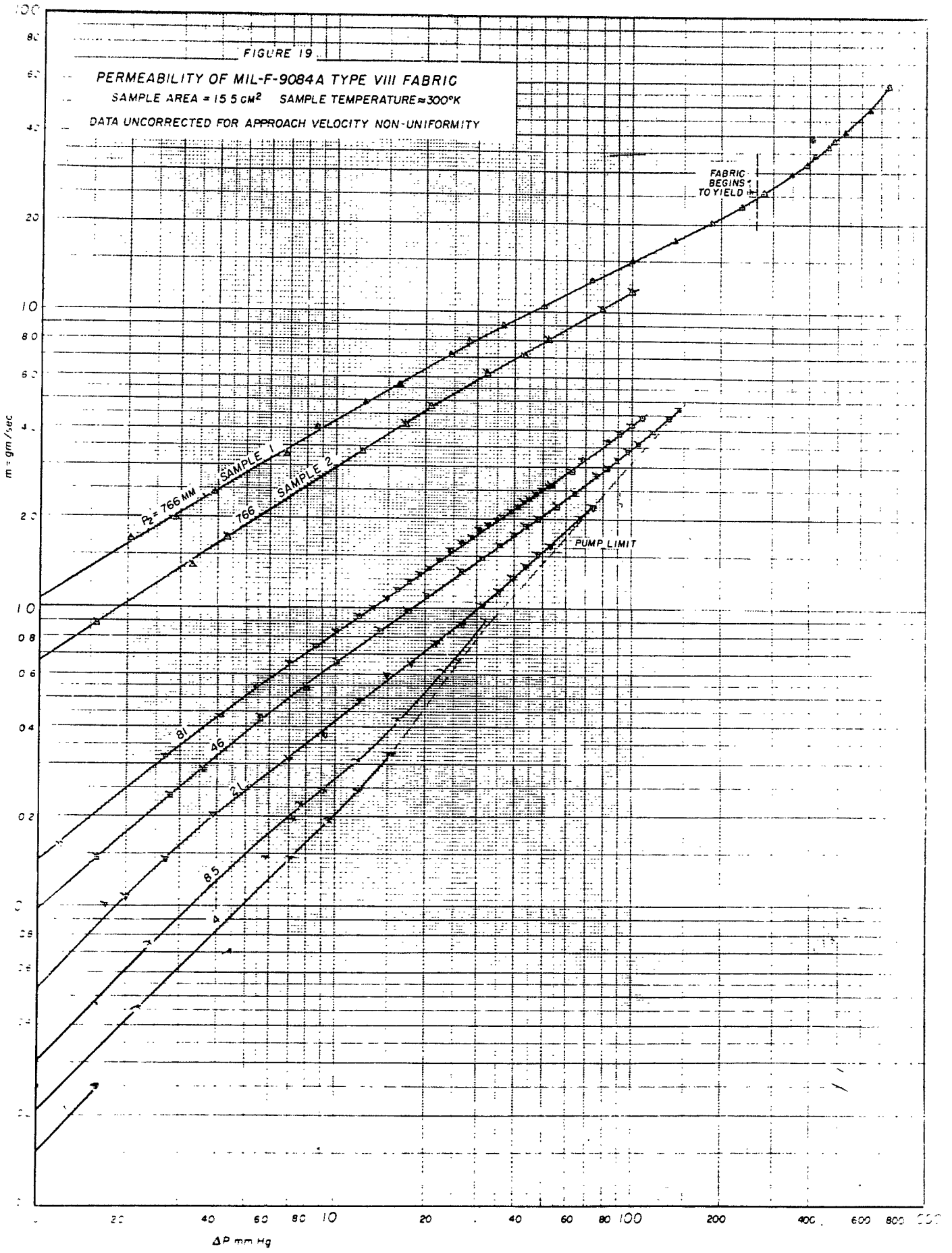

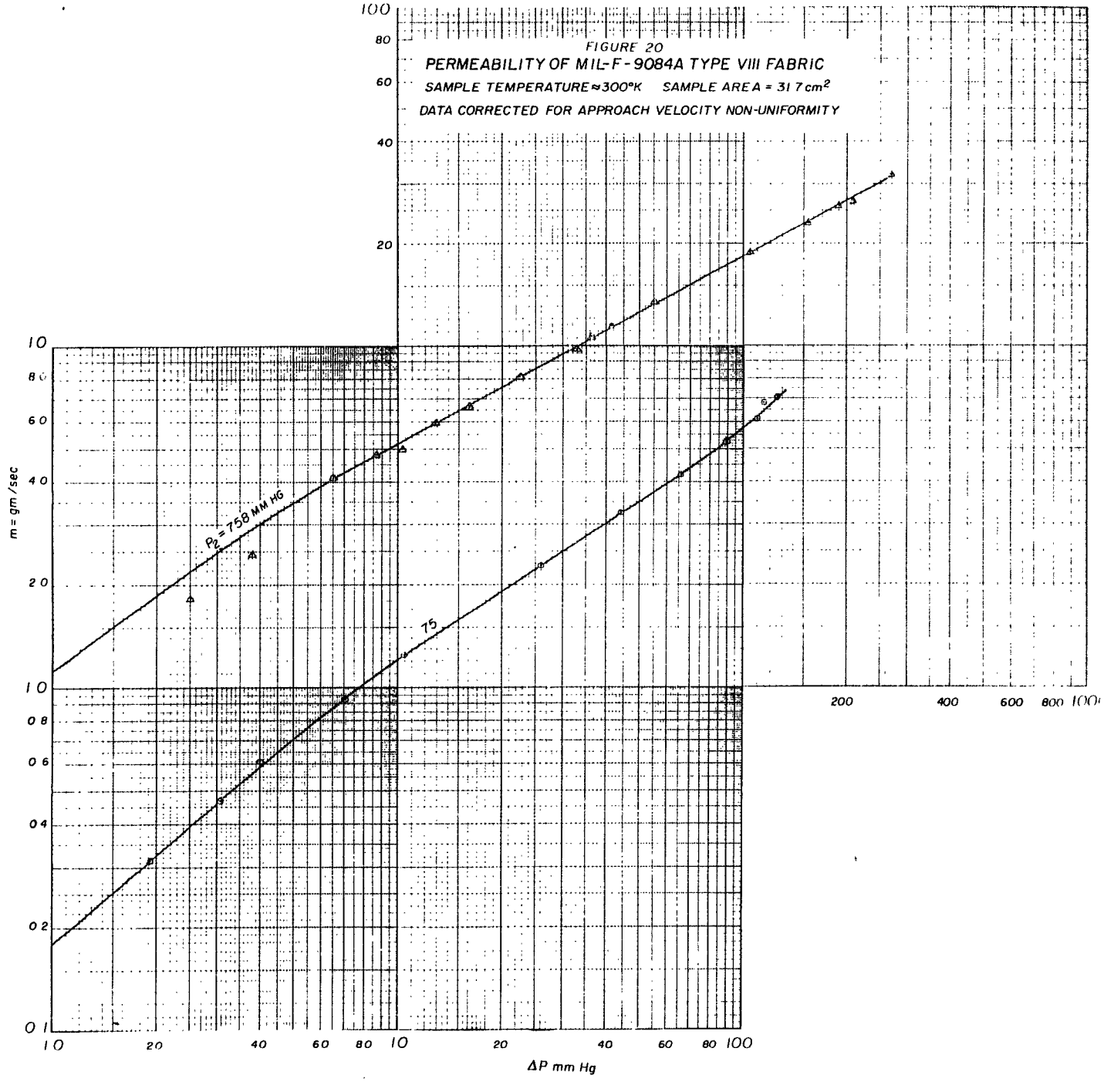
FIGURE 20
PERMEABILITY OF MIL-F-9084A TYPE VIII FABRIC
SAMPLE TEMPERATURE ≈ 300°K SAMPLE AREA = 31 7 cm²
DATA CORRECTED FOR APPROACH VELOCITY NON-UNIFORMITY
m = gm /sec
ΔP mm Hg
P₂ = 758 MM HG
75
100
80
60
40
20
10
8 0
6 0
4 0
2 0
1 0
0 8
0 6
0 4
0 2
0 1
10
20
40
60
80
10
20
40
60
80
100
200
400
600
800
1000

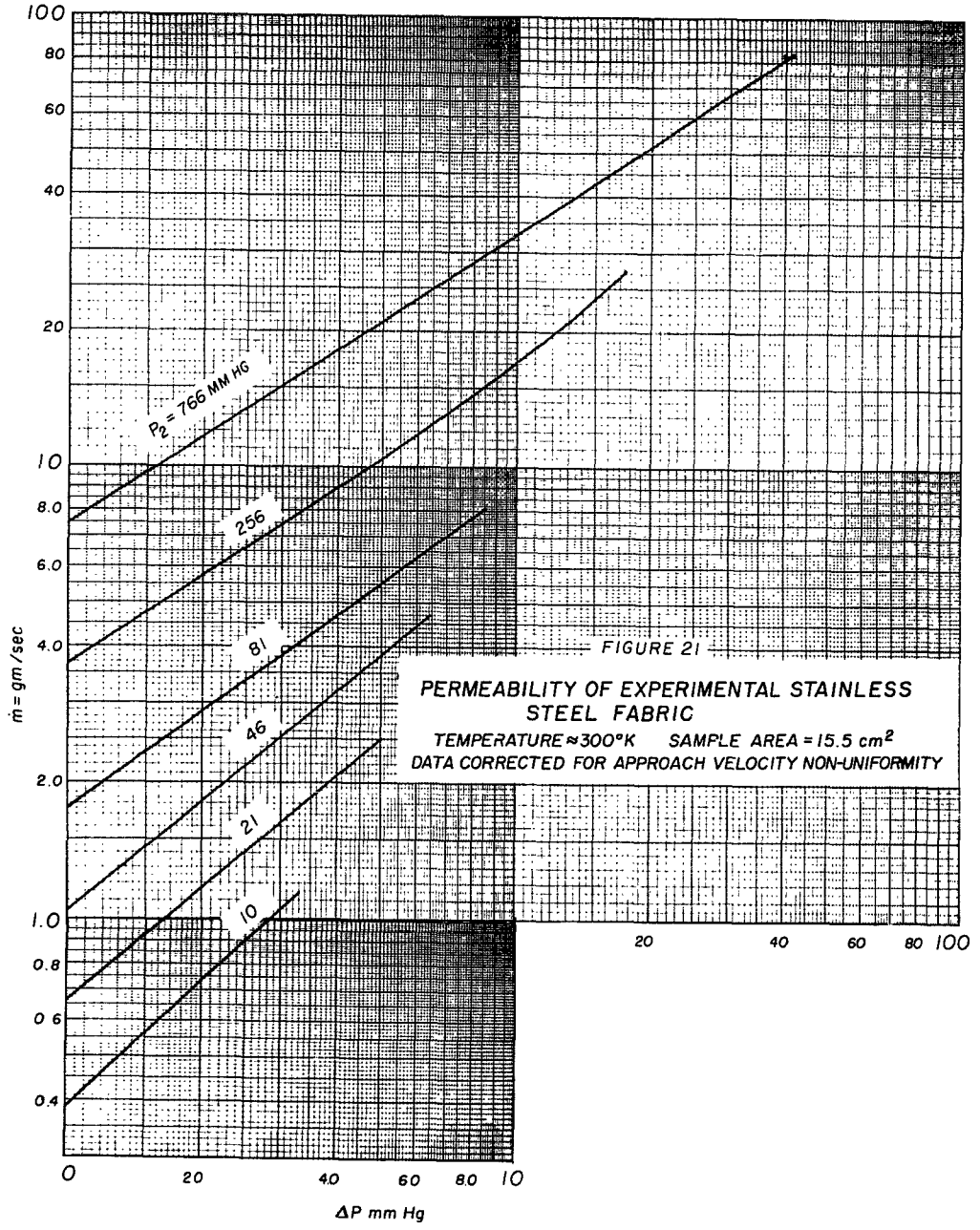

FIGURE 21

PERMEABILITY OF EXPERIMENTAL STAINLESS STEEL FABRIC

TEMPERATURE ≈ 300°K SAMPLE AREA = 15.5 cm^2

DATA CORRECTED FOR APPROACH VELOCITY NON-UNIFORMITY

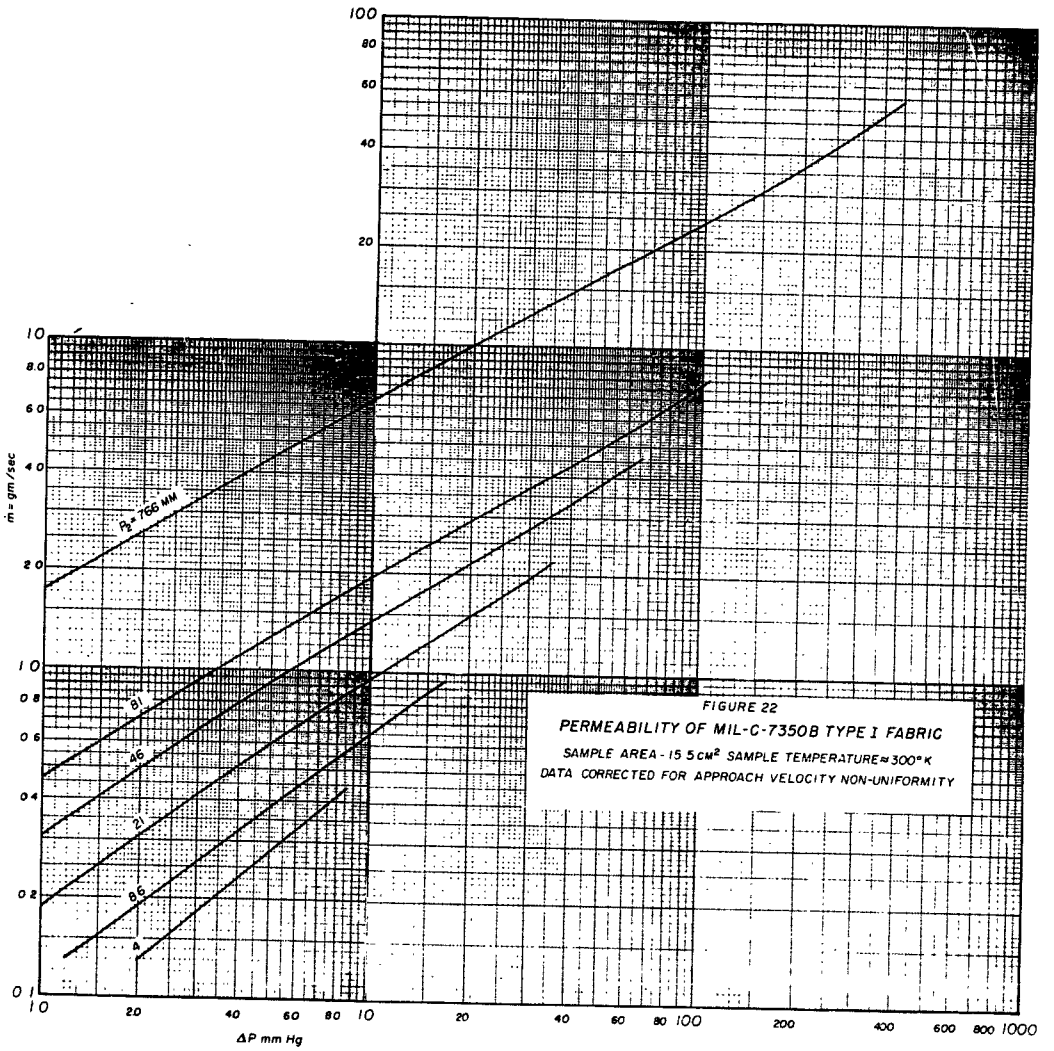

FIGURE 22

PERMEABILITY OF MIL-C-7350B TYPE I FABRIC

SAMPLE AREA - 15.5 cm² SAMPLE TEMPERATURE ≈ 300° K

DATA CORRECTED FOR APPROACH VELOCITY NON-UNIFORMITY

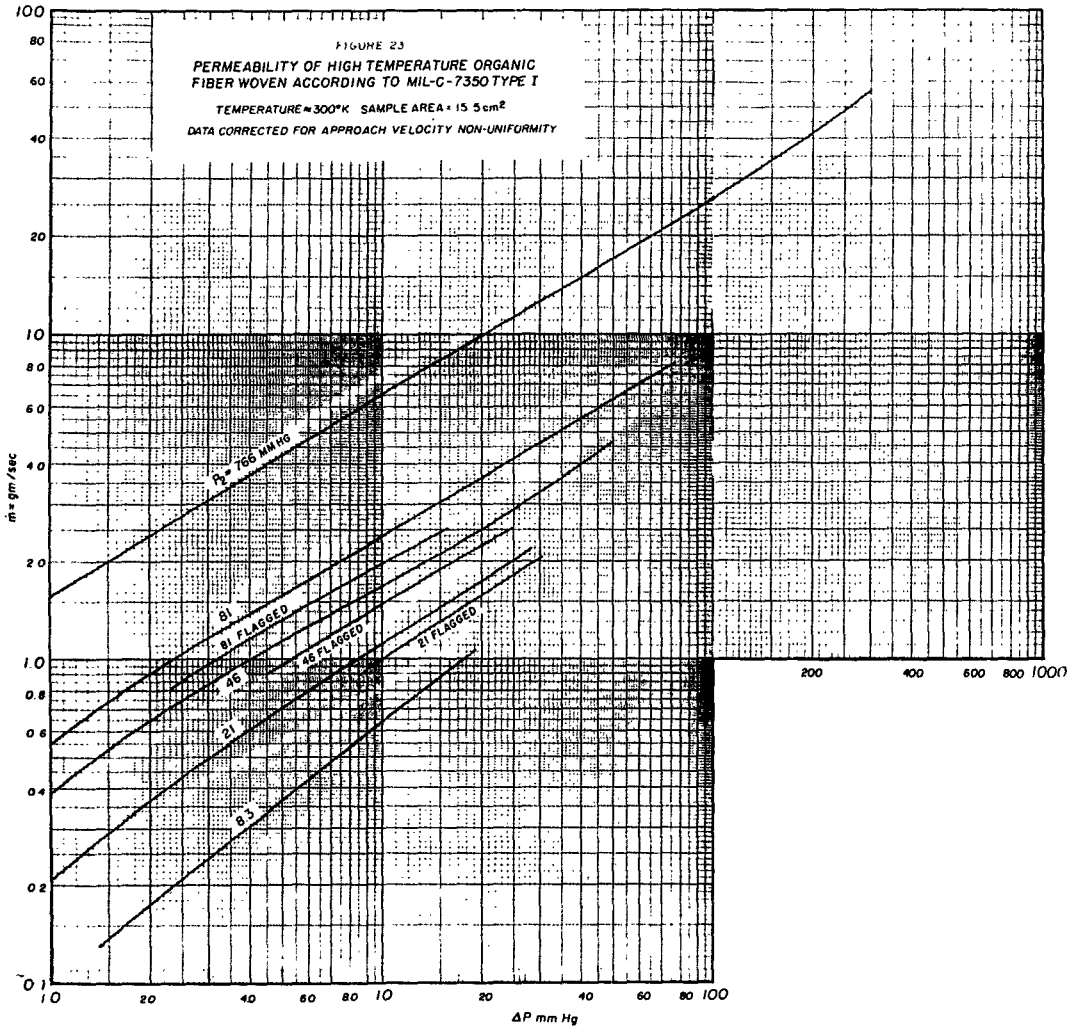

* Flagged Symbols Represent Data from Other Sample

FIGURE 24

PERMEABILITY OF MIL-C-8021B TYPE II FABRIC

SAMPLE. AREA = 15.50 cm^2
TEMPERATURE ~ 300° K
DATA CORRECTED FOR APPROACH VELOCITY NON-UNIFORMITY

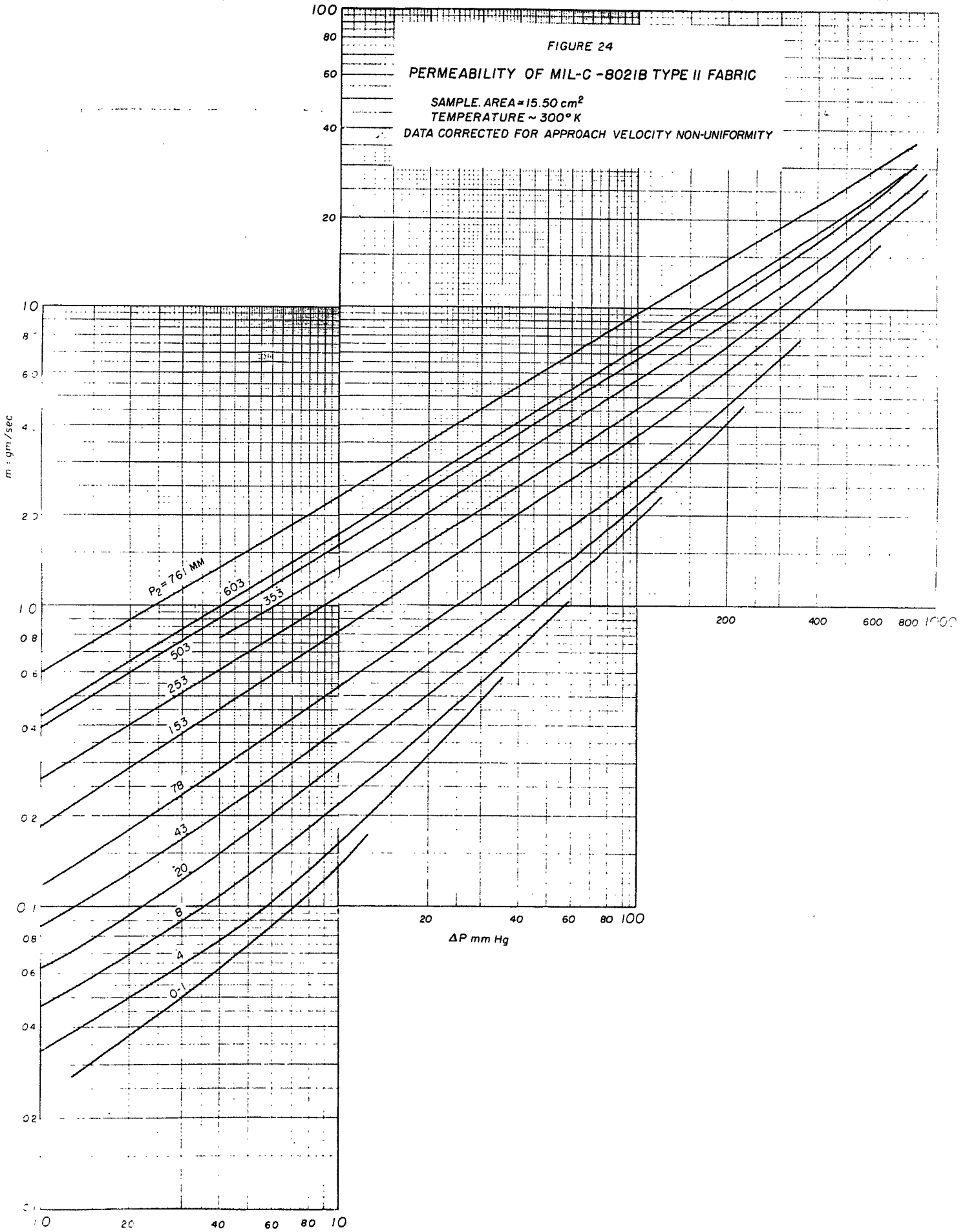

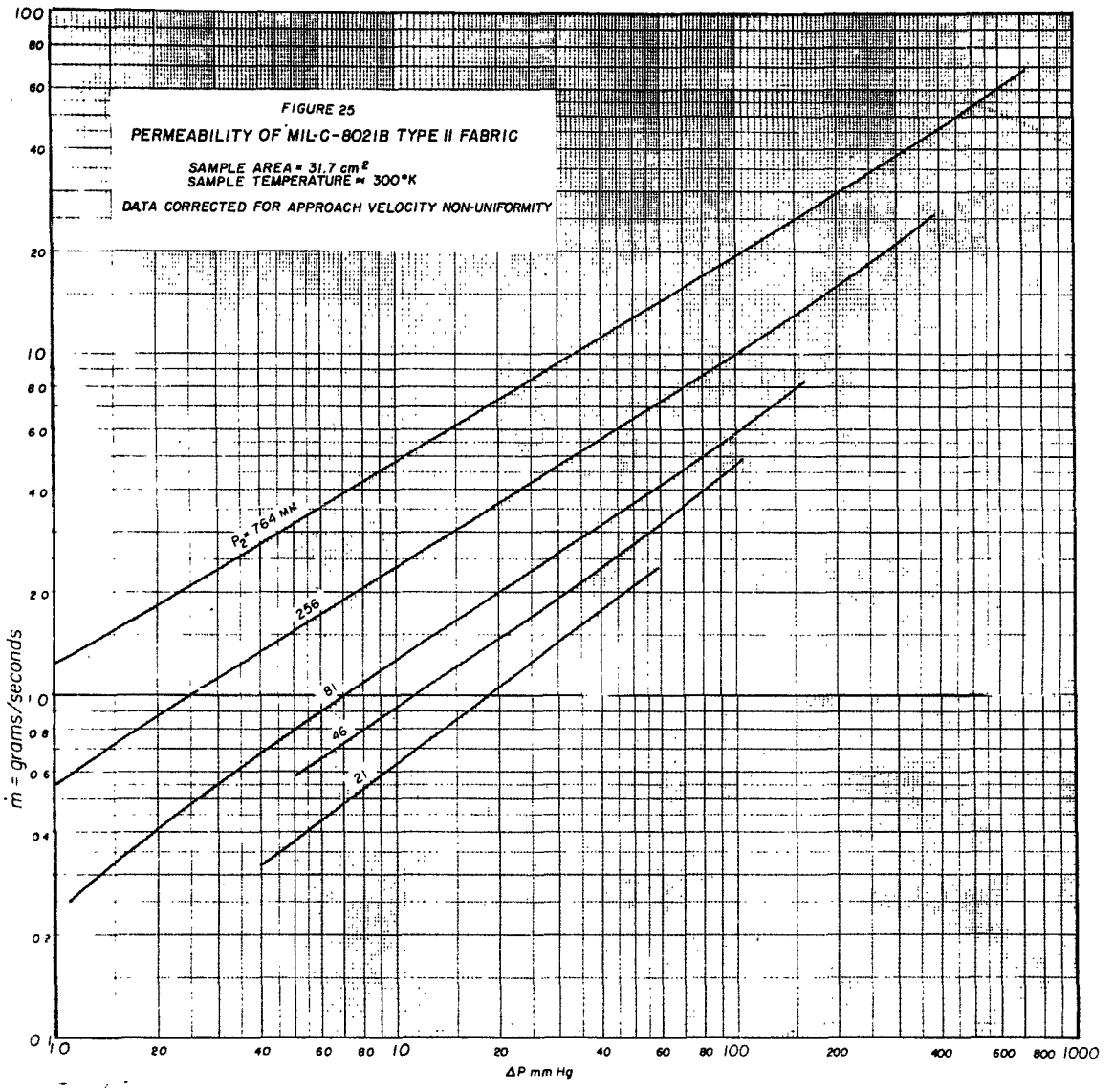
FIGURE 25
PERMEABILITY OF MIL-C-8021B TYPE II FABRIC
SAMPLE AREA = 31.7 cm²
SAMPLE TEMPERATURE ≈ 300°K
DATA CORRECTED FOR APPROACH VELOCITY NON-UNIFORMITY
P₂ = 764 MM
256
81
46
21
ṁ = grams/seconds
ΔP mm Hg

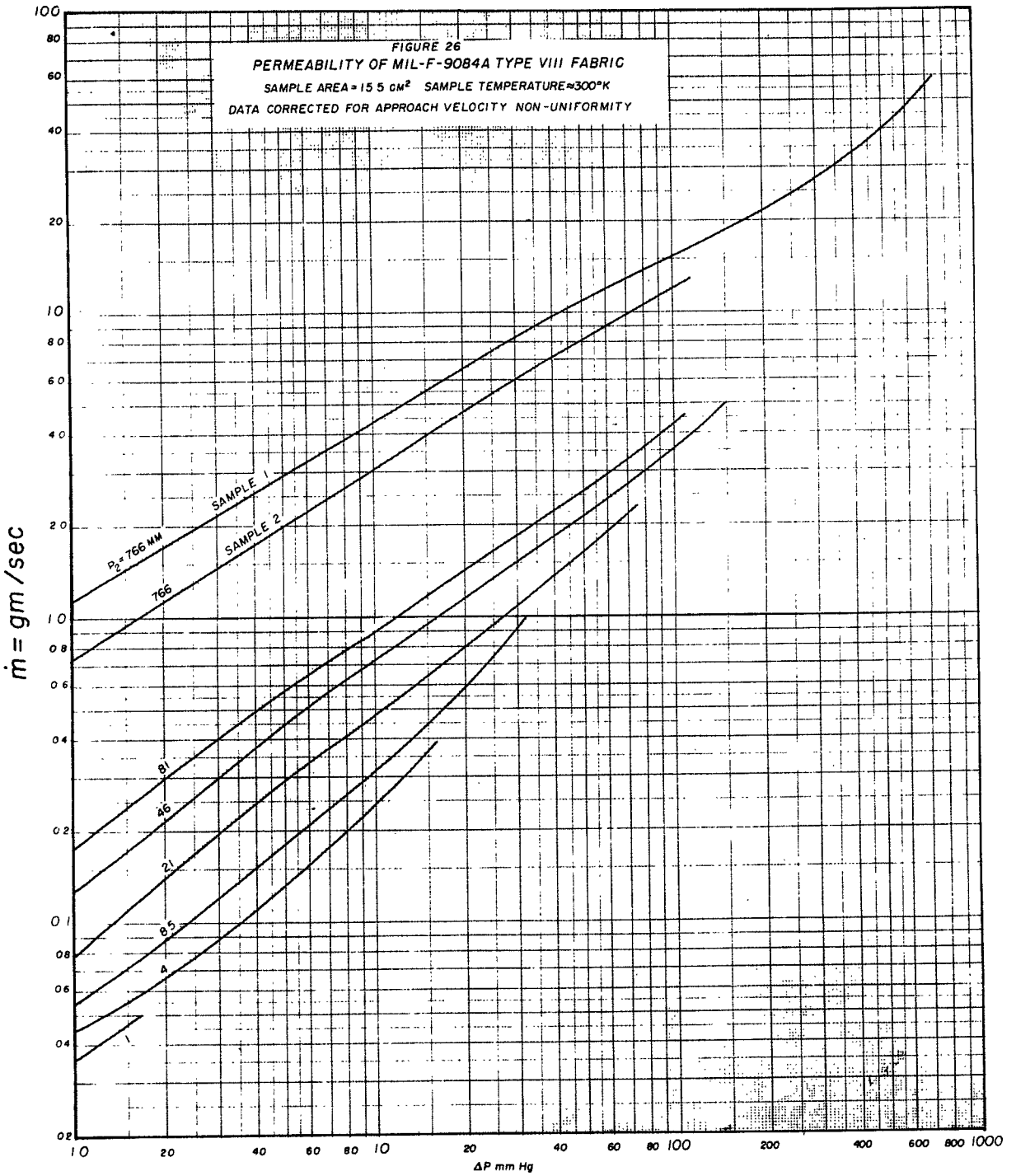
FIGURE 26
PERMEABILITY OF MIL-F-9084A TYPE VIII FABRIC
SAMPLE AREA = 15 5 cm² SAMPLE TEMPERATURE ≈ 300°K
DATA CORRECTED FOR APPROACH VELOCITY NON-UNIFORMITY
ṁ = gm/sec
ΔP mm Hg
SAMPLE 1
SAMPLE 2
P2 = 766 MM
766
81
46
21
8 5
4
1

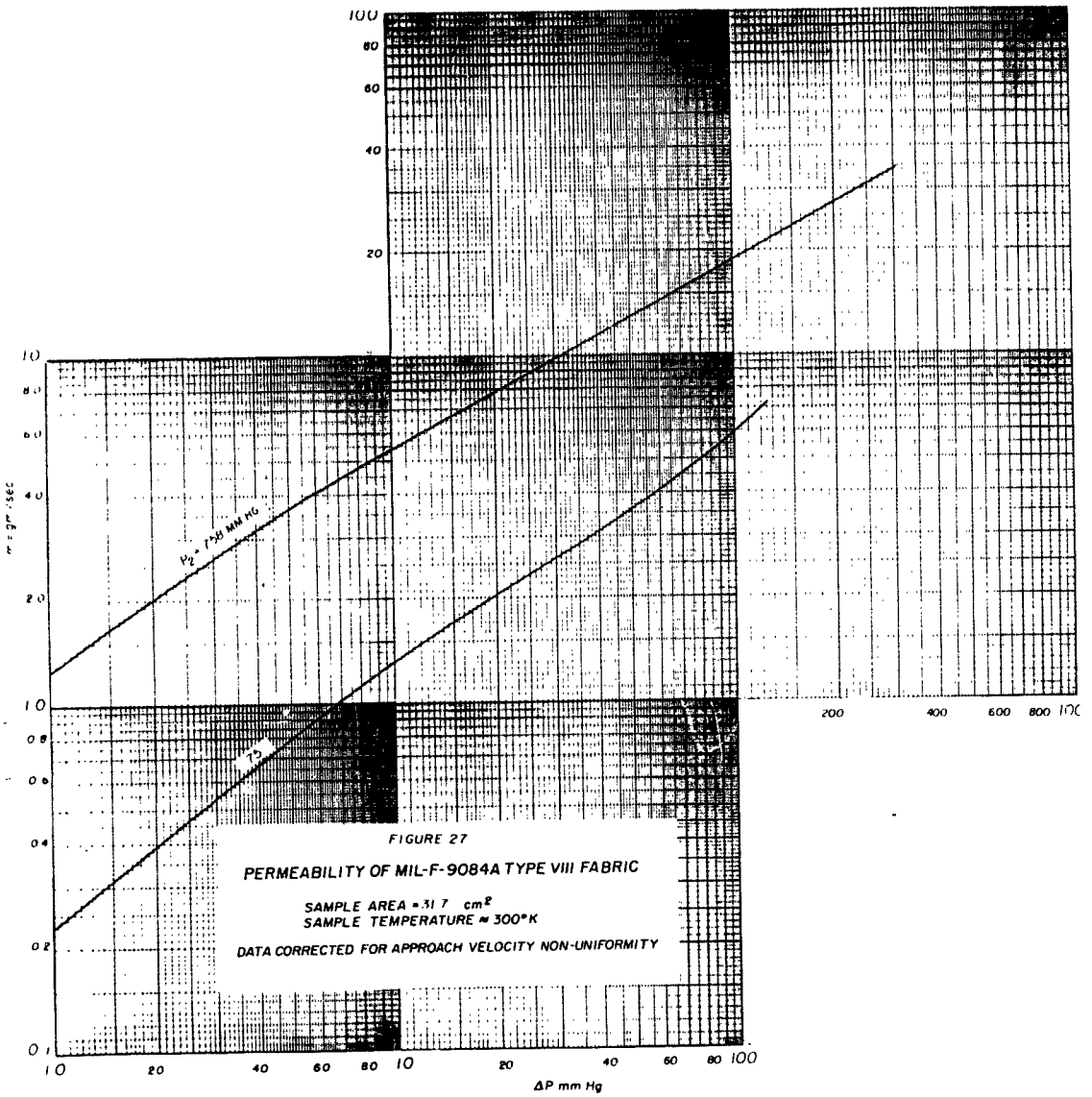

FIGURE 27

PERMEABILITY OF MIL-F-9084A TYPE VIII FABRIC

SAMPLE AREA = 31.7 cm^2
SAMPLE TEMPERATURE ≈ 300°K

DATA CORRECTED FOR APPROACH VELOCITY NON-UNIFORMITY

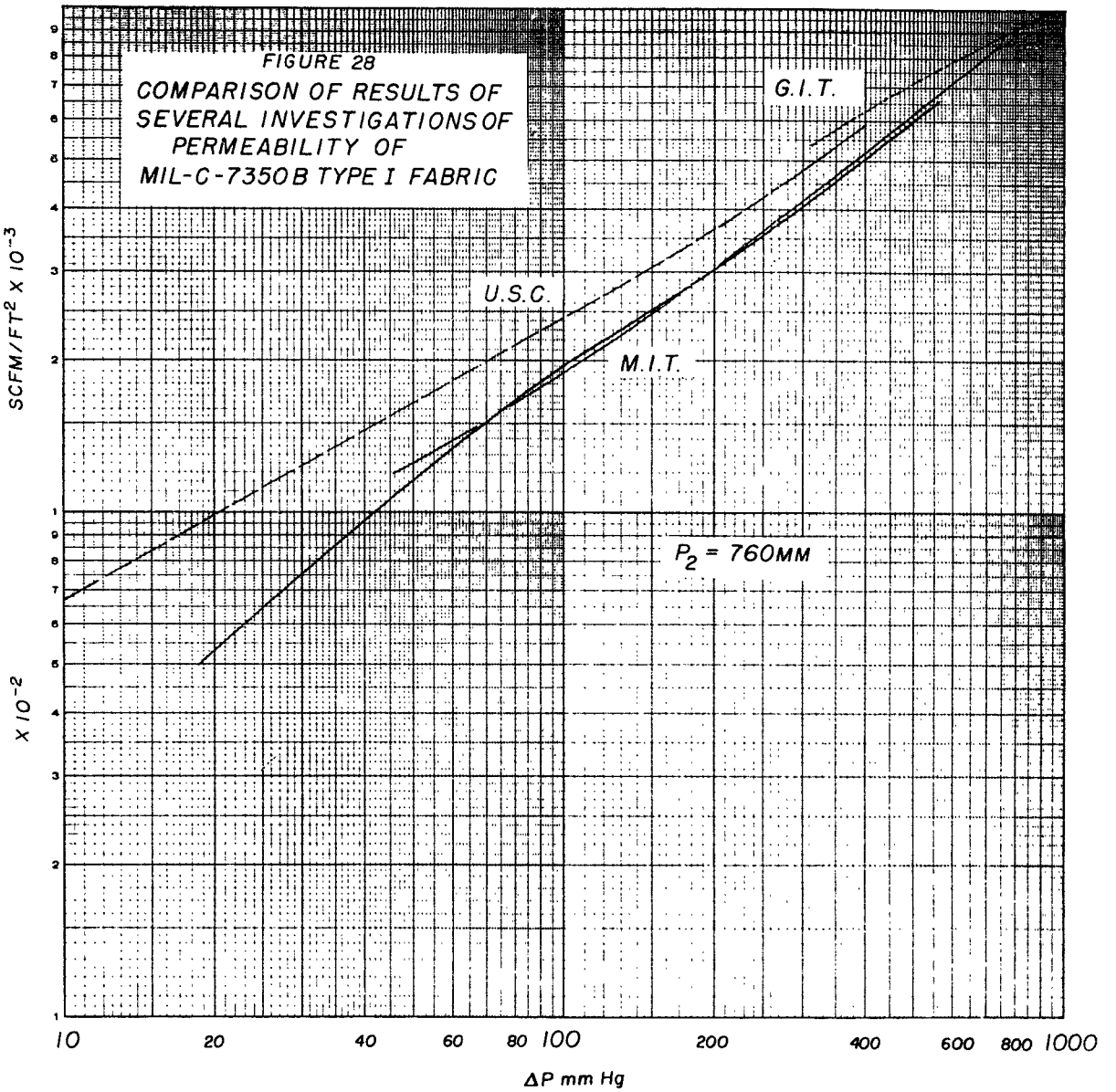
FIGURE 28
COMPARISON OF RESULTS OF SEVERAL INVESTIGATIONS OF PERMEABILITY OF MIL-C-7350B TYPE I FABRIC
G.I.T.
U.S.C.
M.I.T.
P_2 = 760MM
SCFM/FT² X 10⁻³
X 10⁻²
10
20
40
60
80
100
200
400
600
800
1000
ΔP mm Hg

FIGURE 29

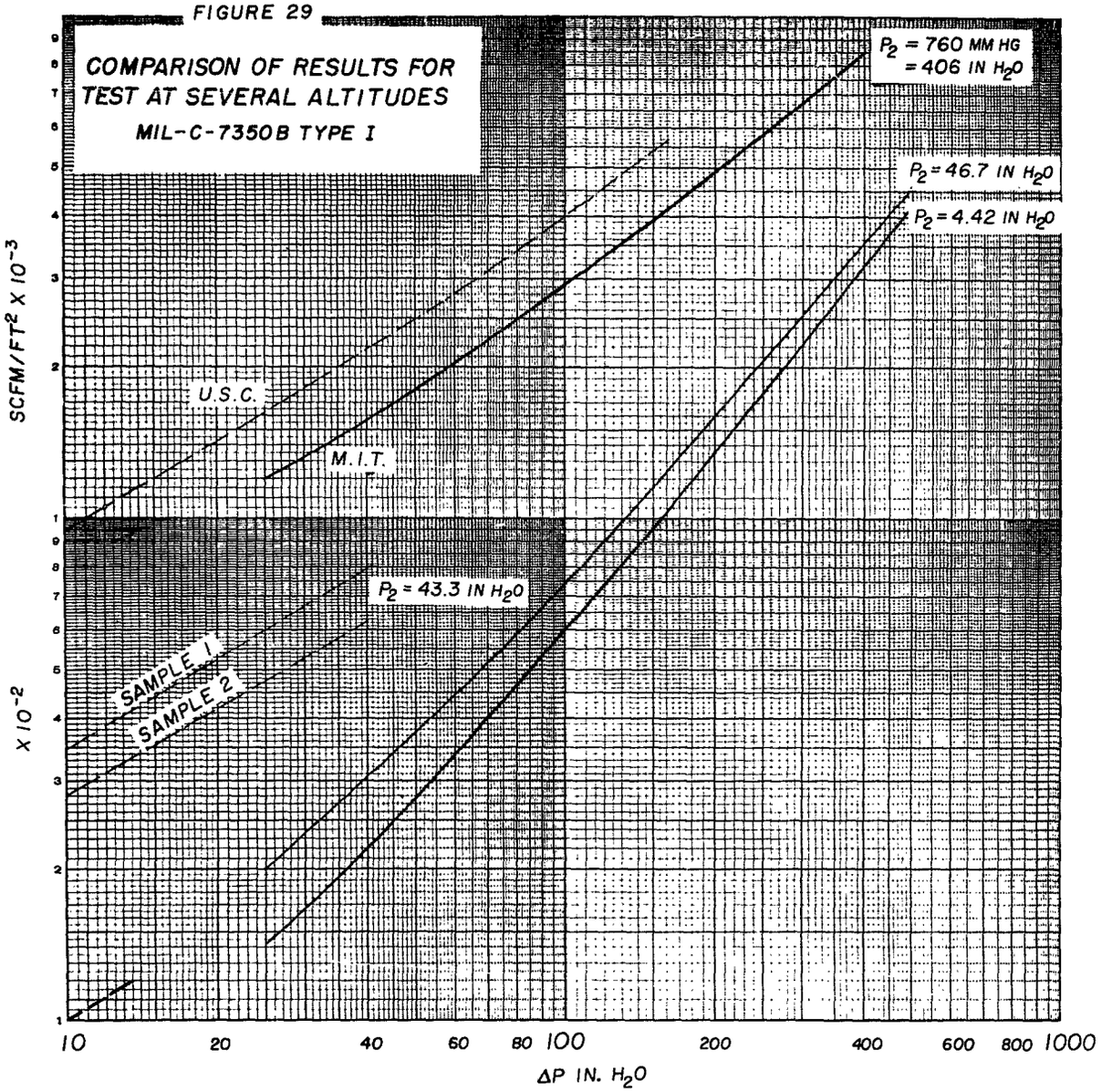
COMPARISON OF RESULTS FOR TEST AT SEVERAL ALTITUDES
MIL-C-7350B TYPE I
P_2 = 760 MM HG = 406 IN H_2O
P_2 = 46.7 IN H_2O
P_2 = 4.42 IN H_2O
P_2 = 43.3 IN H_2O
U.S.C.
M.I.T.
SAMPLE 1
SAMPLE 2
SCFM/FT^2 X 10^{-3}
X 10^{-2}
10
20
40
60
80
100
200
400
600
800
1000
ΔP IN. H_2O

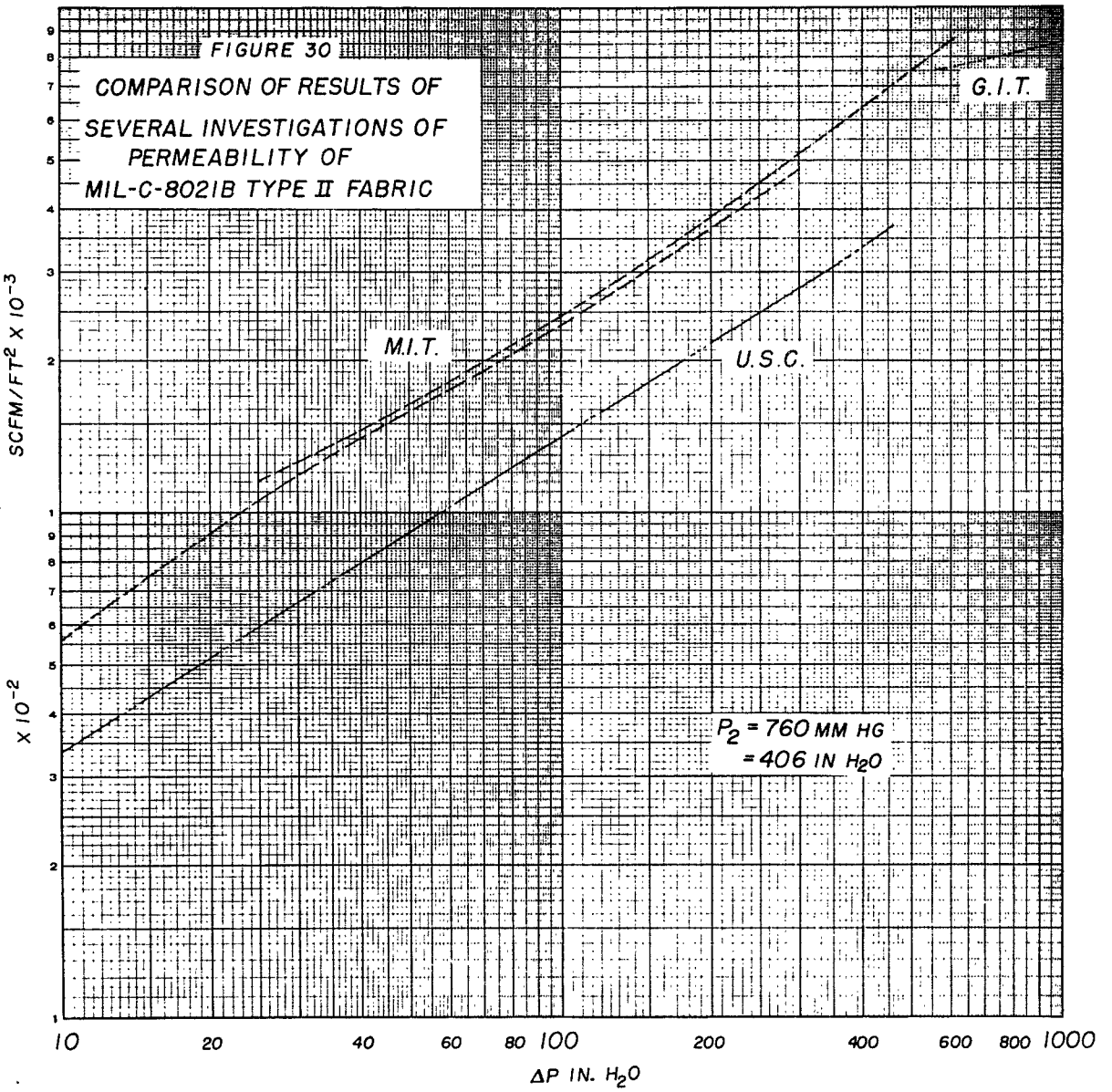
FIGURE 30
COMPARISON OF RESULTS OF
SEVERAL INVESTIGATIONS OF
PERMEABILITY OF
MIL-C-8021B TYPE II FABRIC
G.I.T.
M.I.T.
U.S.C.
P_2 = 760 MM HG
= 406 IN H_2O
SCFM/FT^2 X 10^{-3}
X 10^{-2}
10
20
40
60
80
100
200
400
600
800
1000
ΔP IN. H_2O

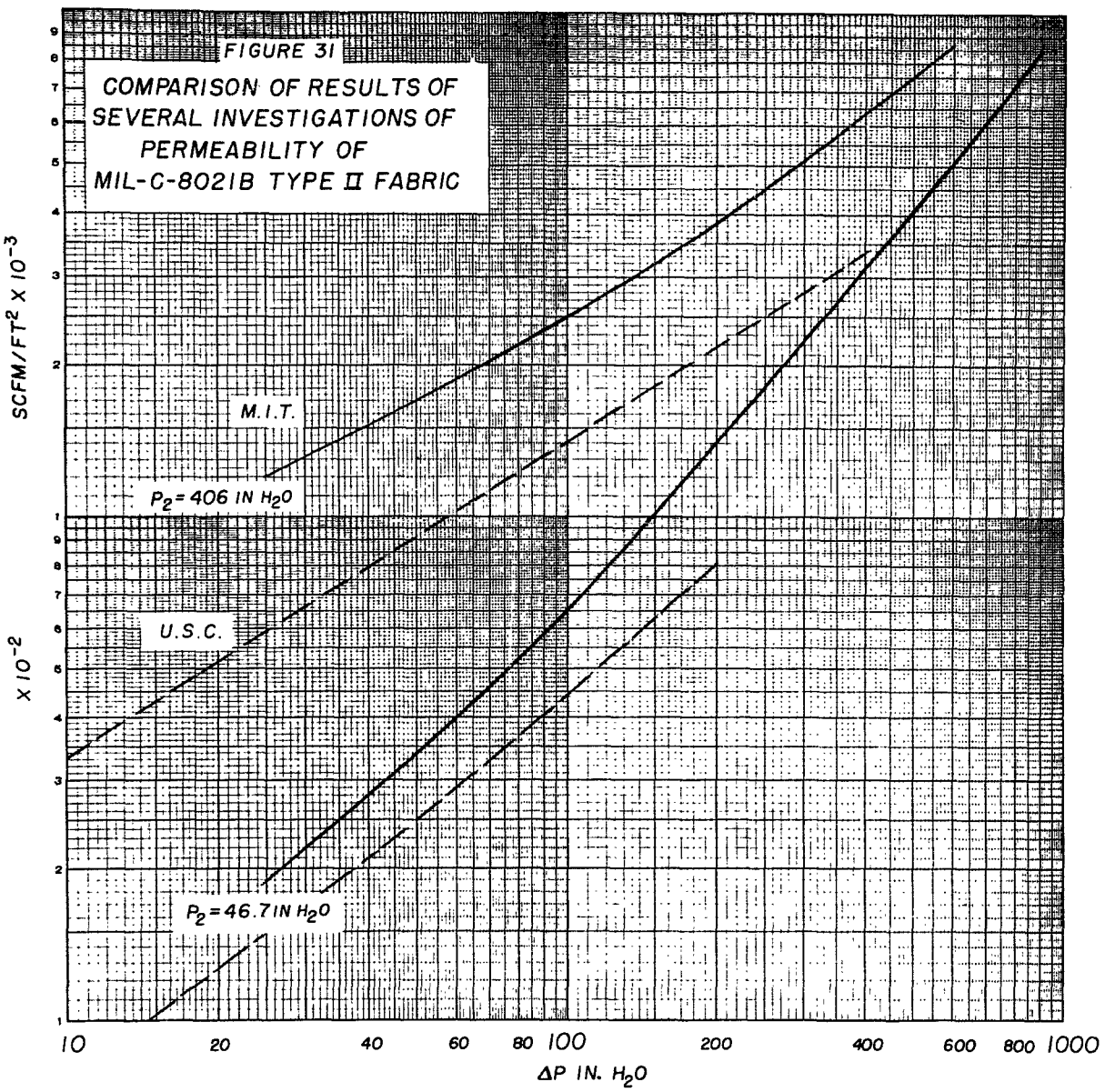
FIGURE 31
COMPARISON OF RESULTS OF SEVERAL INVESTIGATIONS OF PERMEABILITY OF MIL-C-8021B TYPE II FABRIC
SCFM/FT² X 10⁻³
X 10⁻²
M.I.T.
P2 = 406 IN H2O
U.S.C.
P2 = 46.7 IN H2O
10
20
40
60
80
100
200
400
600
800
1000
ΔP IN. H2O

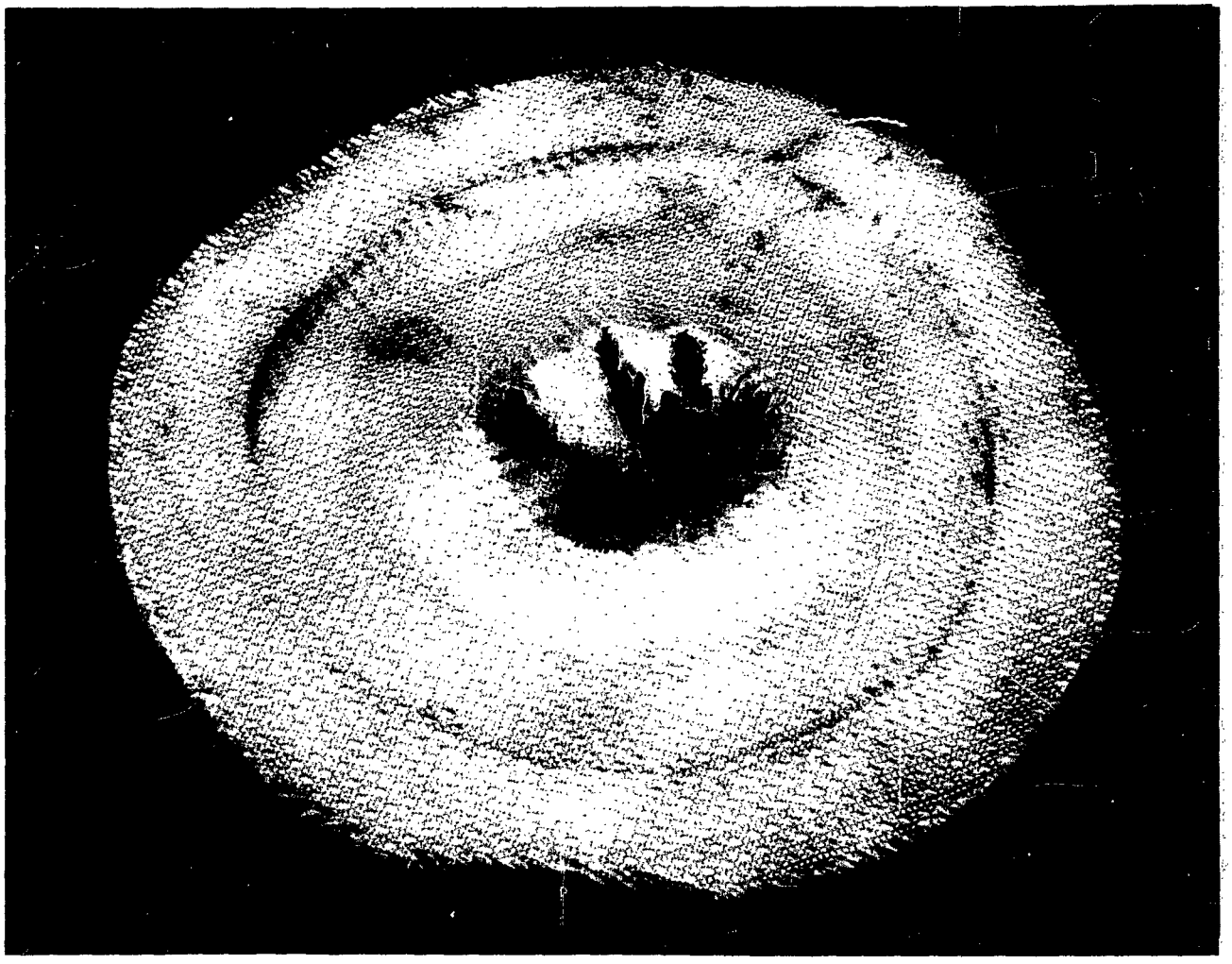

FIGURE 32 MIL-C-8021B TYPE II FABRIC AFTER TESTS DURING WHICH AIRFLOW TEMPERATURE EXCEEDED MELTING TEMPERATURE OF MATERIAL, DIAMETER OF MELTED SECTION IS ABOUT 1".

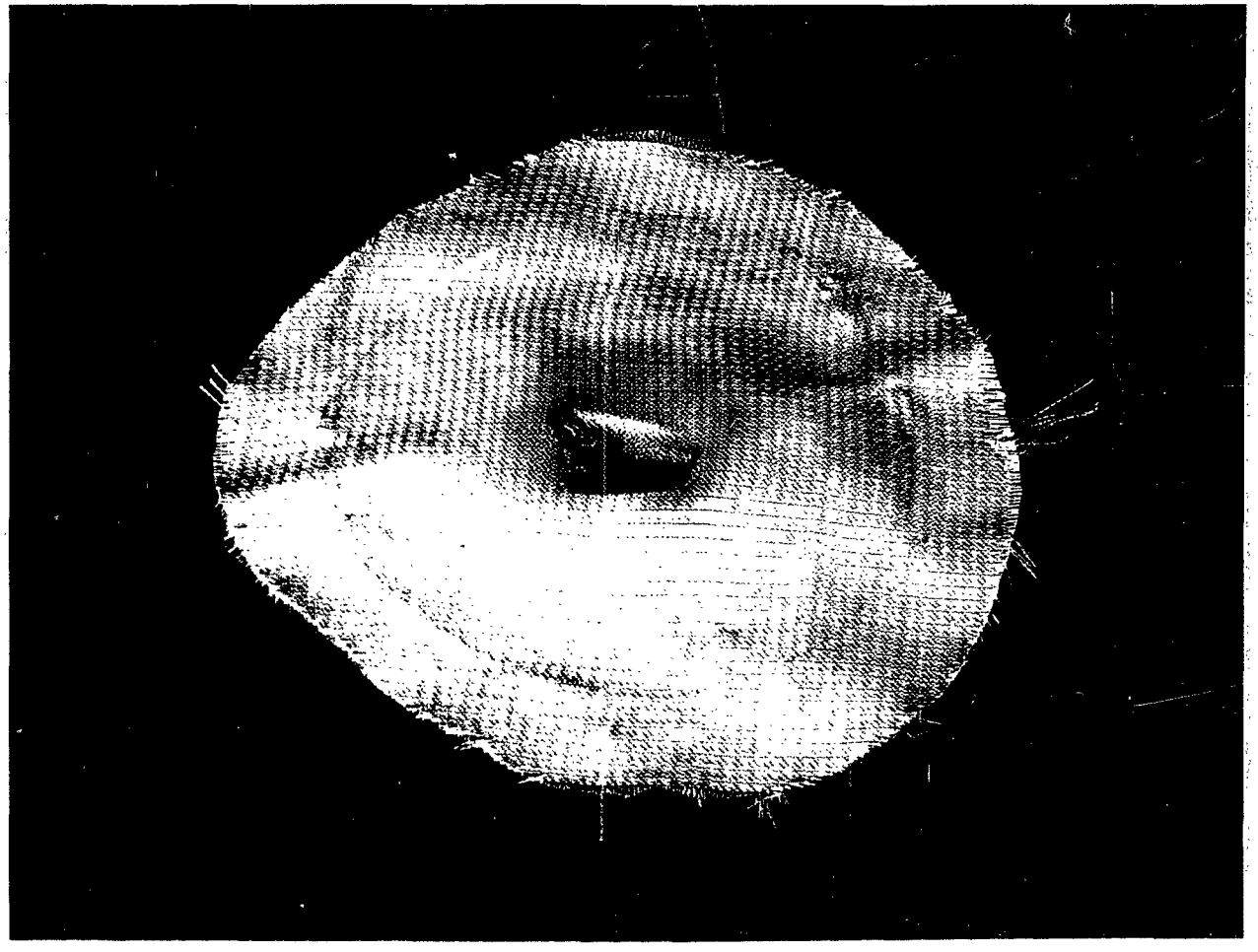

FIGURE 33 HT-1 FABRIC AFTER TESTS DURING WHICH AIRFLOW TEMPERATURE EXCEEDED MELTING TEMPERATURE OF MATERIAL.

FIGURE 34

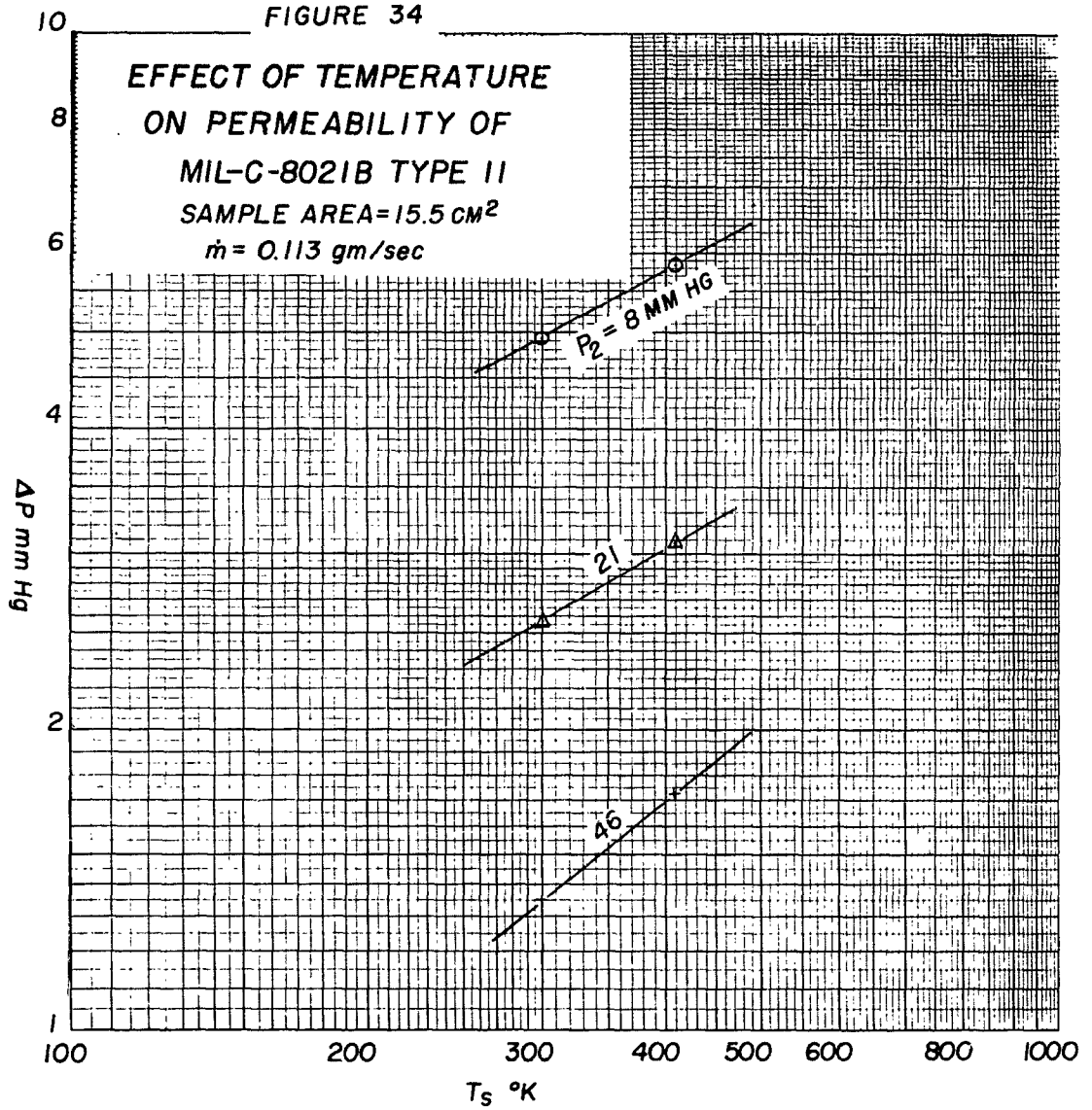
EFFECT OF TEMPERATURE
ON PERMEABILITY OF
MIL-C-8021B TYPE II
SAMPLE AREA=15.5 CM²
ṁ = 0.113 gm/sec
P2 = 8 MM HG
21
46
ΔP mm Hg
Ts °K
10
8
6
4
2
1
100
200
300
400
500
600
800
1000

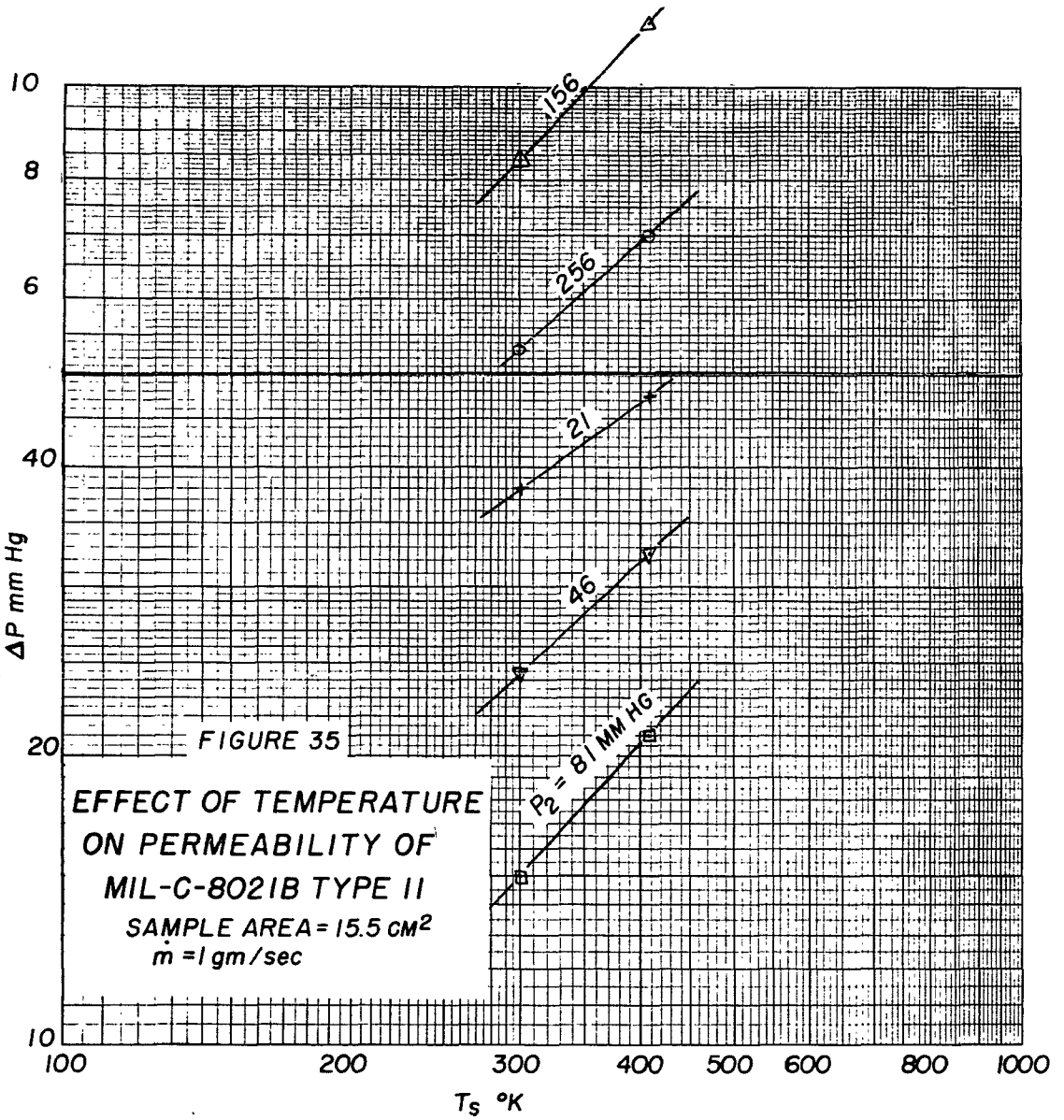

FIGURE 35

EFFECT OF TEMPERATURE ON PERMEABILITY OF MIL-C-8021B TYPE II

SAMPLE AREA = 15.5 cm²

$\dot{m}$ = 1 gm/sec

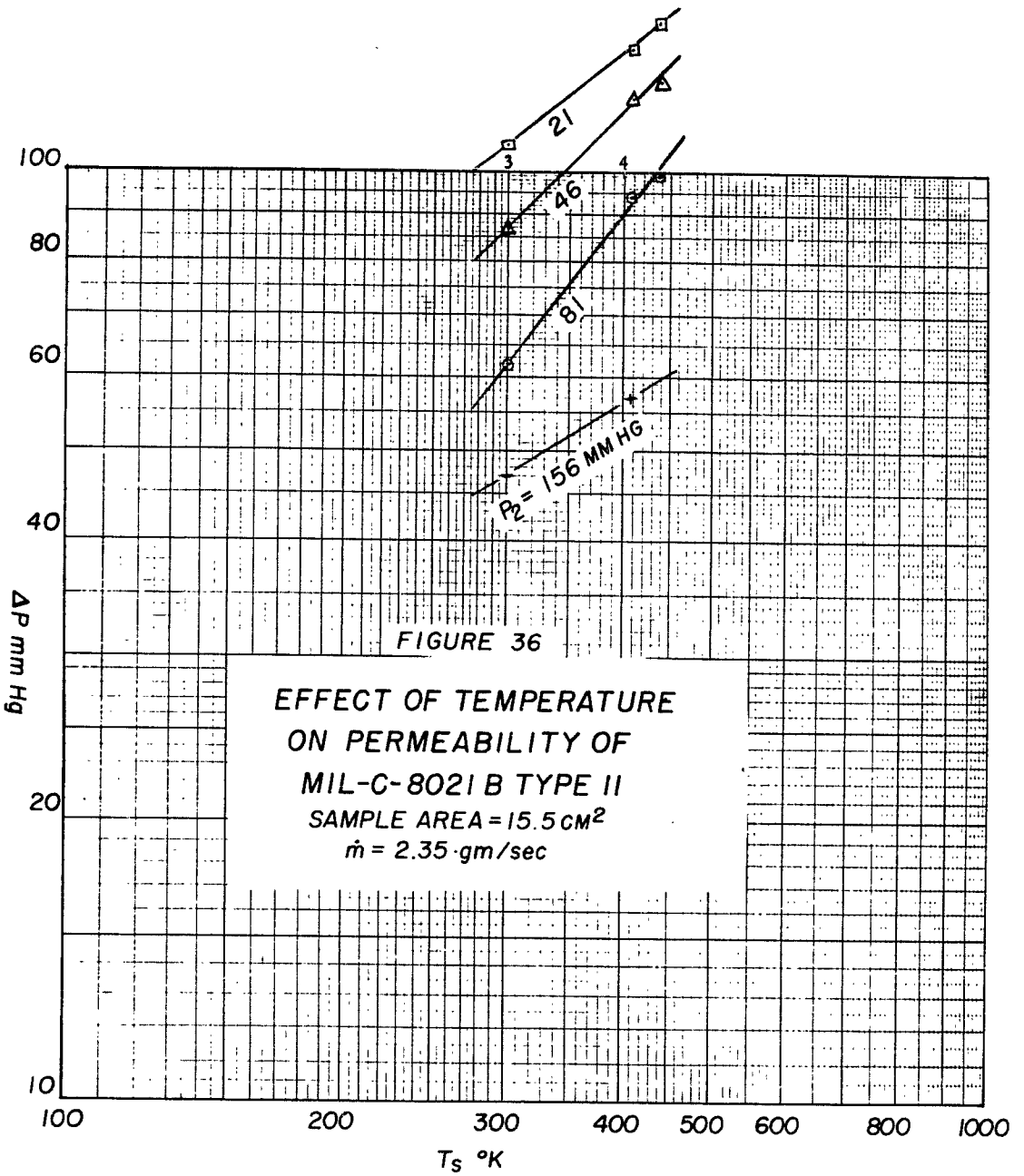

FIGURE 36

EFFECT OF TEMPERATURE ON PERMEABILITY OF MIL-C-8021 B TYPE II

SAMPLE AREA = 15.5 cm^2

$\dot{m}$ = 2.35 gm/sec

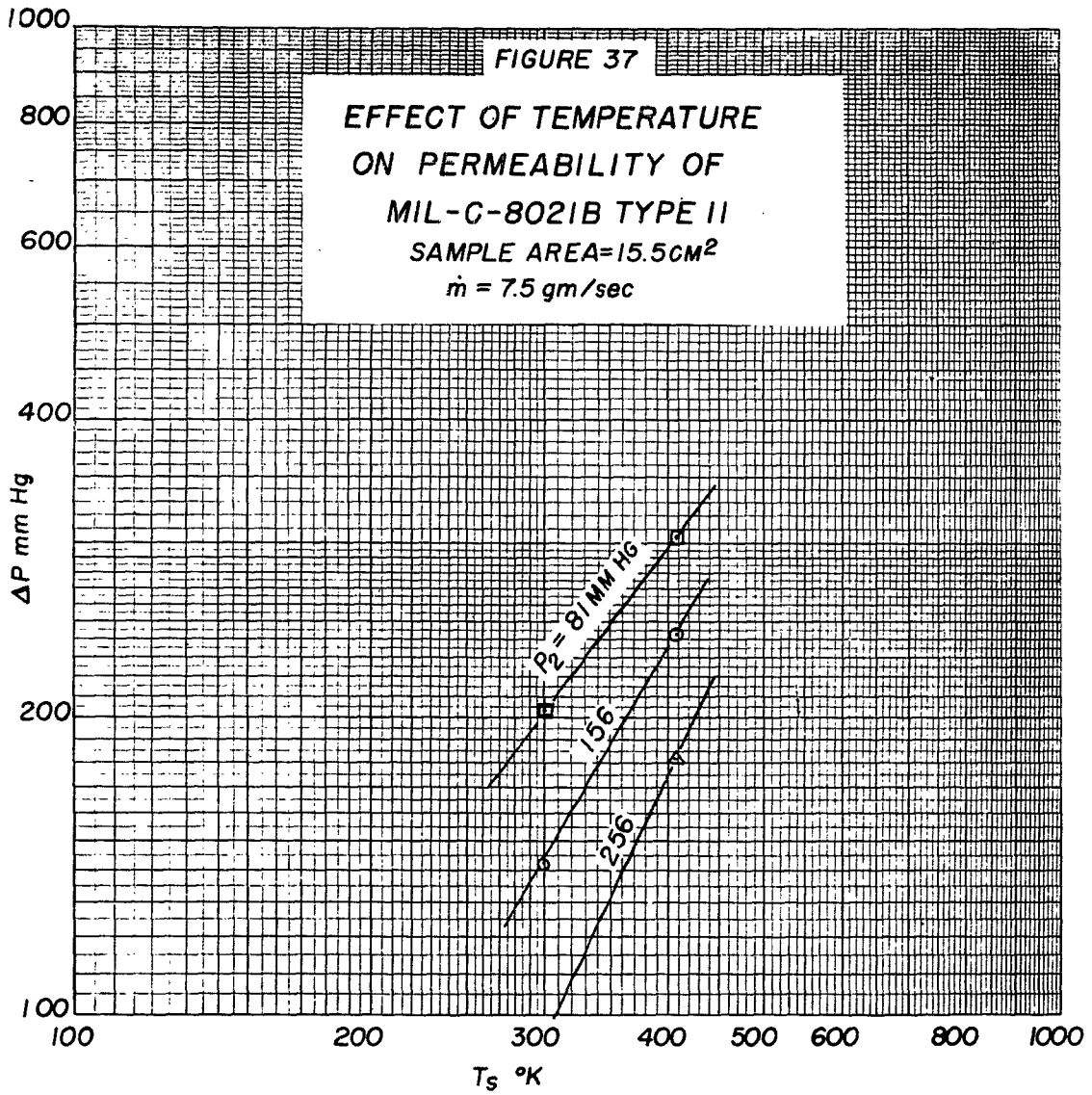
FIGURE 37
EFFECT OF TEMPERATURE ON PERMEABILITY OF MIL-C-8021B TYPE II
SAMPLE AREA=15.5cm²
ṁ = 7.5 gm/sec
ΔP mm Hg
1000
800
600
400
200
100
100
200
300
400
500
600
800
1000
Ts °K
P2 = 81 MM HG
156
256

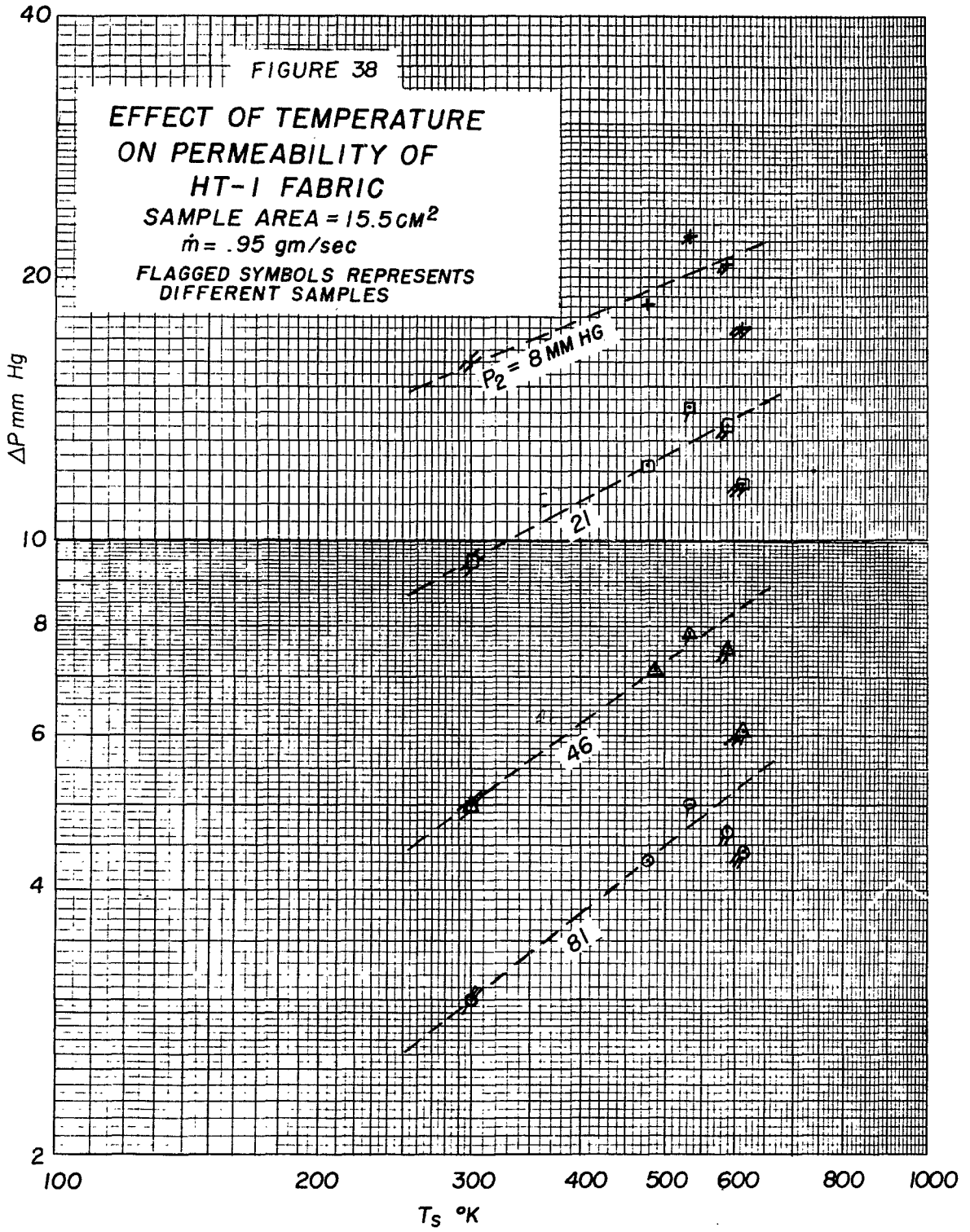
FIGURE 38
EFFECT OF TEMPERATURE ON PERMEABILITY OF HT-1 FABRIC
SAMPLE AREA = 15.5 CM²
ṁ = .95 gm/sec
FLAGGED SYMBOLS REPRESENTS DIFFERENT SAMPLES
P2 = 8 MM HG
21
46
81
ΔP mm Hg
Ts °K
40
20
10
8
6
4
2
100
200
300
400
500
600
800
1000

FIGURE 39

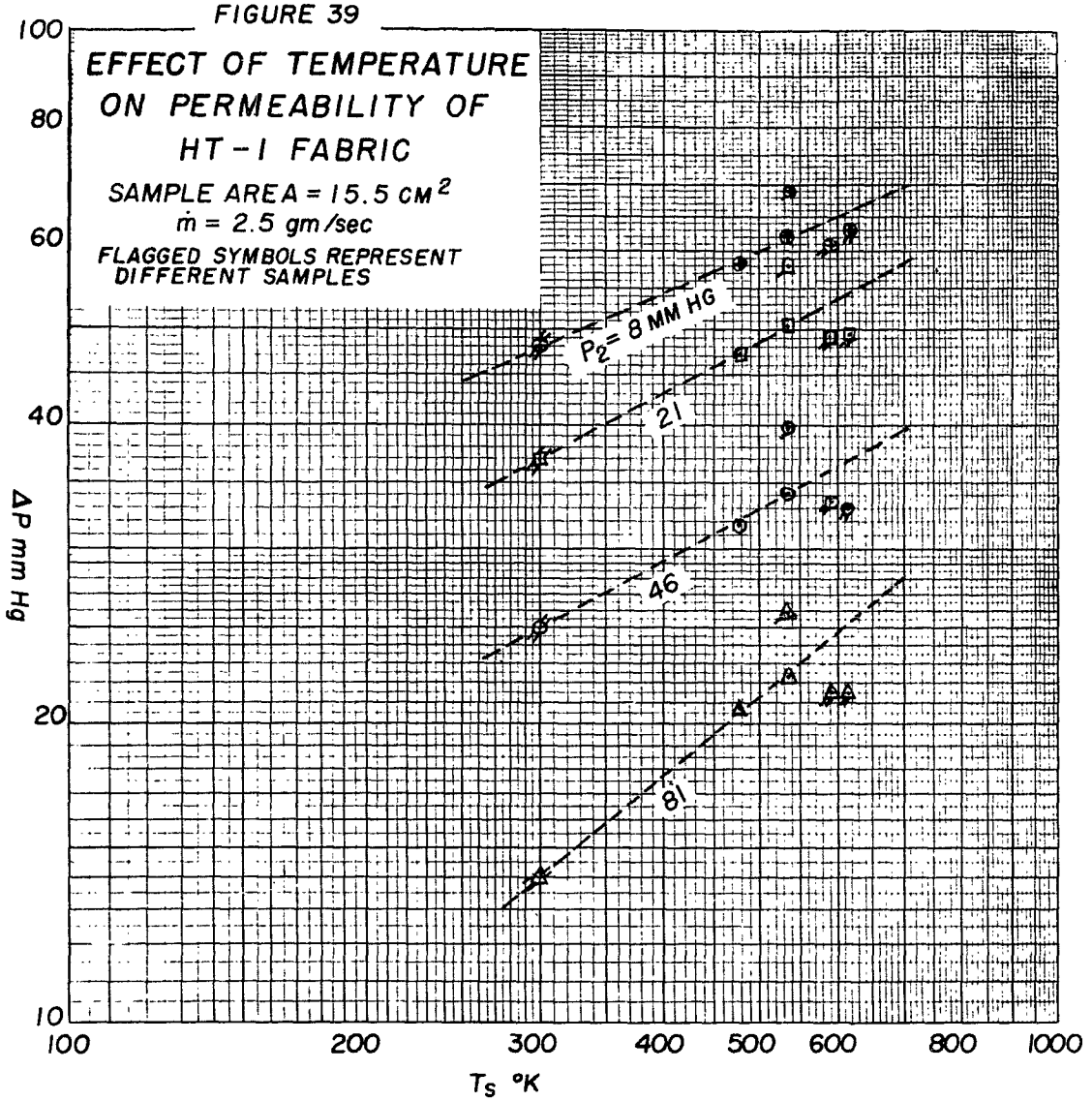
EFFECT OF TEMPERATURE ON PERMEABILITY OF HT-1 FABRIC
SAMPLE AREA = 15.5 CM²
ṁ = 2.5 gm/sec
FLAGGED SYMBOLS REPRESENT DIFFERENT SAMPLES
P₂ = 8 MM HG
21
46
81
ΔP mm Hg
Ts °K
100
80
60
40
20
10
100
200
300
400
500
600
800
1000

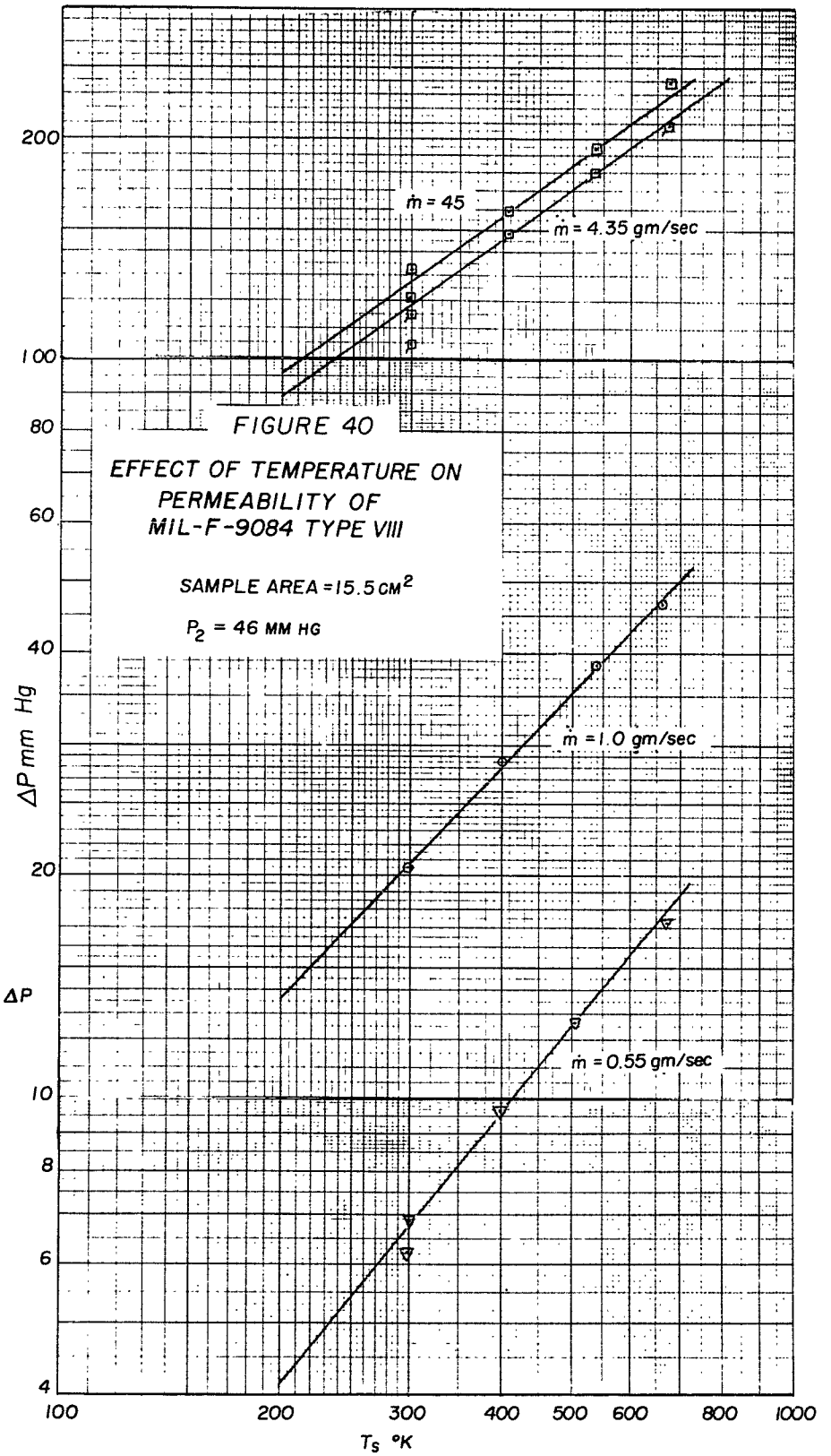

FIGURE 40

EFFECT OF TEMPERATURE ON PERMEABILITY OF MIL-F-9084 TYPE VIII

SAMPLE AREA = 15.5 CM^2

P_2 = 46 MM HG

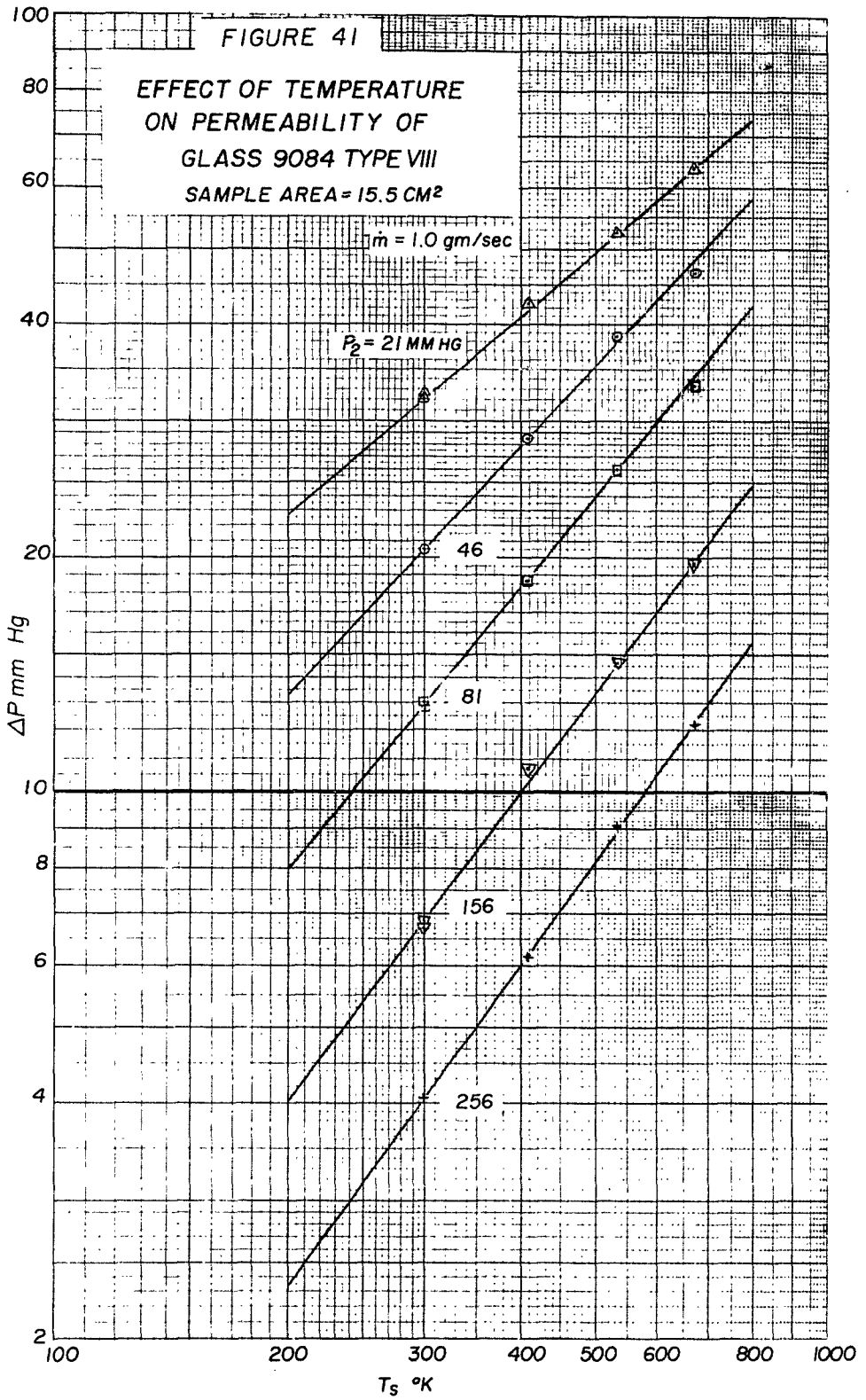
FIGURE 41
EFFECT OF TEMPERATURE ON PERMEABILITY OF GLASS 9084 TYPE VIII
SAMPLE AREA = 15.5 CM²
ṁ = 1.0 gm/sec
P2 = 21 MM HG
46
81
156
256
ΔP mm Hg
Ts °K
100
80
60
40
20
10
8
6
4
2
100
200
300
400
500
600
800
1000

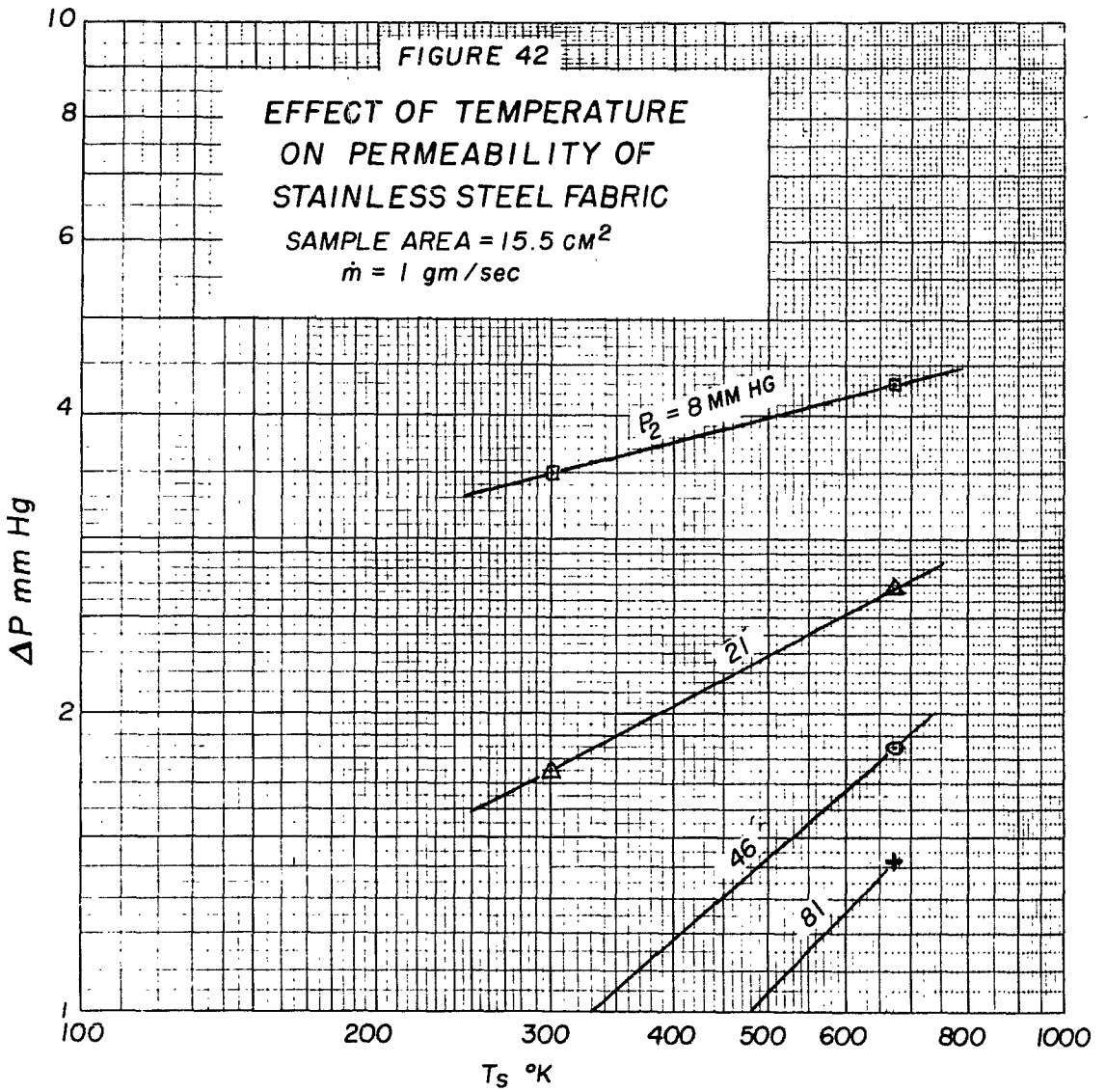
FIGURE 42
EFFECT OF TEMPERATURE ON PERMEABILITY OF STAINLESS STEEL FABRIC
SAMPLE AREA = 15.5 cm²
ṁ = 1 gm/sec
P₂ = 8 MM HG
21
46
81
ΔP mm Hg
Ts °K
10
8
6
4
2
1
100
200
300
400
500
600
800
1000

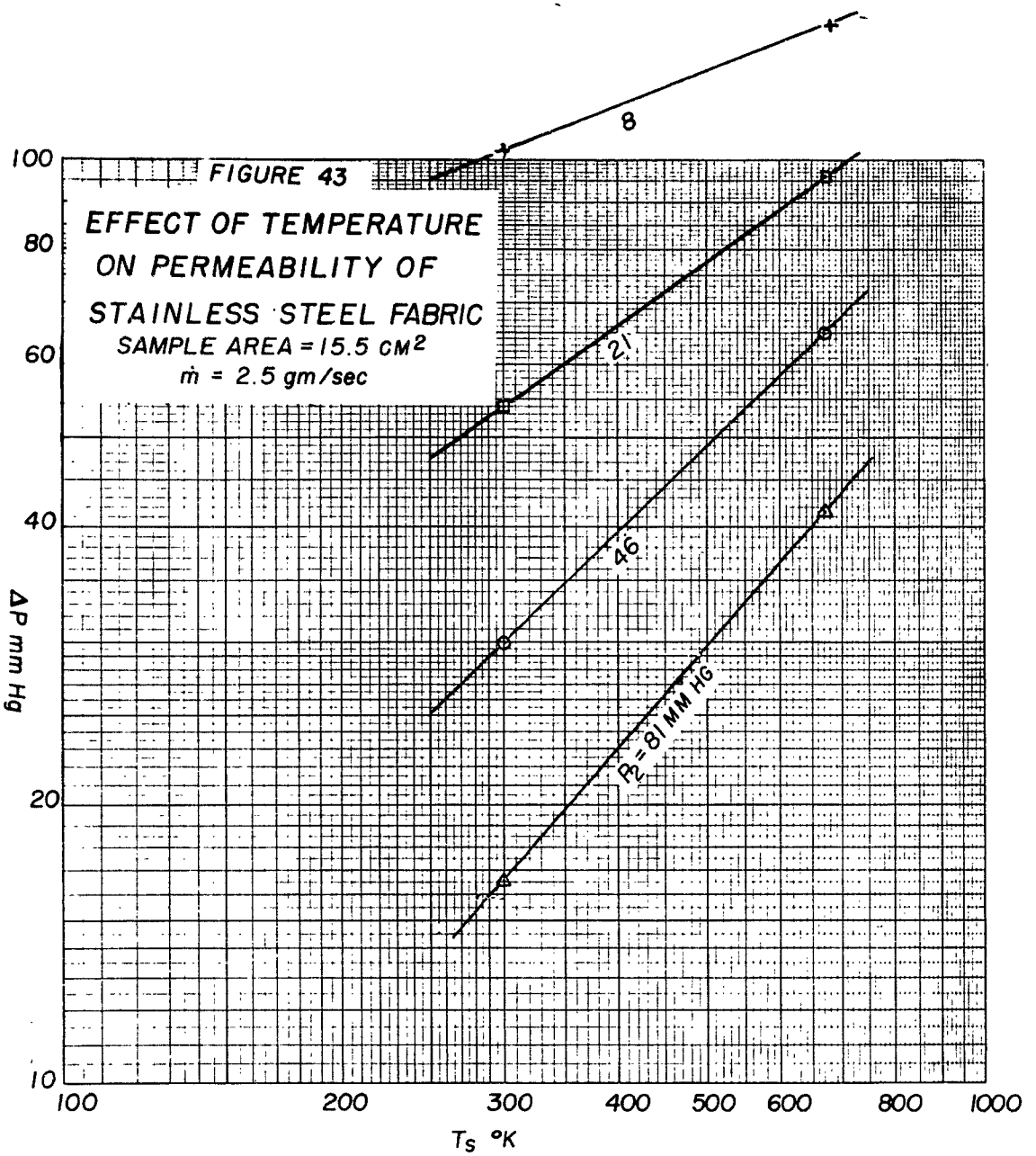
FIGURE 43
EFFECT OF TEMPERATURE ON PERMEABILITY OF STAINLESS STEEL FABRIC
SAMPLE AREA = 15.5 cm²
ṁ = 2.5 gm/sec
8
21
46
P2 = 81 MM HG
ΔP mm Hg
100
80
60
40
20
10
100
200
300
400
500
600
800
1000
Ts °K

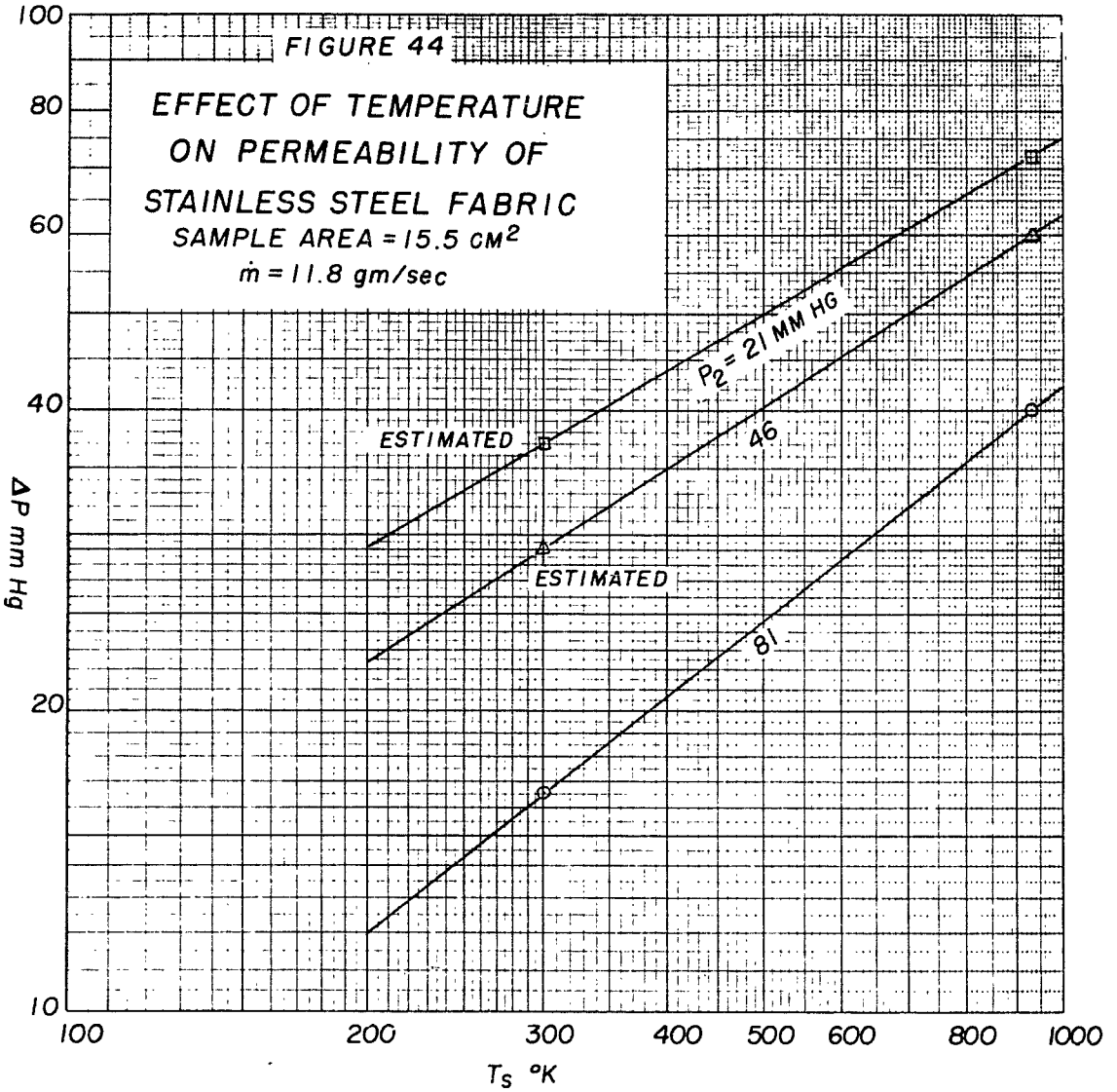
FIGURE 44
EFFECT OF TEMPERATURE ON PERMEABILITY OF STAINLESS STEEL FABRIC
SAMPLE AREA = 15.5 cm²
ṁ = 11.8 gm/sec
P₂ = 21 MM HG
46
81
ESTIMATED
ESTIMATED
ΔP mm Hg
Ts °K
100
80
60
40
20
10
100
200
300
400
500
600
800
1000

UNIVERSITY OF SOUTHERN CALIFORNIA, ENGINEERING CENTER, Los Angeles. A THEORETICAL AND EXPERIMENTAL STUDY OF GAS FLOW THROUGH CLOTH OVER A RANGE OF PRESSURES AND TEMPERATURES, by Frederick O. Smetana, June 1961, 124p. incl. figs., tables and refs. (Project 7320) (ASD TR 61-192) (Contract AF 33(616)-7102)

Unclassified report

Measurements were made of the permeability of five fabrics at downstream pressures from sea level to 150,000', pressure drops across the samples of 1 mm Hg to 900 mm Hg, and stagnation temperatures from 300°K to 930°K. In addition to this basic information, the investigation sought to provide a means of predicting high altitude results from those at sea level. It was found that: (a) the geometry of the test apparatus can have a

(over)

marked influence on the results, (b) the major elastic effects on permeability arise from the change in fabric pore inclination with load rather than through simple extension of the yarn itself, (c) viscous effects are present for all except the very highest pressures, (d) rarefaction effects appear at altitudes above about 60,000', (e) the most satisfactory model for explaining the results appears to be one likening the flow to that between two noninteracting cylinders, and (f) as long as the fabric retains its elasticity and does not take a permanent set, temperature changes affect the permeability only insofar as the air density is changed. Some of these findings have not as yet been described quantitatively; for this reason, a satisfactory prediction procedure is not yet available.

Unclassified

Unclassified

Unclassified

Unclassified

UNIVERSITY OF SOUTHERN CALIFORNIA, ENGINEERING CENTER, Los Angeles. A THEORETICAL AND EXPERIMENTAL STUDY OF GAS FLOW THROUGH CLOTH OVER A RANGE OF PRESSURES AND TEMPERATURES, by Frederick O. Smetana, June 1961, 124p. incl. figs., tables and refs. (Project 7320) (ASD TR 61-192) (Contract AF 33(616)-7102)

Unclassified report

Measurements were made of the permeability of five fabrics at downstream pressures from sea level to 150,000', pressure drops across the samples of 1 mm Hg to 900 mm Hg, and stagnation temperatures from 300°K to 930°K. In addition to this basic information, the investigation sought to provide a means of predicting high altitude results from those at sea level. It was found that: (a) the geometry of the test apparatus can have a

(over)

marked influence on the results, (b) the major elastic effects on permeability arise from the change in fabric pore inclination with load rather than through simple extension of the yarn itself, (c) viscous effects are present for all except the very highest pressures, (d) rarefaction effects appear at altitudes above about 60,000', (e) the most satisfactory model for explaining the results appears to be one likening the flow to that between two noninteracting cylinders, and (f) as long as the fabric retains its elasticity and does not take a permanent set, temperature changes affect the permeability only insofar as the air density is changed. Some of these findings have not as yet been described quantitatively; for this reason, a satisfactory prediction procedure is not yet available.

Unclassified

Unclassified

Unclassified

Unclassified

UNIVERSITY OF SOUTHERN CALIFORNIA, ENGINEERING CENTER, Los Angeles. A THEORETICAL AND EXPERIMENTAL STUDY OF GAS FLOW THROUGH CLOTH OVER A RANGE OF PRESSURES AND TEMPERATURES, by Frederick O. Smetana, June 1961, 124p. incl. figs., tables and refs. (Project 7320) (ASD TR 61-192) (Contract AF 33(616)-7102)

Unclassified report

Measurements were made of the permeability of five fabrics at downstream pressures from sea level to 150,000', pressure drops across the samples of 1 mm Hg to 900 mm Hg, and stagnation temperatures from 300°K to 930°K. In addition to this basic information, the investigation sought to provide a means of predicting high altitude results from those at sea level. It was found that: (a) the geometry of the test apparatus can have a

(over)

Unclassified

Unclassified

marked influence on the results, (b) the major elastic effects on permeability arise from the change in fabric pore inclination with load rather than through simple extension of the yarn itself, (c) viscous effects are present for all except the very highest pressures, (d) rarefaction effects appear at altitudes above about 60,000', (e) the most satisfactory model for explaining the results appears to be one likening the flow to that between two noninteracting cylinders, and (f) as long as the fabric retains its elasticity and does not take a permanent set, temperature changes affect the permeability only insofar as the air density is changed. Some of these findings have not as yet been described quantitatively; for this reason, a satisfactory prediction procedure is not yet available.

Unclassified

UNIVERSITY OF SOUTHERN CALIFORNIA, ENGINEERING CENTER, Los Angeles. A THEORETICAL AND EXPERIMENTAL STUDY OF GAS FLOW THROUGH CLOTH OVER A RANGE OF PRESSURES AND TEMPERATURES, by Frederick O. Smetana, June 1961, 124p. incl. figs., tables and refs. (Project 7320) (ASD TR 61-192) (Contract AF 33(616)-7102)

Unclassified report

Measurements were made of the permeability of five fabrics at downstream pressures from sea level to 150,000', pressure drops across the samples of 1 mm Hg to 900 mm Hg, and stagnation temperatures from 300°K to 930°K. In addition to this basic information, the investigation sought to provide a means of predicting high altitude results from those at sea level. It was found that: (a) the geometry of the test apparatus can have a

(over)

Unclassified

Unclassified

marked influence on the results, (b) the major elastic effects on permeability arise from the change in fabric pore inclination with load rather than through simple extension of the yarn itself, (c) viscous effects are present for all except the very highest pressures, (d) rarefaction effects appear at altitudes above about 60,000', (e) the most satisfactory model for explaining the results appears to be one likening the flow to that between two noninteracting cylinders, and (f) as long as the fabric retains its elasticity and does not take a permanent set, temperature changes affect the permeability only insofar as the air density is changed. Some of these findings have not as yet been described quantitatively; for this reason, a satisfactory prediction procedure is not yet available.

Unclassified